This Page is Inserted by IFW Indexing and Scanning Operations and is not part of the Official Record

BEST AVAILABLE IMAGES

Defective images within this document are accurate representations of the original documents submitted by the applicant.

Defects in the images include but are not limited to the items checked:

- ☐ BLACK BORDERS
- ☐ IMAGE CUT OFF AT TOP, BOTTOM OR SIDES
- ☐ FADED TEXT OR DRAWING
- ☐ BLURRED OR ILLEGIBLE TEXT OR DRAWING
- ☐ SKEWED/SLANTED IMAGES
- ☐ COLOR OR BLACK AND WHITE PHOTOGRAPHS
- ☐ GRAY SCALE DOCUMENTS
- ☐ LINES OR MARKS ON ORIGINAL DOCUMENT
- ☐ REFERENCE(S) OR EXHIBIT(S) SUBMITTED ARE POOR QUALITY
- ☐ OTHER: _____

IMAGES ARE BEST AVAILABLE COPY.
As rescanning these documents will not correct the image problems checked, please do not report these problems to the IFW Image Problem Mailbox.

IN THE UNITED STATES PATENT AND TRADEMARK OFFICE

In re application of:
UMAÑA *et al.*.
Appl. No.: 10/633,699
Filed: August 5, 2003
For: **Glycosylation Engineering of Antibodies for Improving Antibody-Dependent Cellular Cytotoxicity**

Confirmation No.: 5489
Art Unit: 1646
Examiner: Riggins, P.
Atty. Docket: 1975.0010004/TJS

Declaration Under 37 C.F.R. § 1.132 of Pablo Umaña, Ph.D.

Commissioner for Patents
PO Box 1450
Alexandria, VA 22313-1450

Sir:

The undersigned, Pablo Umaña, Ph.D., declares and says as follows:

1. I am an inventor of the above-captioned application, U.S. Patent Application Number 10/633,699, filed August 5, 2003, entitled "Glycosylation Engineering of Antibodies for Improving Antibody-Dependent Cellular Cytotoxicity."

2. I am currently Chief Scientific Officer and Member of the Board at GlycArt Biotechnology AG in Zurich, Switzerland. I am an expert in the fields of molecular biology and immunology, with particular expertise in the area of antibody engineering. My qualifications as an expert are established by the attached curriculum vitae and the publications listed therein. (Exhibit A)

3. I have read and understood the subject matter of U.S. Pat. Appl. No. 10/633,699.

4. Glycoengineered antibodies produced according to the techniques we described in the above-captioned patent application are characterized by a substantial increase in the proportion of nonfucosylated oligosaccharides in their Fc region and

exhibit significantly increased binding to Fc receptors and antibody-dependent cellular cytotoxicity. Our studies confirming this are set forth in the attached Exhibits B-D.

5. The present application teaches that glycoengineered antibodies with increased Fc receptor binding can be obtained, according to one method, by engineering a host cell to coexpress an antibody and a glycoprotein-modifying glycosyltransferase. The application specifically identifies GnT III and ManII as useful glycoprotein modifying glycosyltransferases for this purpose. In addition, the application teaches that glycoengineered antibodies can be obtained by coexpressing the antibody with *multiple* glycoprotein-modifying glycosyltransferases, such as GnTIII + ManII. (*See* page 13, lines 18-30; page 21, lines 15-25.)

6. Exhibit B is U.S. Pat. Appl. Pub. No. U.S. 2004/0241817, which published December 2, 2004, and is entitled "Fusion Constructs and Use of Same to Produce Antibodies with Increased Fc Receptor Binding Affinity and Effector Function." I am a named inventor on that application. Example 6 of the application describes experiments that I and my colleagues conducted to study the effect of coexpression in a host cell of the human α-Mannosidase II ("hManII") gene or, alternatively, a polynucleotide encoding the Golgi localization domain of hManII fused to the catalytic domain of human galactosyltransferase, and an expression vector encoding the recombinant anti-CD20 antibody C2B8.

7. Specifically, to study the effect of hManII coexpression, we transfected HEK 293-EBNA cells with expression vectors coding for each the light and heavy chain of the anti-CD20 monoclonal antibody and the hManII gene. At day 5 post-transfection, supernatant was harvested and the monoclonal antibody was then purified from the supernatant by sequential chromatography. (Paragraph Nos. 0434 - 0436.)

8. We analyzed the oligosaccharide structures of the purified antibody by enzymatically cleaving the oligosaccharides from the antibodies by PNGaseF digestion and, optionally, EndoH glycosidase digestion. The enzymatic digests containing the released oligosaccharides were subsequently analyzed by MALDI/TOF-MS. (Paragraph Nos. 0437-0446.)

9. The oligosaccharide profile of the anti-CD20 antibody cocxpressed with hManII and the relative percentages of the structures found associated to the Fc portion of the antibody are shown in FIG. 34. As noted in the application, the oligosaccharides found associated to the Fc portion of the antibody are complex structures, 48% of which lack core fucose. The α-Mannosidase II competes with the core-fucosyltransferase, generating 48% non-fucosylated oligosaccharide structures. In the absence of α-Mannosidase II, the oligosaccharides of the Fc portion of the antibody are composed of only fucosylated structures (wild-type antibody). (*See* Paragraph No. 0448).

10. The oligosaccharide profile of the anti-CD20 antibody coexpressed with the hManII-GalT fusion protein is shown in FIG. 35A-B. Antibody produced in the presence of hManII-GalT shows almost 100% non-fucosylated structures. (Paragraph No. 0449.)

11. We also assayed antibodies produced in the presence of hManII or hManII-GalT fusion protein for binding to Fc receptors and ADCC activity. The binding assay experiment utilized the cell line CHO-1708-37, which expresses on its surface the FcγRIIIA receptor (CD16) and the γ chain of the FcγRI receptor. The expression of the FcγRIIIA receptor was assessed by FACS analysis using the 3G8-FITC monoclonal antibody. As shown in FIG. 36, the anti-CD20 antibody produced in the presence of α-

Mannosidase II binds to the FcγRIIIA receptor with higher affinity than the wild-type antibody that was not produced in the presence of ManII. (Paragraph No. 0457.)

12. Exhibit C is a manuscript that I and my colleagues have submitted to the journal Biotechnology & Bioengineering for publication. It is currently being reviewed. The title of the manuscript is "Modulation of Therapeutic Antibody Effector Functions by Glycosylation Engineering." In general, it describes the generation of anti-CD20 antibody glycovariants by coexpression in a host cell of GnT-III or chimeric GnTIII proteins.

13. In these studies, we analyzed two anti-CD20 antibodies produced either by 1) coexpression with a fusion protein comprising the catalytic domain of human GnTIII fused to the Golgi localization domain of human Mannosidase II (termed "Glyco-1 antibodies") or by 2) coexpression with the GnT-III/ManII fusion construct and a gene encoding ManII ("Glyco-2") for their affinity for FcγRIIIa compared to either the unmodified (i.e., not glycoengineered) antibody, or to an antibody glycovariant produced under the same conditions by co-expression of GnT-III ("Glyco-0"). (Page 5, right hand column.)

14. We evaluated the binding of the glycoengineered antibodies to FcγRIIIA on peripheral human natural killer (NK) cells, which are known to be important mediators of ADCC, and to constitutively express FcγRIIIA. Both Glyco-1 and Glyco-2 were found to bind with a considerably higher affinity to NK cells than unmodified antibody. (*See* FIG. 5A). The Glyco-0 antibody produced by wild-type GnT-III coexpression was found to have intermediate FcγRIIIA binding affinity between that of the unmodified antibody and Glyco-1/Glyco-2. (Page 5, right hand column.)

15. Exhibit D shows the results of a study we conducted to determine the effect of constitutive coexpression of recombinant, wild-type β1,4-N-acetylglucosaminyltransferase III (GnT-III) *and* Golgi α-mannosidase II (ManII) in stable, industrial grade CHO cells on a recombinant anti-CD20 antibody produced by those cells.

16. FIG. 1 of Exhibit D shows the glycosylation profile (as determined by MALDI/TOF-MS) for the Fc-region oligosaccharides of a nonglycoengineered recombinant antibody produced in CHO cells. The level of nonfucosylated oligosaccharides is below 10%, which is typical for a nonglycoengineered antibody produced by CHO cells.

17. FIG 2 of Exhibit D shows the glycosylation profile for the Fc-region oligosaccharides of a *glycoengineered* anti-CD20 antibody produced in CHO cells. The glycoengineered antibodies had significantly increased levels of nonfucosylated oligosaccharides relative to the nonglycoengineered antibodies. In particular, peaks at m/z 1339, 1543 and 1705 correspond to nonfucosylated, complex oligosaccharides, which represent over 70% of the total oligosaccharides.

18. FIG. 3 of Exhibit D depicts the binding to FcγRIII receptors achieved by the glycoengineered antibodies compared to the nonglycoengineered antibodies. Substantially increased binding to FcγRIII receptors was observed for the glycoengineered antibody.

19. FIG. 4 of ExhibitD depicts the increased antibody-dependent cellular cytotoxicity observed for a glycoengineered antibody with increased levels of nonfucosylated Fc-region oligosaccharides compared to the nonglycoengineered antibody.

20. Thus, the attached Exhibits show that anti-CD20 antibodies coexpressed either with wild-type hManII or wild-type GnT-III or wild-type GnTIII *and* wild-type ManII have substantially increased affinity for the FcγRIIIA receptor compared to the corresponding nonglycoengineered antibody. This demonstrates that the techniques taught in the present application can be used to produce glycoengineered antibodies having increased binding affinity for Fc receptors.

21. The undersigned further declares that all statements made herein of his knowledge are true, and that all statements made on information and belief are believed to be true, and that these statements were made with the knowledge that willful false statements or the like so made are punishable by fine, imprisonment, or both under § 1001 of Title 18, United States Code, and that such willful false statements may jeopardize the validity of any patent application or patent issued thereon.

July 15, 2005
Date

Pablo Umaña, Ph.D.

CURRICULUM VITAE

Dr. Pablo Umaña

GlycArt Biotechnology AG
Einsteinstrasse
Zurich 8093, Switzerland
Email: pablo.umana@glycart.com

PROFILE

Scientific researcher experienced in molecular biology, biochemistry, immunology, cell biology and gene therapy, with an emphasis in the field of antibody glycosylation. Obtained PhD from the California Institute of Technology (carrying out a major part of the experimental work at the ETH-Zurich). Carried postdoctoral research in gene therapy vectors at the University of Manchester, U.K. Co-founder of GlycArt Biotechnology AG, Zurich, a company spinning out of research carried out at the ETH-Zurich during doctoral studies. Joined GlycArt Biotecnhology AG as a full-time employee in 2001 as Chief Scientific Officer.

EDUCATION

1993-1998. **California Institute of Technology/ ETH-Zurich.** PhD from Caltech, experimental work carried out at the ETH-Zurich. Thesis: Genetic engineering of protein glycosylation in Chinese hamster ovary cells.

1991-1993. **California Institute of Technology**. MSc. Thesis: Genetic engineering of protein glycosylation in the insect cell/baculovirus expression system.

1985-1990. **University of Costa Rica**. Licenciatura in Chemical Engineering.

ACADEMIC HONORS

Top Engineering Student Award. University of Costa Rica, 1988.

PUBLICATIONS

Umaña, P., Gerdes, C.A., Stone, D., Davies, J.R.E., Ward, D., Castro, M.G. and Lowenstein, P.R.. 2001. Efficient FLPe recombinase enables scalable production of helper-dependent adenoviral vectors with negligible helper-virus contamination. *Nature Biotechnology* 19: 582-585.

Umaña, P.,Jean-Mairet, J., and Bailey, J.E. 1999. Tetracycline-Regulated Overexpression of Glycosyltransferases in CHO Cells. *Biotechnology and Bioengineering* 65: 542-549.

Umaña, P., Jean-Mairet, J., Moudry, R., Amstutz, H., and Bailey, J.E. 1999. Engineered Glycoforms of an Anti-Neuroblastoma IgG1 with Optimized Antibody-Dependent Cellular Cytotoxic Activity. *Nature Biotechnology* 17: 176-180.

Sburlati, A., Umaña, P., Prati, E. and Bailey, J.E. 1998. Synthesis of Bisected Glycoforms of Recombinant IFN-Beta by Overexpression of GnTIII in Chinese Hamster Ovary Cells. *Biotechnology Progress* 14: 189-192.

Umaña, P. and Bailey, J.E. 1997. A Mathematical Model of N-linked Glycoform Biosynthesis. *Biotechnology and Bioengineering* **55**: 890-908.

Lowenstein, P.R.. Thomas, C.E., Umaña, P., Gerdes, C.A., Verakis, T., Boyer, O., Tondeur S., Klatzmann D. and Castro, M.G. 2002. High-capacity, helper-dependent, "gutless" adenoviral vectors for gene transfer into brain. *Methods in Enzymology* 346: 292-311.

Bailey, J. E., Umaña, P., Minch, S., Harrington, M., Page, M., and Sburlati, A. 1997. Metabolic Engineering of N-linked Glycoform Synthesis Systems in Chinese Hamster Ovary Cells. In: Animal Cell Technology, Kluwer, p. 489-494.

Umaña, P., Kellis, J.T. and Arnold, F.H. 1993. Recombinant Protein Stabilization through Engineered Metal-Chelating Sites. In: Biocatalyst Design for Stability and Specificity, ACS Sysmposium Series **516**: 102-108.

SUPERVISORY/TEACHING EXPERIENCE

Chief Scientific Officer (GlycArt Biotechnology AG, 2001-present)
Supervision of a Diploma project (ETH-Zürich, 1995-1996).
Teaching assistant for Enzyme Technology practical course (ETH-Zürich, 1995).
Teaching assistant for Experimental Physical Chemistry (1989), Thermodynamics (1988-1991), and Reaction Kinetics and Reactor Design (1990) at the University of Costa Rica.

PERSONAL DETAILS

Date of Birth: 23.09.67; Nationality: Costa Rican; Marital Status: married.
Fluent in written and spoken English. Mother tongue: Spanish.

RESEARCH PROJECTS

2001 – present. Chief Scientific Officer:	Engineering therapeutic antibody glycosylation GlycArt biotechnology AG, Zürich.
1999 – 2001. Postdoctoral Research:	Development of a new production system for helper-dependent, fully-deleted adenoviral vectors Anti-angiogenic gene therapy for intracranial tumors.
Supervisor: Prof. Pedro R. Lowenstein.	University of Manchester, U.K.
1993-1998. PhD Project:	Genetic engineering of protein glycosylation in CHO cells
Supervisor: Prof. James E. Bailey	California Institute of Technology/ETH-Zurich
1992-1993. MSc Project:	Genetic engineering of protein glycosylation in the insect cell/ baculovirus expression system
Supervisor: Prof. James E. Bailey	California Institute of Technology
1991 Summer Project:	Recombinant protein stabilization by engineered metal chelating sites
Supervisor: Prof. Frances H. Arnold	California Institute of Technology

MODULATION OF THERAPEUTIC ANTIBODY EFFECTOR FUNCTIONS BY GLYCOSYLATION ENGINEERING:

Influence of Golgi enzyme localization domain and co-expression of heterologous β1,4-N-acetylglucosaminyltransferase III and Golgi α-mannosidase II

Ferrara C.[1,2], Brünker P.[1], Suter T.[1,3], Moser S.[1], Püntener U.[1], Umaña P.[1]
1 Glycart Biotechnology AG, Wagistrasse 18, CH-8952 Schlieren, Switzerland
2 Institute of Biotechnology, ETH Zürich, CH-8093 Zürich, Switzerland

Running Title: MODULATION OF THERAPEUTIC ANTIBODY EFFECTOR FUNCTIONS BY GLYCOSYLATION ENGINEERING

Address correspondence to: Pablo Umaña, Glycart Biotechnology AG, Wagistrasse 18, CH-8952 Schlieren-Zurich, Switzerland, Tel.+41 1 755 61 61; Fax. +41 1 755 61 60; E-mail: pablo.umana@glycart.com

3 Current address: Section of Clinical Immunology, University Hospital, CH-8044 Zürich, Switzerland

The effector functions elicited by IgG antibodies strongly depend on the carbohydrate moiety linked to the Fc region of the protein. Therefore several approaches have been developed to rationally manipulate these glycans and improve the biological functions of the antibody. Overexpression of recombinant β1,4-N-acetylglucosaminyl-transferase III (GnT-III) in production cell lines leads to antibodies enriched in bisected oligosaccharides. Moreover, GnT-III over-expression leads to increases in non-fucosylated and hybrid oligosaccharides. Such antibody glycovariants have increased antibody-dependent cellular cytotoxicity (ADCC). To explore a further variable besides overexpression of GnT-III, we exchanged the localization domain of GnT-III with that of other Golgi-resident enzymes. Our results indicate that chimeric GnT-III can compete even more efficiently against the endogenous core α1,6-fucosyltransferase (α1,6-FucT) and Golgi α-mannosidase II (ManII) leading to higher proportions of bisected non-fucosylated hybrid glycans ("Glyco-1" antibody). The co-expression of GnT-III and ManII led to a similar degree of non-fucosylation as that obtained for Glyco-1, but the majority of the oligosaccharides linked to this antibody ("Glyco-2") are of the complex type. These glycovariants feature strongly increased ADCC activity compared to the unmodified antibody, while Glyco-1 (hybrid-rich) features reduced CDC compared to Glyco-2 or unmodified antibody. We show that apart from GnT-III overexpression, engineering of GnT-III localization is a versatile tool to modulate the biological activities of antibodies relevant for their therapeutic application.

Antibodies of the IgG class have proven to be useful anticancer therapeutics (1). Their high specificity for an antigen, for targeting a cancerous cell, and the simultaneous recruitment of immune effector cells, by binding to Fcγ receptors (FcγRs) *via* their Fc region, make them a powerful tool for immunotherapies. This linker function of the antibodies results in the elimination of the cancerous cell by cell-mediated effector functions, such as antibody-dependent cellular cytotoxicity (ADCC).

Many therapeutic antibodies depend on Fc-mediated effector functions and it was concluded that they require a higher *in vivo* efficacy to increase their potential as therapeutic drugs. The recruitment of FcγR-expressing cells relies on an efficient binding to the Fc region of IgG (2). The affinity of this interaction can be improved by amino acid mutations of the polypeptide (3), which bear the risk of immunogenicity. On the other hand the presence of specific oligosaccharide structures linked to the Cγ2 domain of the Fc fragment was reported

to affect the biological activity of the antibody (4, 5, 6) by influencing the interaction with Fcγ receptors (7). In this context, modification of the carbohydrate moiety associated to the Fc region of IgG has proven to be a successful approach to enhance ADCC (8, 9, 10).

Recombinant DNA-based glyco-engineering for increased antibody effector function was first achieved by overexpression of heterologous β1,4-N-acetylglucosaminyl-transferase III (GnT-III), in antibody-producing cells (8). GnT-III catalyzes the addition of a bisecting N-acetylglucosamine (GlcNAc) to N-linked oligosaccharides, as long as they have been modified by N-acetylglucosaminyltransferase I (GnT-I) and have not been modified by β1,4 galactosyltransferase (GalT, FIG. 1). Once a glycan is bisected, other central reactions of the biosynthetic pathway such as core-fucosylation and conversion of hybrid to complex glycans are blocked (11, FIG. 1). This gives GnT-III a high degree of control over the the glycosylation process in the Golgi apparatus. Overexpression of GnTIII in antibody-producing cells results in the formation of bisected, non-fucosylated oligosaccharides linked to the antibodies that mediate increased ADCC (8, 9, 10).

Previously, we have shown that the GnT-III expression level has a large impact on the relative levels of complex and hybrid, fucosylated or non-fucosylated oligosaccharides (8). Besides the expression level, the Golgi localization domain of GnT-III, which controls its spatial distribution relative to other enzymes, is another variable influencing the impact of GnT-III on the glycosylation pathway (12). Here we explore the localization variable by fusing the catalytic domain of GnT-III to the localization domain (cytoplasmic, transmembrane and stem region) of other Golgi-resident enzymes of the N-glycosylation pathway. The resulting chimeric proteins were expressed in antibody-producing cells to engineer the antibody glycosylation pattern and the associated antibody effector functions.

EXPERIMENTAL PROCEDURES

Construction of expression vectors - The DNA for the variable heavy (VH) and variable light (VL) chain of the anti-CD20 antibody was assembled by polymerase chain reaction (PCR) on the basis of the published sequence of the murine C2B8 antibody (13, 14). The IgG1 constant regions were amplified from a human leukocyte cDNA library (BD Biosciences, Allschwil/Switzerland). The rat GnT-III gene was amplified using specific primers from a rat kidney cDNA library (BD Biosciences, Allschwil/Switzerland) and a sequence coding for a C-terminal c-myc-epitope tag was added. The construction of the GnT-III-chimeric genes was performed by subsequent overlapping PCR reactions. The DNA fragments coding for the localization domains (cytoplasmic, transmembrane and stem regions) of human GnT-I (102 amino acids), ManII (100 amino acids), GnT-II (103 amino acids) and α1,6-FucT (101 amino acids) were amplified from different material of human origin using the specific primers. The gene coding for Golgi α-mannosidase II was amplified by PCR from human DNA using specific primers. The gene coding for the human N-acetylglucosaminyltransferase II (GnT-II) was amplified from pGnTII (RG002551, Invitrogen AG, Basel/Switzerland) by polymerase chain reaction (PCR) using specific primers. The construction of the catalytically inactive GnT-III^{ManII} (iGnT-III^{ManII}) was performed as described (15). The construction of two mutant GnT-III^{mutManII} was accomplished by site-directed PCR mutagenesis, where the mutations R60Q, R73N, L79S and E81S (GnT-III$^{mutManII(4aa)}$) or R73N, L79S and E81S (GnT-III$^{mutManII(3aa)}$) were introduced into ManII (12). All expression vectors were combined with an origin of replication from the Epstein Barr virus (oriP) for episomal vector replication and maintenance in cells producing the Epstein Barr virus nuclear antigen (EBNA). Expression of the protein was confirmed by western blot detection of GnT-III C-terminal c-myc tag.

For the generation of the FcγRIIIa-expressing CHO cell line, an expression vector for FcγRIIIa-Val158 α-chain, γ-chain and the gene conferring puromycin resistance was constructed. The cDNAs coding for the FcγRIIIA and the γ-chain were amplified from a healthy donor using specific primers. Genotyping for the FcγRIIIA-Val/Phe158 and FcγRIIC polymorphisms were performed as described (16, 17).

Production and purification of glyco-engineered anti-CD20 antibodies in HEK293-EBNA cells - HEK293-EBNA cells, a kind gift from Rene Fischer (Laboratory of Organic Chemistry, ETH Zürich, Switzerland), were grown as adherent monolayer cultures using DMEM culture medium supplemented with 10% FCS (Invitrogen AG,

Basel/Switzerland) and were transfected essentially as described (18). Glyco-engineered antibodies were produced by co-transfection of the cells with two plasmids coding for antibody and chimeric GnT-III, at a ratio of 4:1 respectively, while for unmodified antibody the plasmids coding for the carbohydrate-modifying enzymes were omitted. For the combination of the chimeric GnT-III^{ManII} and ManII (or GnT-II), cells were co-transfected with three expression vectors coding for antibody, GnT-III^{ManII} and ManII (or GnT-II) at a ratio of 3:1:1. At day 5 post-transfection, supernatant was harvested and monoclonal antibody purified using two sequential chromatographic steps as described (8), followed by size exclusion chromatography (HiLoad™ 16/60 Superdex™ 200 column, Amersham Biosciences, Otelfingen/Switzerland).

Oligosaccharide analysis - Oligosaccharides were enzymatically released from the antibodies by N-Glycosidase digestion (PNGaseF, EC 3.5.1.52, QA-Bio, San Mateo,CA/USA) at 0.05 mU/μg protein in 2 mM Tris, pH7 for 3 hours at 37°C. A fraction of the PNGaseF-treated sample was subsequently digested with Endoglycosidase H (EndoH, EC 3.2.1.96, Roche, Basel/Switzerland) at 0.8 mU/μg protein and incubated for 3 hours at 37°C. The released oligosaccharides were incubated in mild acid (150 mM acetic acid) prior to purification through a cation exchange resin (AG50W-X8 resin, hydrogen form, 100-200 mesh, BioRad, Reinach/Switzerland) packed into a micro-bio-spin chromatography column (BioRad, Reinach/Switzerland) as described (19). The oligosaccharide samples were then analyzed with sDHB as matrix (19) using an Autoflex MALDI/TOF (Bruker Daltonics, Faellanden/Switzerland) in positive ion mode. For the assignment of an oligosaccharide structure to each peak, Endoglycosidase H was used due to its specificity. It digests most hybrid and high mannose, but not complex oligosaccharides. Upon EndoH digestion, the peaks at m/z 1664 and 1810 shift to 1460, and those at 1826 and 1972 to 1622, confirming the increase in bisected, non-fucosylated hybrid (m/z 1664 and 1826) and their fucosylated versions (m/z 1810 and 1972) upon recombinant expression of GnT-III or chimeric GnT-III proteins (FIG. 3). A refined oligosaccharide analysis was necessary to distinguish between bisected hybrid and complex (m/z 1339 and 1502) and their fucosylated versions (m/z 1648 and 1810), as both structures are not digested by EndoH. For this purpose, EndoH analysis was combined with *in vitro* galactosylation of the whole antibody performed as described (20). The aim was to distinguish between hybrid or complex oligosaccharides by making use of the fact that hybrid oligosaccharides can be galactosylated only at one terminal GlcNAc residue. Although the *in vitro* galactosylation was not complete the majority of peaks of m/z 1339 and 1502 could be assigned to non-fucosylated, complex glycan structures, with only minor contribution of bisected, non-fucosylated hybrid structures (FIG. 3, Table I).

Binding of monomeric IgG1 glycovariants to NK cells and FcγRIIIa-expressing CHO cell line - Human NK cells were isolated from freshly isolated peripheral blood mononuclear cells (PBMC) applying a negative selection enriching for CD16- and CD56-positive cells (MACS system, Miltenyi Biotec GmbH, Bergisch Gladbach/Germany). The purity determined by CD56 expression was between 88-95 %. Freshly isolated NK cells were incubated in PBS without calcium and magnesium ions (3 x 10^5 cells/ml) for 20 minutes at 37°C to remove NK cell-associated IgG. Cells were incubated at 10^6 cells/ml at different concentrations of anti-CD20 antibody (0, 0.1, 0.3, 1, 3, 10 μg/ml) in PBS, 0.1% BSA. After two washes with PBS, 0.1% BSA antibody, binding was detected by incubating with 1:200 FITC-conjugated F(ab')$_2$ goat anti-human, F(ab')$_2$ specific IgG (Jackson ImmunoReasearch, West Grove, PA/USA) and anti-human CD56-PE (BD Biosciences, Allschwil/Switzerland, 9). The anti-FcγRIIIa 3G8 F(ab')$_2$ fragments (Ancell, Bayport, MN/USA) were added at a concentration of 10 μg/ml to compete binding of antibody glycovariants (3 μg/ml). Fluorescence intensity was determined for CD56-positive cells on a FACSCalibur (BD Biosciences, Allschwil /Switzerland) and refers to the geometric mean measured for different antibody concentrations, from which the geometric mean of cells incubated without primary antibody was subtracted.

CHO cells were transfected by electroporation (280 V, 950 μF, 0.4 cm) with an expression vector coding for the FcγRIIIa-Val158 α-chain and the γ-chain. Transfectants were selected by addition of 6 μg/ml puromycin and stable clones were analyzed by FACS using 10 μl FITC-conjugated anti-FcγRIII 3G8 monoclonal antibody (BD Biosciences, Allschwil/Switzerland) for 10^6 cells. Binding of

IgG1 to FcγRIIIa-Val158-expressing CHO cells was performed analogously to the NK cell binding described above by omitting CD56-staining.

Biological activities of anti-CD20 monoclonal antibodies glycovariants - Antibody-dependent cellular cytotoxicity (ADCC) assay: CD20-positive Raji cells (DMEM, 10% FCS, 1% Glutamax, Invitrogen AG, Basel/Switzerland) were labeled with the fluorescent dye Calcein AM for 20 min, according to the manufacturer's instruction (Molecular Probes, Leiden/The Netherlands). Antibodies were serially diluted in AIM-V (Invitrogen AG, Basel/Switzerland) and incubated with the target cells for 10 min at room temperature prior to the addition of effector cells. Peripheral blood mononuclear cells (PBMC) were prepared from a donor heterozygous for FcγRIIIa-Val/Phe158 and lacking FcγRIIc expression using Histopaque-1077 (Sigma-Aldrich, Buchs/Switzerland) following the manufacturer's instructions. These were added to the wells at an effector to target ratio of 25:1. After four hours incubation at 37°C, the cells were spun down, washed twice with PBS without calcium and magnesium ions and lysed by addition of 50 mM borate, 0.1% Triton X-100 solution. The content of the wells was subsequently transferred to a 96-well black flat-bottomed plate. Retention of the fluorescent dye by intact target cells was measured with a fluorometer (485 nm excitation, 520 nm emission, FLUOstar Optima, BMG Labtechnologies Inc., Durham/USA). Specific lysis was calculated relative to the total lysis control, resulting from incubating the target cells with 1% Triton X-100. Percentage of specific antibody-mediated cytotoxicity was calculated as follows: ((fluorescence at concentration x – fluorescence of Spontaneous Release)/(fluorescence Maximal Release – fluorescence Spontaneous Release)*100. Each antibody dilution was analyzed in quadruplicate.
Complement-dependent cytotoxicity (CDC) assay: CD20 positive human B lymphoblastoid SKW 6.4 cells (DMEM, 10% FCS, 1% Glutamax, Invitrogen AG, Basel/Switzerland) were incubated with increasing concentrations of antibody for 10 minutes at room temperature prior to the addition of normal human serum (NHS, FcγRIIIA-Val158 and FcγRIIC homozygous donor), prepared from the blood of healthy volunteers, as source of complement. The blood was allowed to coagulate for one hour at room temperature and then centrifuged at 1200xg for 20 min. The serum was diluted 3-fold with AIM-V and added to the wells to obtain a final concentration of 20% NHS. The assay plates were incubated for two hours at 37°C. Maximal release was determined by incubating the cells in the presence of 1% Triton X-100. Relative cytotoxicity was determined using the alamarBlue™ Assay (Serotec Inc, Düsseldorf/Germany). Fluorescence was monitored on a fluorometer (540 nm excitation, 590 nm emission, FLUOstar Optima, BMG Labtechnologies Inc., Durham/USA). Each antibody concentration was measured in quadruplicate.
Whole blood B cell depletion assay: 490 µl heparinized blood from a healthy FcγRIIIA-Val/Phe158 and FcγRIIC negative donor, was incubated at 37°C with 10 µl PBS or 50-fold concentrated antibody glycovariants (final concentrations of 0.1, 1, 10, 100, 1000 ng/ml). After 24 hours 50 µl blood were stained with a mixture of anti-CD19-PE, anti-CD3-FITC and anti-CD45-CyChrome (BD Biosciences, Allschwil/Switzerland) for 15 min at room temperature. Before analysis, 500 µl PBS containing 2% FCS and 5mM EDTA were added to the tubes. The CD3-FITC and CD19-PE fluorescence of the blood samples were flowcytometrically analyzed by gating on all CD45-positive cells. B cell-depletion was determined by plotting the ratio of CD19-positive B cells to CD3-positive T cells. Each antibody concentration was analyzed in triplicate.

RESULTS

Generation of anti-CD20 antibody glycovariants achieved by co-expression of GnT-III or chimeric GnT-III proteins

Modulation of antibody glycosylation was achieved by co-expression of the genes coding for antibody and chimeric GnT-III proteins in HEK293-EBNA cells. In the chimeric proteins, the localization domain of GnT-III was replaced with those of various other Golgi-resident enzymes of the N-linked glycosylation pathway (FIG. 2). The oligosaccharide profiles obtained for the expressed antibodies indicate a significant impact of the enzyme localization on the outcome of the glycosylation process (FIG. 3). The use of the localization domain of GnT-I, α1,6-FucT, GnT-II or ManII, instead of that of GnT-III results in an increase in the proportion of bisected non-fucosylated hybrid oligosaccharides linked to the secreted antibody.

Among these chimeric proteins, GnT-III fused to the localization domain of ManII (GnT-III^{ManII}) leads to the highest content of these carbohydrates (Table I, FIG. 3).

To assess if the localization domain of ManII itself and not the enzymatic activity of the catalytic domain of GnT-III accounts for any of the oligosaccharide modifications, a catalytically inactive GnT-III^{ManII} chimeric protein was prepared by replacing residues Asp321 and Asp323 of GnT-III by alanine residues (15) (FIG. 2). This inactive chimeric protein did not influence the carbohydrate pattern, which was that of an unmodified antibody (FIG. 3). To ascertain if a different expression level of the enzymes may account for the differences in the oligosaccharide patterns, the expression of GnT-III was quantified by western blot analysis *via* a C-terminal c-myc tag (FIG. 4). Both GnT-III^{ManII} and GnT-III showed a slightly reduced expression compared to those of the other GnT-III chimeric proteins.

We also evaluated the hypothesis that the existence of relatively well organized functional glycosylation reaction subcompartments within the *medial* and *trans* Golgi cisternae may account for the glycosylation profiles derived from the chimeric GnT-III proteins. Given that pairs of charged amino acid residues in the stem regions of GnT-I and ManII have been postulated as critical for oligomer formation between enzymes (12), it was investigated if such a pairing could account for the GnT-III^{ManII}-derived antibody glycosylation profile. Therefore the amino acid mutations R73N, L79S and E81S (GnT-III$^{mutManII(3aa)}$) or R60Q, R73N, L79S and E81S (GnT-III$^{mutManII(4aa)}$) were introduced into the stem region of ManII (FIG. 2, 12). Both mutants were expressed in similar amounts (FIG. 4) and yielded antibody glycovariants featuring substantially reduced proportions of bisected non-fucosylated oligosaccharides compared to the non-mutated GnT-III^{ManII} (FIG. 3, Table I).

The co-expression of GnT-III^{ManII} and ManII or GnT-III and ManII (FIG. 3) was also explored with the intention to shift the biosynthetic pathway from hybrid to complex bisected oligosaccharides (FIG. 1). The expression of both enzyme combinations lead to the generation of antibodies characterized by high proportions of complex type glycans lacking core-fucosylation, with the majority being bisected (FIG. 3, Table I). GnT-III^{ManII} was also co-expressed with GnT-II, an enzyme that similarly to ManII directs the glycosylation pathway toward the formation of complex type glycans. This led to the accumulation of high mannose structures and a low proportion of bisected non-fucosylated oligosaccharides (data not shown) and this enzyme combination was not investigated further.

Two glyco-engineered antibodies, namely those produced either by transient co-expression with GnT-III^{ManII} (termed "Glyco-1", bearing mainly hybrid non-fucosylated bisected glycans) or with GnT-III^{ManII} and ManII ("Glyco-2", bearing mainly complex non-fucosylated bisected glycans), were examined for their affinity for FcγRIIIa and compared either to the unmodified antibody or to an antibody glycovariant produced under the same conditions by transient co-expression of GnT-III ("Glyco-0").

FcγRIIIa binding of Glyco-0, Glyco-1 and Glyco-2 anti-CD20 monoclonal antibodies

Binding of glyco-engineered antibodies to FcγRIIIa was evaluated on peripheral human natural killer (NK) cells, which are known to be important mediators of ADCC, and to constitutively express FcγRIIIa. Binding to NK cells was performed by incubating the antibody glycovariants with freshly isolated NK cells from a donor who was genotyped as heterozygous for FcγRIIIA-Val/Phe158 (16). Both Glyco-1 and Glyco-2 bind with a considerably higher affinity to NK cells than unmodified antibody (FIG. 5A). Under the transient gene expression levels of this study, GnT-III co-expression leads to an antibody (Glyco-0) with a lower level of bisected non-fucosylated oligosaccharides with intermediate FcγRIIIa binding affinity. Antibody binding to NK cells occurred exclusively *via* FcγRIIIa as it could be outcompeted by the addition of blocking anti-FcγRIIIa F(ab')$_2$ fragments (FIG. 5B). Similar results were obtained using a recombinant CHO cell line stably expressing the FcγRIIIa-Val158 α-chain receptor (FIG. 5C).

Biological activities of Glyco-1 and Glyco-2 anti-CD20 monoclonal antibodies

In a next step we investigated whether increased FcγRIIIa binding correlates with an improvement in the biological activities of the glyco-engineered antibodies, which are characterized by bisected non-fucosylated oligosaccharides. Both glycovariants mediate an enhanced antibody-dependent cellular cytotoxicity (ADCC) against CD20-positive Raji

cells, independently of the Fc-linked glycans being of complex or hybrid type (FIG. 6A).

Glyco-1 and Glyco-2 were also evaluated for complement-dependent cytotoxicity (CDC) against CD20-positive tumor cells SKW6.4 in the presence of human serum (FIG. 6B). Glyco-2, bearing complex oligosaccharides, performs similarly to the unmodified antibody in CDC. For Glyco-1, on the contrary, a reduction in CDC is observed, correlating with high proportion of hybrid oligosaccharides that are characteristic for this glycovariant.

To asses whether both ADCC and CDC can contribute to the elimination of target cells, we evaluated these glyco-engineered antibodies for B cell depletion in a whole blood assay (FIG. 6C). Glyco-1 and Glyco-2 anti-CD20 variants were over 100-fold more potent than unmodified anti-CD20 in depleting B cells, while no significant difference could be observed between the two glycovariants, indicating a minor contribution of CDC.

DISCUSSION

Chimeric GnT-III proteins

GnT-III is an ideal enzyme to manipulate the N-glycosylation of expressed proteins (glyco-engineering), as it exerts a large degree of control over the glycosylation process by blocking the action of α1,6-FucT, ManII and GnT-II (8, 11). In the present study the impact of the localization domain of GnT-III on the antibody glycosylation profile was evaluated. We obtained antibodies with engineered carbohydrate moieties by co-expression of chimeric GnT-III proteins, composed of the catalytic domain of GnT-III fused to the localization domain of GnT-I, α1,6-FucT, GnT-II, or ManII (FIG. 2). The resulting glycovariants feature a bisecting N-acetylglucosamine (GlcNAc) residue on almost all oligosaccharide structures, indicating that all chimeric GnT-III proteins were active (Table I, FIG. 3). These glycovariants are also characterized by a high proportion of non-fucosylated oligosaccharides, indicating a more efficient competition against α1,6-FucT for GnT-I-processed glycans, and of hybrid glycans, which are by-products of GnT-III expression resulting from its competition against ManII (FIG. 1).

Among the chimeric GnT-III proteins, GnT-III^{ManII} is the most efficient in the competition against the above mentioned enzymes, leading to the antibody glycovariant with the highest proportion of bisected non-fucosylated hybrid oligosaccharides. The oligosaccharide modifications derived from GnT-III^{ManII} were solely dependent on the enzymatic activity of GnT-III, as shown by co-expression of a catalytically inactive iGnT-III^{ManII}. Since the expression level of GnT-III^{ManII} was not higher than for the other chimeric proteins or GnT-III, we propose that the higher efficiency of GnT-III^{ManII} results either from a different distribution in Golgi compartments or from a different functional organization of enzymes within a compartment. This allows GnT-III to act immediately after GnT-I, leading to higher levels of bisected, non-fucosylated hybrid oligosaccharides (FIG. 1) relative to the other chimeric GnT-III proteins.

Influence of the ManII stem region residues on the glycosylation pattern

The higher efficiency of the chimeric protein GnT-III^{GnT-I}, compared to the unmodified GnT-III, for the synthesis of bisected hybrid and bisected non-fucosylated oligosaccharides can be explained by an earlier Golgi distribution, in the *cis*-to-*trans* direction of glycoprotein substrate transport, of GnT-I relative to GnT-III. The fine Golgi distributions of GnT-I and ManII have been determined previously by quantitative immunoelectron microscopy (21). Both enzymes co-distribute along the Golgi, being localized mainly in the medial and *trans* cisternae (21, 22, 23). The fine quantitative spatial distributions of α1,6-FucT and GnT-II have not yet been determined, but rat GnT-III has been found predominantly in the *trans* Golgi cisternae (24). This, however, does not explain why the chimeric GnT-III^{ManII} is significantly more efficient than GnT-III^{GnT-I} at synthesizing bisected, hybrid and bisected, non-fucosylated oligosaccharides, since both GnT-I and ManII have identical spatial distributions along the Golgi subcompartments. Additionally, the slightly lower expression level of GnT-III^{ManII} compared to those of the other chimeric GnT-III proteins, indicates that the antibody glycoprofile is not a result of an increased enzyme expression level (FIG. 4) but a consequence of a more efficient processing of GnT-I-modified oligosaccharides, denoted here as "functional pairing" of GnT-III^{ManII} with GnT-I.

To assess if this functional pairing relies on a physical interaction between the two enzymes, we evaluated GnT-III^{ManII} mutants with amino acid substitutions in the localization domain of ManII which were reported to be critical determinants for the formation of hetero-

oligomers of GnT-I and ManII (12). Although it has been suggested that these residues are not essential for incorporation into high molecular weight complexes of Golgi enzymes or even for Golgi localization (25), it is possible that they are involved in a finer pairing of the catalytic domains during oligosaccharide biosynthesis. We observed a significant reduction in bisected non-fucosylated hybrid oligosaccharides with these mutants (FIG. 3). Both GnT-III^{mutManII} mutants were expressed at comparable levels as GnT-III^{ManII}, excluding the expression level of the latter as being responsible for higher proportions of bisected non-fucosylated glycans (FIG. 4). However, the exchanged residues do not seem to be the sole determinant of the resulting oligosaccharide product distribution, suggesting either additional contributions of the rest of the stem or catalytic regions to functional enzyme pairing, or an enrichment of these enzymes in subcompartments caused by different mechanisms. Altogether these data indicate that by virtue of the ManII localization domain, a physical and/or a functional pairing seems to take place between the catalytic domains of the endogenous GnT-I and the recombinant GnT-III^{ManII} chimeric protein.

Co-expression of GnT-III^{ManII} and ManII

With the described approach, we are able to modulate the glycosylation pattern of antibodies from fucosylated complex glycans to bisected non-fucosylated hybrid oligosaccharides by overexpressing GnT-III^{ManII}. The co-expression of GnT-III^{ManII} and ManII or of GnT-III and ManII led to the formation of bisected non-fucosylated glycans of the complex type. ManII overexpression redirects the biosynthetic pathway causing the product shift from hybrid to complex carbohydrates (FIG.1). Although equally high levels of bisected non-fucosylated complex oligosaccharides can be synthesized by high level expression of GnT-III, the results presented here show that GnT-III^{ManII} is more efficient at adding a bisecting GlcNAc residue to the GnT-I-processed oligosaccharides prior to the reactions catalyzed by ManII, GnT-II and α1,6-FucT.

Similarly to ManII, GnT-II was co-expressed with GnT-III^{ManII} with the intent of forming complex type glycans linked to the antibody. The resulting glycovariant had lower proportions of bisected non-fucosylated (37%) and complex (22%) glycans compared to the GnT-III^{ManII}/ManII-derived antibody (data not shown). Moreover, a significant fraction of high mannose oligosaccharides characterized this glycovariant, suggesting an influence of the overexpression of GnT-II on the maturation process of high mannose glycans. Under these conditions, the enzyme seems to inhibit the GnT-I-mediated reaction (FIG.1) by unknown mechanisms. A similar phenomenom was reported for overexpression of β1,4-galactosyltransferase (GalT), which led to an enrichment of high mannose oligosaccharides on recombinantly co-expressed IFN-γ (26). Although the cellular localization of GnT-II is yet to be discovered, high molecular weight complexes between GnT-I and GnT-II have been found in Golgi extracts of mammalian cells (25). The formation of such complexes might be disturbed by GnT-II overexpression.

We could show that the formation of a desired carbohydrate profile can be achieved by the combination and overexpression of enzymes, although not all the potential enzymes are suitable for this purpose, indicating that the glycosylation process is governed by a well-balanced system of enzymes that needs further elucidation.

Biological activity of glyco-engineered antibodies

A high affinity to FcγRIIIa is important for ADCC, which is mediated by unconjugated therapeutic antibodies in humans. This was deduced from pioneering pharmacogenomic studies evaluating the impact of the FcγRIIIA polymorphisms on the activity of rituximab in lymphoma patients (27). In that study, the objective response rates at two/twelve months were 100/90% for homozygous FcγRIIIA-Val158 and 67/51% for FcγRIIIA-Phe158 carriers respectively. The superior response of the former seems to be the result of a significantly increased binding of the antibody to FcγRIIIa-Val158 compared to FcγRIIIa-Phe158 (16).

Glyco-1, featuring mainly bisected non-fucosylated hybrid glycans, and Glyco-2, bearing mainly bisected non-fucosylated complex carbohydrates, were examined for their binding to FcγRIIIa and their reactivity in cytotoxicity assays. Both Glyco-1 and Glyco-2 have an increased affinity for FcγRIIIa, which correlates with high proportions of bisected non-fucosylated oligosaccharides but seems independent of the glycans being of the hybrid or complex type. It has been reported that the absence of core fucose is responsible for an

increased affinity to FcγRIIIa (9). Moreover, the absence of core fucose but not the presence of galactose or bisecting GlcNAc was reported to be responsible for increased ADCC under the tested conditions (10).

Both Glyco-1 and Glyco-2 mediate an increased ADCC to a similar extent compared to the unmodified antibody, but feature a different reactivity in CDC assays. While Glyco-2 acts similarly to the unmodified antibody, Glyco-1 displays a reduced CDC, suggesting a significant influence of the glycan type (complex vs. hybrid). The main difference between Glyco-1 and Glyco-2 is the structure of their carbohydrate α1,6-arm. In contrast to Glyco-1, carrying hybrid glycans with mannose residues α1,3- and α1,6-linked to the α-6 arm, Glyco-2 and unmodified antibodies have mainly β1,2-linked GlcNAc residues at this position (complex glycans), which may be followed by galactose. This carbohydrate arm is in close contact with the IgG-Cγ2 domain polypeptide and may therefore influence domain conformations required for binding to C1q (28, 29, 30). An even larger reduction in CDC was reported for antibodies featuring only high mannose oligosaccharides (31).

The glyco-engineered antibodies also performed better than their unmodified counterparts in the depletion of B-cells in a whole blood assay, where both ADCC and CDC contribute to the elimination of target cells. The reduction in CDC activity, observed for Glyco-1, does not seem to affect our model of B-cell depletion in whole blood, suggesting that ADCC is the predominant mechanism in this assay. Moreover as first-dose-related side-effects *in vivo* have been recently attributed to complement activation (32, 33), Glyco-1 may provide a tool to prevent these problems.

We could therefore demonstrate that apart from modulating glycosyltransferase expression levels, engineering of Golgi localization domains can also be exploited for the production of tailored glyco-engineered therapeutic antibodies with unique combinations of biological activities.

REFERENCES

1. Carter, P. (2001) *Nat. Rev. Cancer* **1**, 118-129
2. Dall'Ozzo, S., Tartas, S., Paintaud, G., Cartron, G., Colombat, P., Bardos, P., Watier, H., and Thibault, G. (2004) *Cancer Res.* **64**, 4664-4669
3. Shields, R.L., Namenuk, A.K., Hong, K., Meng, Y.G., Rae, J., Briggs, J., Xie, D., Lai, J., Stadlen, A., Li, B., Fox, J.A., and Presta, L.G. (2001) *J. Biol. Chem.* **276** (9):6591-604
4. Lifely, M.R., Hale, C., Boyce, S., Keen, M.J., and Phillips, (1995) *J. Glycobiology* **5**, 813-822
5. Jefferis, R., Lund, J., and Pound, J.D. (1998) *Immunol. Rev.* **163**, 59-76
6. Wright, A., and Morrison, S.L. (1997) *Trends Biotechnol.* **15**, 26-32
7. Tao, M.H., and Morrison, S.L. (1989) *J. Immunol.* **143**, 2595-2601
8. Umaña, P., Jean-Mairet, J., Moudry, R., Amstutz, H., and Bailey, J.E. (1999) *Nat. Biotechnol.* **17**, 176-180
9. Shields, R.L., Lai, J., Keck, R., O'Connell, L.Y., Hong, K., Meng ,Y.G., Weikert, S.H., and Presta, L.G. (2002) *J. Biol. Chem.* **277**, 26733-26740
10. Shinkawa, T., Nakamura, K., Yamane, N., Shoji-Hosaka, E., Kanda, Y., Sakurada, M., Uchida, K., Anazawa, H., Satoh, M., Yamasaki, M., Hanai, N., and Shitara, K. (2003) *J. Biol. Chem.* **278**, 3466-3473
11. Schachter, H. (1986) *Biochem. Cell Biol.* **64**, 163-181
12. Nilsson, T., Rabouille, C., Hui, N., Watson, R., and Warren, G. (1996) *J. Cell. Sci.* **109** (Pt 7), 1975-1989
13. Reff, M.E., Carner, K., Chambers, K.S., Chinn, P.C., Leonard, J.E., Raab, R., Newman, R.A., Hanna, N., and Anderson, D.R. (1994). *Blood* **83**, 435-445
14. Kobayashi, N., Soderlind, E., and Borrebaeck, C.A. (1997) *Biotechniques* **23**, 500-503
15. Ihara, H., Ikeda, Y., Koyota, S., Endo, T., Honke, K., and Taniguchi, N. (2002) *Eur. J. Biochem.* **269**, 193-201
16. Koene, H.R., Kleijer, M., Algra, J., Roos, D., von dem Borne, A.E., and de Haas, M. (1997) *Blood* **90**, 1109-1114
17. Metes, D., Gambotto, A.A., Nellis, J., Ruscin, A., Stewart-Akers, A.M., Morel, P.A., and Rao, A.S. (2001) *J. Immunol. Methods* **258**, 85-95
18. Jordan, M., Schallhorn, A., and Wurm, F.M. (1996) *Nucleic Acids Res.* **24**, 596-601

19. Papac, D.I., Briggs, J.B., Chin, E.T., and Jones, A.J. (1998) *Glycobiology* **8**, 445-454
20. Raju, T.S., Briggs, J.B., Chamow, S.M., Winkler, M.E., and Jones, A.J. (2001) *Biochemistry* **40**, 8868-8876
21. Rabouille, C., Hui, N., Hunte, F., Kieckbusch, R., Berger, E.G., Warren, G., and Nilsson, T. (1995) *J. Cell. Sci.* **108** (Pt 4):1617-1627.
22. Dunphy, W.G., Brands, R., and Rothman, J.E. (1985) *Cell* **40** (2):463-72
23. Velasco, A., Hendricks, L., Moremen, K.W., Tulsiani, D.R., Touster, O., and Farquhar, M.G. (1993) *J. Cell. Biol.* **122** (1):39-51
24. Umaña, P. 155 (California Institute of Technology, Pasadena, CA; 1998).
25. Fukuta, K., Abe, R., Yokomatsu, T., Minowa, M.T., Takeuchi, M., Asanagi, M., and Makino, T. (2001) *Arch. Biochem. Biophys.* **392** *(1)*:79-86
26. Opat, A.S., Houghton, F., and Gleeson, P.A. (2000) *J. Biol. Chem.* **275**, 11836-11845
27. Cartron, G., Dacheux, L., Salles, G., Solal-Celigny, P., Bardos, P., Colombat, P., and Watier, H. (2002) *Blood* **99**, 754-758
28. Huber, R., Deisenhofer, J., Colman, P.M., Matsushima, M., and Palm, W. (1976) *Nature* **264**(5585):415-420
29. Duncan, A.R., and Winter, G. (1988) *Nature* **332**(6166):738-740
30 Idusogie, E.E., Presta, L.G., Gazzano-Santoro, H., Totpal, K., Wong, P.Y., Ultsch, M., Meng, Y.G., and Mulkerrin, M.G. (2000) *J. Immunol.* **164**(8):4178-4184
31. Wright, A., and Morrison, S.L. (1994) *J. Exp. Med.* **180**(3):1087-1096
32. van der Kolk, L.E., Grillo-Lopez, A.J., Baars, J.W., Hack, C.E., and van Oers, M.H. (2001) *Br. J. Haematol.* **115**, 807-811
33. Winkler, U., Jensen, M., Manzke, O., Schulz, H., Diehl, V., and Engert, A. (1999) *Blood* **94**, 2217-2224

FOOTNOTES

We would like to thank Rene Fischer (Laboratory of Organic Chemistry, ETH Zürich, Switzerland) for providing the HEK293-EBNA cell line and Patrik Buholzer, Christian Gerdes, Samuel Haldane, Saskia Karg, Julia Maria Martinez, Peter Sondermann and Manuel Späni for assistance and useful comments on this manuscript.

FIGURE LEGENDS

FIG. 1. **N-linked oligosaccharide biosynthetic pathway leading to complex or hybrid structures bearing a bisecting GlcNAc.** The mass to charge (m/z) value of the sodium-associated oligosaccharide ion obtained by MALDI/TOF-MS analysis is indicated next to the corresponding oligosaccharide structure. The presence of a fucose (+f) α1,6-linked to the N-acetylglucosamine residue attached to Asn is indicated by the corresponding m/z value. The shaded monosaccharides belong to the core of the oligosaccharide, shared by all naturally occurring N-linked glycoforms, the presence of the other sugars is variable. A bisecting N-acetylglucosamine (grey) is β1,4 linked to the core mannose by the enzyme GnT-III. Complex and hybrid glycans structures are defined by the structure of the α1,6-arm.

FIG. 2. **N-acetylglucosaminyltransferase III (GnT-III) chimeric proteins.** GnT-III with different localization domains were constructed by fusing the catalytic domain of GnT-III (grey) to the localization domain CTS (white), consisting of cytoplasmic tail, transmembrane domain and stem region, of other Golgi-resident enzymes. The length of the respective regions is indicated. In the last three constructs single amino acid substitutions are indicated.

FIG. 3. **MALDI-TOF-MS spectra of neutral oligosaccharides from recombinant anti-CD20 IgG1 glycovariants.** The antibodies were produced in HEK293-EBNA cells engineered for expression of various forms of GnT-III (see FIG. 2). Furthermore, combinations of GnT-III^{ManII} with ManII or GnT-III with ManII were tested. Endoglycosidase H digestion (+ EndoH) and *in vitro* galactosylation (ivg)

were performed to refine the oligosaccharide analysis. The m/z value corresponds to the sodium-associated oligosaccharide ion.

FIG. 4. **Western blot detection of GnT-III.** 15 μg of cell lysates were separated on a 4-12% NU-PAGE gel (Invitrogen AG, Basel/Switzerland) and electroblotted to nitrocellulose membrane. Detection of GnT-III was performed *via* its C-terminal c-myc tag, while beta-actin detection served as an internal control for the amount of loaded extracts (Abcam Ltd, Cambridge/UK).

FIG. 5. **FcγRIIIa binding of monomeric anti-CD20 glycovariant antibodies.** Binding to purified NK cells from a donor heterozygous for FcγRIIIA-Val/Phe158 and negative for FcγRIIC was evaluated. A, Binding of antibodies at concentrations ranging from 0.1 to 10 μg/ml. B, Antibody binding (3 μg/ml) to FcγRIIIA was competed by addition of blocking anti-FcγRIIIa 3G8 F(ab')2 fragments (10 μg/ml). C, binding to a CHO cell line stably expressing human FcγRIIIa-Val158 α-chain and γ-chain was evaluated to confirm the dependence of antibody binding to FcγRIIIa. All assays were performed in quadruplicate. ○, unmodified; ●, Glyco-0; ▲, Glyco-1 and □, Glyco-2 antibodies.

FIG. 6. **Biological activity assays of anti-CD20 antibody glycovariants.** A, ADCC using PBMCs (FcγRIIIA-Val/Phe158, FcγRIIC negative donor) as effectors and human lymphoma Raji cells as targets. B, CDC against B lymphoblastoid SKW6.4 cells in the presence of human serum as a source of complement. C, B-cell depletion in whole blood (FcγRIIIA-Val/Phe158, FcγRIIC negative donor), which was calculated from the ratio of CD19-positive B cells to CD3-positive T cells as measured by FACS analysis. ○, unmodified; ▲, Glyco-1 and □, Glyco-2 antibodies.

TABLE I

Oligosaccharide distributions (relative percentages) of anti-CD20 monoclonal antibody glycoforms

	Unmodified	GnT-III	GnT-III^{GnT-I}	GnT-III^{GnT-II}	GnT-III$^{\alpha1,6\text{-}FucT}$	GnT-III^{ManII}	GnT-III$^{mutManII(3aa)}$	GnT-III$^{mutManII(4aa)}$	iGnT-III^{ManII}	GnT-III^{ManII} / ManII	GnT-III / ManII
high mannose	0.9	1.7	20.9	5.5	3.3		2.6	2.9	1.1		0.9
non-fuc, hybrid, bisected		21.6	64.7	52.1	65.0	90.2	55.8	62.0	1.6	17.5	3.2
fuc, hybrid, bisected		29.0	12.8	35.6	27.3	9.8	38.9	32.7		0.8	
non-fuc, complex, bisected										42.8	49.1
fuc, complex, bisected		42.1		1.3						15.6	25.7
non-fuc, complex	0.9								7.9	15.4	12.8
total bisected		92.7	77.5	89.0	92.3	100.0	94.7	94.7	1.6	76.7	78.0
total non-fuc		21.6	64.7	52.1	65.0	90.2	55.8	62.0	9.5	75.7	65.1
total non-fuc, complex	0.9								7.9	58.2	61.9
total complex	95.4	47.6	1.6	6.8	4.4		2.6	2.3	91.6	81.7	95.9

Designation according to FIG. 2.

Fuc, fucosylated

Figure 1

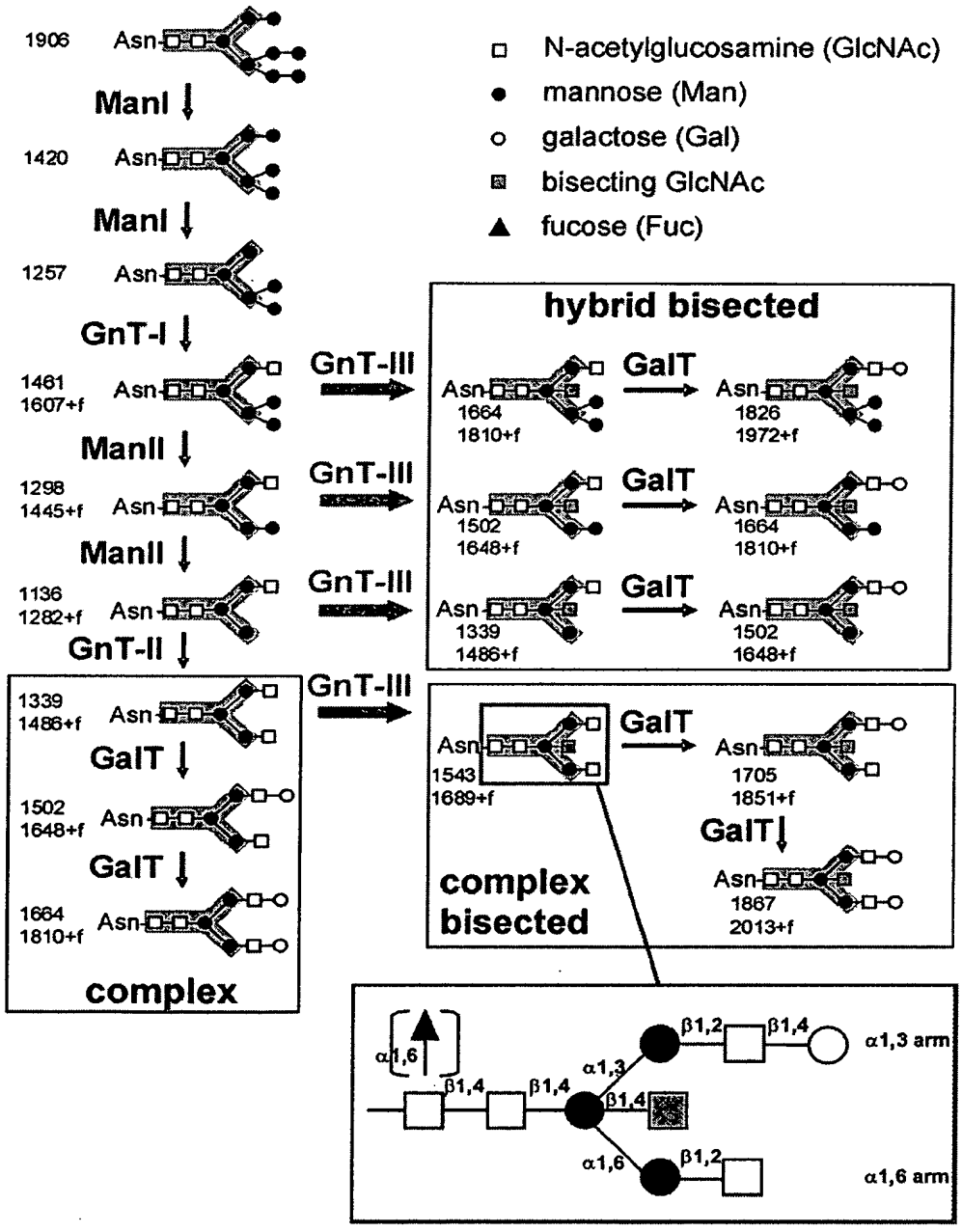
1906
Asn
ManI
1420
Asn
ManI
1257
Asn
GnT-I
1461
1607+f
Asn
ManII
1298
1445+f
Asn
ManII
1136
1282+f
Asn
GnT-II
1339
1486+f
Asn
GalT
1502
1648+f
Asn
GalT
1664
1810+f
Asn
complex
GnT-III
GnT-III
GnT-III
GnT-III
hybrid bisected
Asn
1664
1810+f
GalT
Asn
1826
1972+f
Asn
1502
1648+f
GalT
Asn
1664
1810+f
Asn
1339
1486+f
GalT
Asn
1502
1648+f
Asn
1543
1689+f
GalT
Asn
1705
1851+f
GalT
Asn
1867
2013+f
complex
bisected
N-acetylglucosamine (GlcNAc)
mannose (Man)
galactose (Gal)
bisecting GlcNAc
fucose (Fuc)
α1,6
β1,4
β1,4
α1,3
β1,2
β1,4
α1,3 arm
β1,4
α1,6
β1,2
α1,6 arm

Figure 2

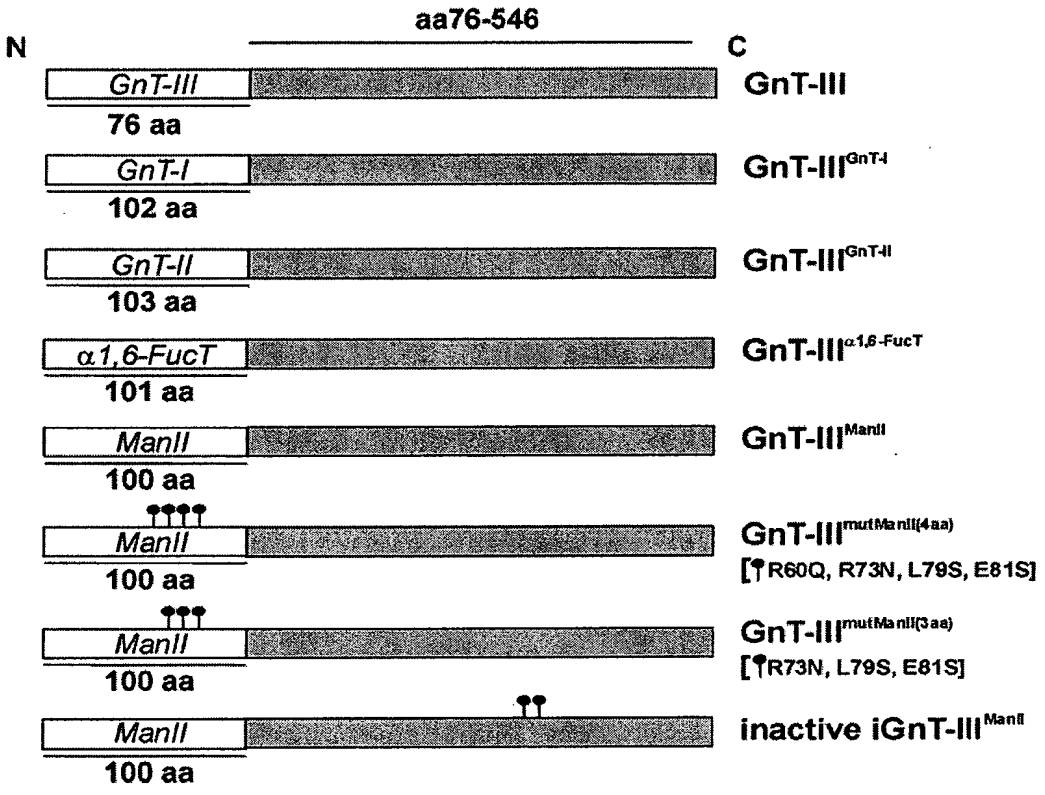
aa76-546
N
C
GnT-III
76 aa
GnT-III
GnT-I
102 aa
GnT-III^GnT-I
GnT-II
103 aa
GnT-III^GnT-II
α1,6-FucT
101 aa
GnT-III^α1,6-FucT
ManII
100 aa
GnT-III^ManII
ManII
100 aa
GnT-III^mutManII(4aa)
[R60Q, R73N, L79S, E81S]
ManII
100 aa
GnT-III^mutManII(3aa)
[R73N, L79S, E81S]
ManII
100 aa
inactive iGnT-III^ManII

Figure 3

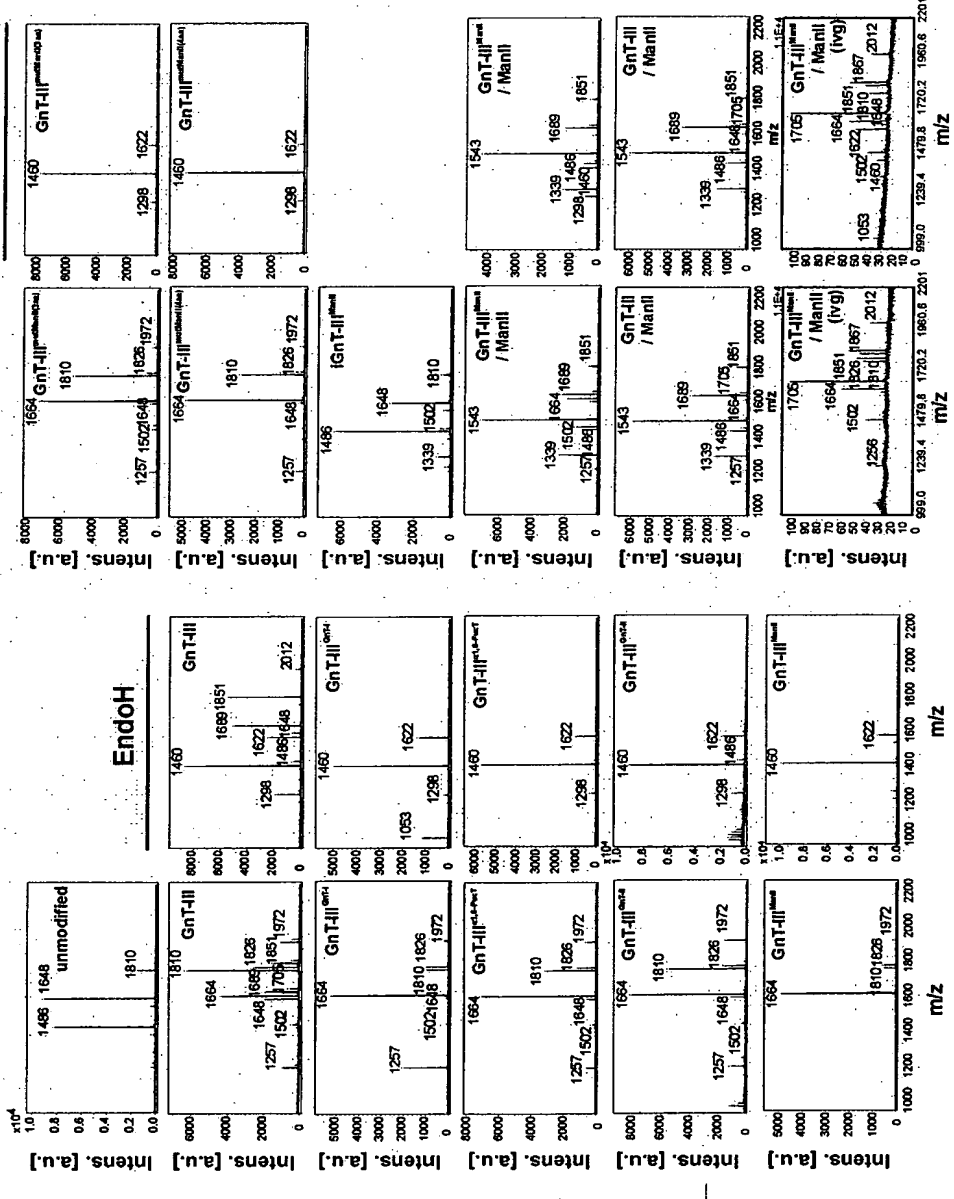
EndoH
EndoH
unmodified
GnT-III
GnT-III
iGnT-III
GnT-III / ManII
GnT-III / ManII
GnT-III / ManII (ivg)
Intens. [a.u.]
m/z

Figure 4

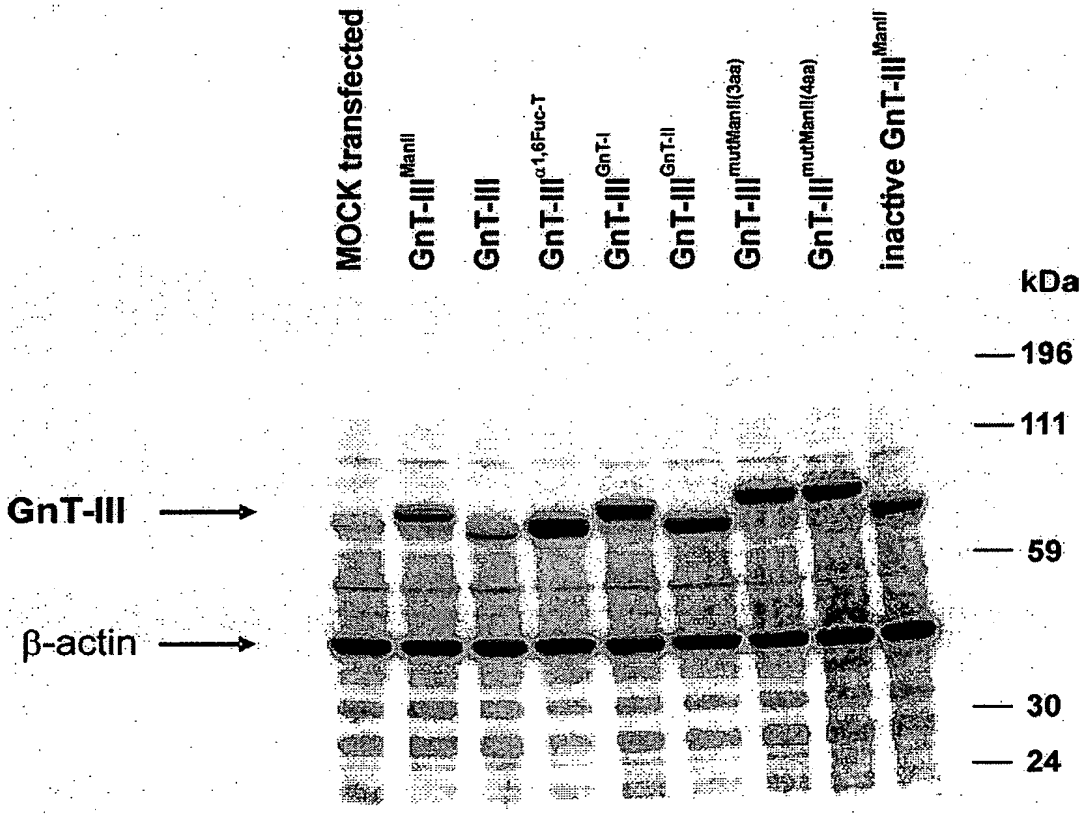
MOCK transfected
GnT-III^ManII
GnT-III
GnT-III^α1,6Fuc-T
GnT-III^GnT-I
GnT-III^GnT-II
GnT-III^mutManII(3aa)
GnT-III^mutManII(4aa)
inactive GnT-III^ManII
kDa
196
111
59
30
24
GnT-III
β-actin

Figure 5

(A)

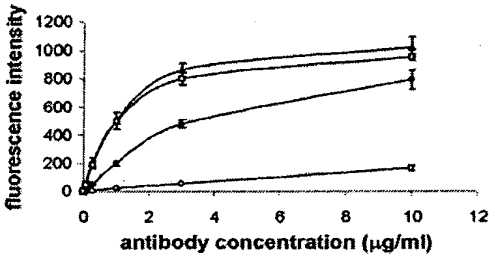
fluorescence intensity
1200
1000
800
600
400
200
0
0
2
4
6
8
10
12
antibody concentration (μg/ml)

(B)

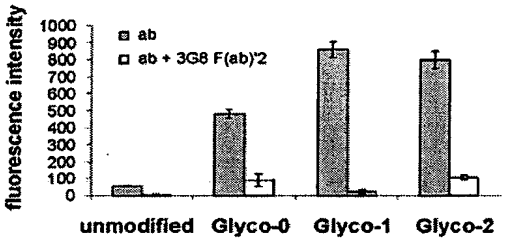
fluorescence intensity
1000
900
800
700
600
500
400
300
200
100
0
ab
ab + 3G8 F(ab')2
unmodified
Glyco-0
Glyco-1
Glyco-2

(C)

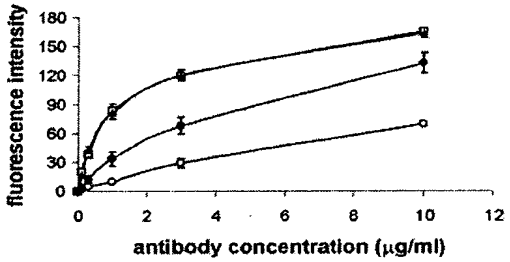
fluorescence intensity
180
150
120
90
60
30
0
0
2
4
6
8
10
12
antibody concentration (μg/ml)

Figure 6

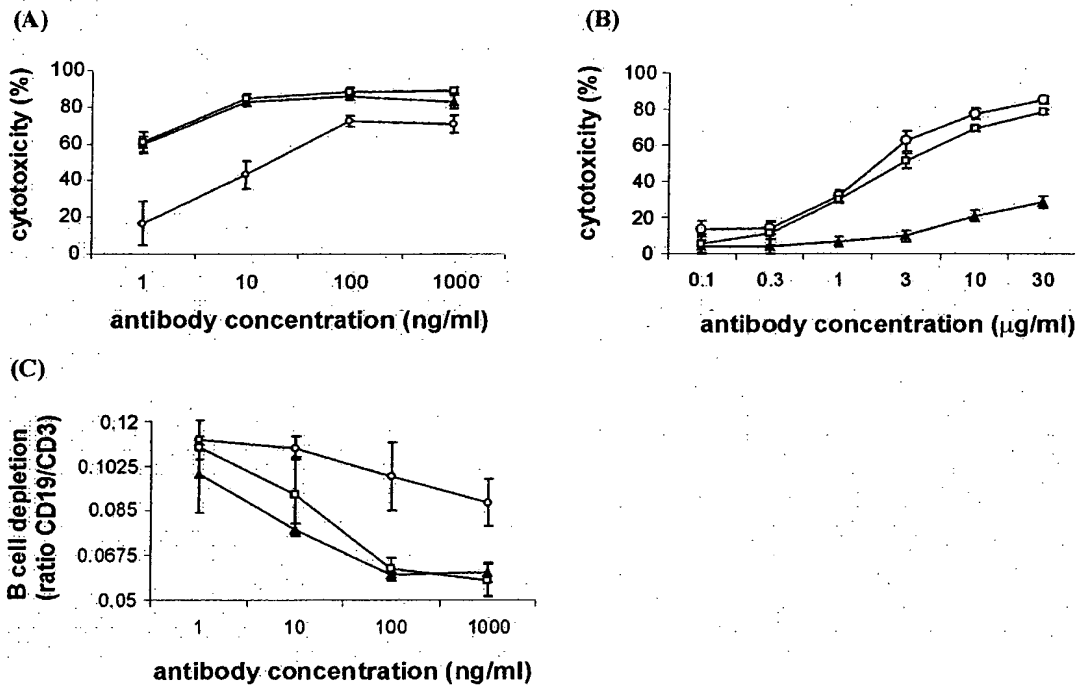
(A)
cytotoxicity (%)
100
80
60
40
20
0
1
10
100
1000
antibody concentration (ng/ml)
(B)
cytotoxicity (%)
100
80
60
40
20
0
0.1
0.3
1
3
10
30
antibody concentration (μg/ml)
(C)
B cell depletion (ratio CD19/CD3)
0.12
0.1025
0.085
0.0675
0.05
1
10
100
1000
antibody concentration (ng/ml)

Antibody glycoengineering by constitutive co-expression of recombinant, wild-type β1,4-N-acetylglucosaminyltransferase III (GnT-III) and Golgi α-mannosidase II (ManII) in stable, industrial grade CHO cells producing a recombinant antibody

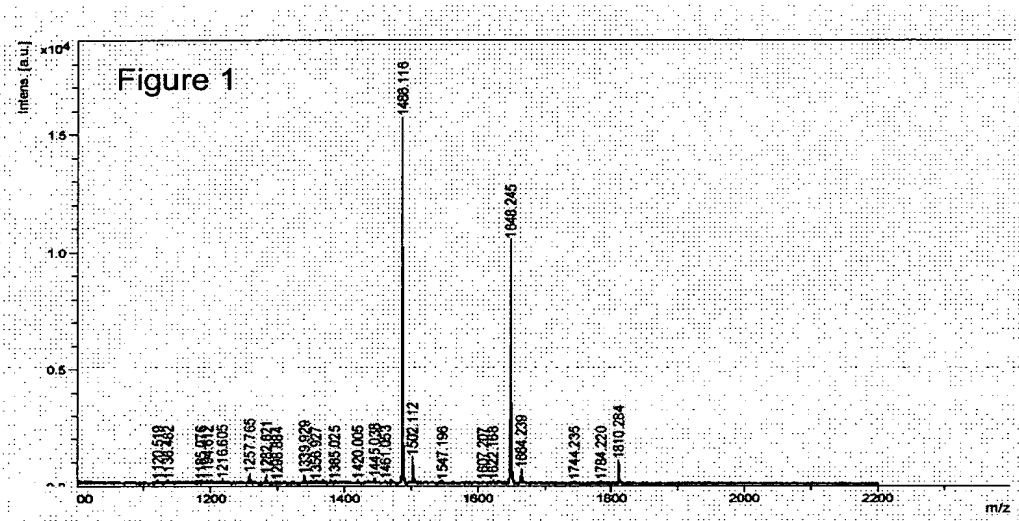

m/z	Rel. Intens.	Res.	Intens.	SN
1120.519	1	3265	83.15	1.9
1136.482	1	3844	75.95	1.7
1165.076	1	2710	84.34	1.8
1194.612	1	3161	100.81	2.2
1216.605	1	3007	127.53	2.9
1257.765	3	3968	390.78	9.0
1282.821	2	3571	326.31	7.7
1298.884	1	4607	80.16	2.0
1339.929	2	4346	337.85	7.9
1356.927	1	6364	97.78	2.2
1385.025	1	4464	115.97	2.7
1420.005	1	3549	109.16	2.6
1445.038	1	3653	190.86	4.5
1461.053	1	4645	93.06	2.3
1486.116	100	6181	14431.82	218.7
1502.112	7	5596	1067.78	14.7
1547.196	1	4963	88.25	2.2
1607.207	1	3733	73.31	1.9
1622.168	1	4301	114.35	2.7
1648.245	68	6909	9855.74	170.4
1664.239	4	5758	575.74	11.6
1744.235	1	3777	104.22	3.0
1784.220	1	6776	92.51	2.6
1810.284	6	7072	933.25	24.7

Figure 1 shows the glycosylation profile for the Fc-region oligosaccharides of a **non-glycoengineered recombinant antibody** produced in CHO cells. The three major peaks (m/z 1486, 1648 and 1810) correspond to fucosylated complex oligosaccharides, and level of non-fucosylated oligosaccharides is below 10%, which is typical for non-glycoengineered antibodies produced by CHO cells. The oligosaccharide profile was determined by MALDI/TOF-MS in positive ion mode for oligosaccharides enzymatically released from the antibody by PNGaseF treatment.

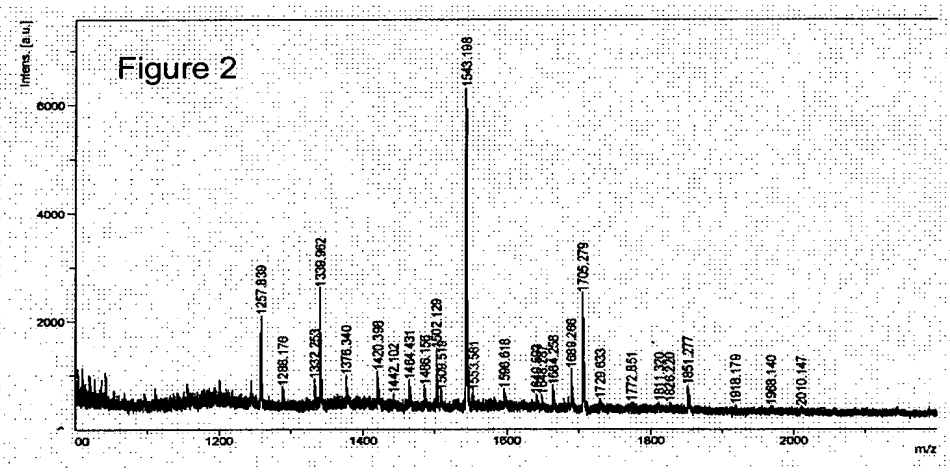

m/z	Rel. Intens.	Res.	Intens.	SN
1257.839	28	4009	1637.78	20.4
1288.176	6	3286	362.68	4.9
1332.253	8	4145	470.63	6.1
1338.962	38	3807	2172.75	28.2
1376.340	9	4352	515.04	6.8
1420.398	11	4403	606.68	8.1
1442.102	3	3908	156.50	2.1
1464.431	8	4497	486.40	6.6
1486.156	7	4279	376.64	5.2
1502.129	18	4676	1042.51	14.4
1509.519	5	4711	271.92	3.8
1543.198	100	4717	5770.25	79.9
1553.581	5	5397	280.13	3.9
1596.618	6	8077	323.03	4.7
1640.593	4	5489	224.84	3.4
1648.287	4	5230	222.18	3.3
1664.258	7	5233	417.30	6.2
1689.266	12	4592	701.39	10.0
1705.279	37	5729	3135.71	29.8
1729.633	3	8479	167.58	2.6
1772.851	2	12836	121.92	2.1
1811.320	2	10340	121.72	2.0
1826.220	2	9903	96.33	1.6
1851.277	8	5048	444.05	7.4
1918.179	2	22801	118.87	2.0
1968.140	2	8509	102.83	1.9
2010.147	2	19033	100.39	1.8

Figure 2 shows the glycosylation profile for the Fc-region oligosaccharides of a **glycoengineered recombinant antibody** produced in CHO cells. Glycoengineering was achieved by constitutive co-expression of recombinant, wild-type β1,4-N-acetylglucosaminyltransferase III (GnT-III) and Golgi α-mannosidase II (ManII) in stable, industrial grade CHO cells producing a recombinant antibody. Industrial grade means that the cells grow (with a doubling time lower than 40 hours) in suspension in chemically-defined protein-free medium and produce over 0.5 g/l of antibody under batch process conditions. Glycoengineering leads to increased levels of non-fucosylated oligosaccharides relative to levels produced in non-glycoengineered CHO cells (peaks at m/z 1339, 1543 and 1705 are

non-fucosylated complex oligosaccharides and represent over 70% of the oligosaccharides). The oligosaccharide profile was determined by MALDI/TOF-MS in positive ion mode for oligosaccharides enzymatically released from the antibody by PNGaseF treatment.

Figure 3 **Fc-FcR binding of antibodies to CHO cells stably expressing recombinant human FcgRIII**

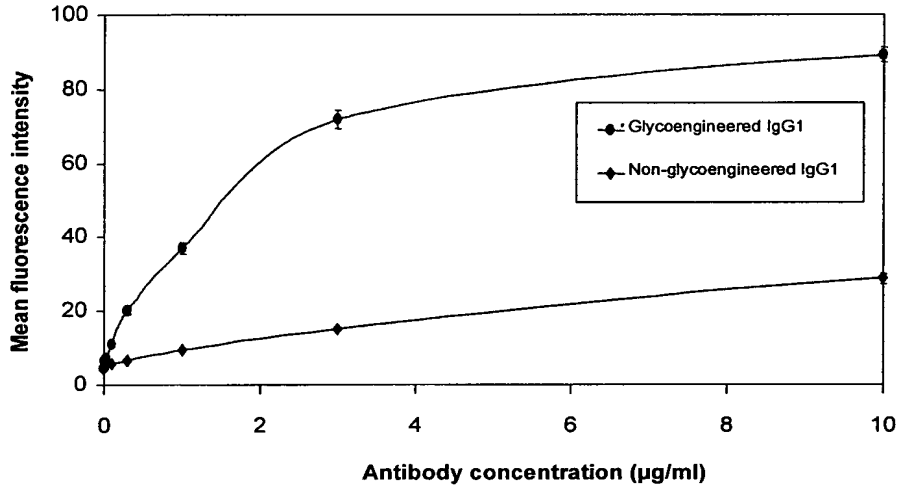

Figure 3 shows increased binding to FcgRIII for a glycoengineered antibody, having increased levels of non-fucosylated Fc-oligosaccharides (glycoengineering as described above for Figure 2), relative to a non-glycoengineered antibody with identical Fc polypeptide region. Binding assay was performed as described in .

Figure 4 **Increased biological activity (antibody dependent killing of B-cells in whole blood) by a glycoengineered antibody with increased levels of non-fucosylated oligosaccharides**

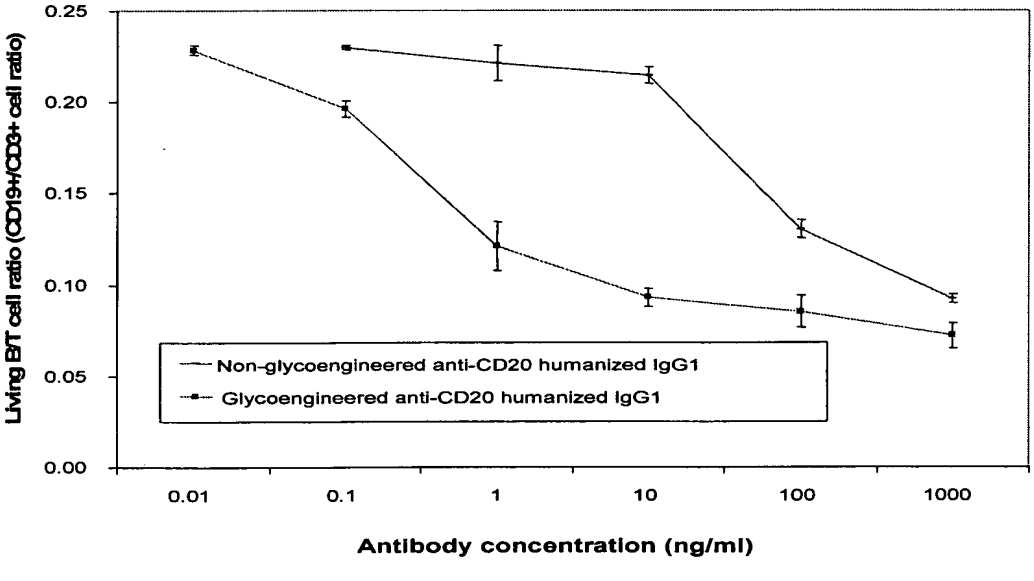

Figure 4 shows increased antibody-dependent killing of target cells for a glycoengineered antibody with increased levels of non-fucosylated Fc-oligosaccharides (glycoengineered as

described above for Figure 2) relative to a non-glycoengineered antibody with identical Fc polypeptide region. B-cell antibody-dependent-depletion assay performed by incubating antibodies with whole blood overnight and measuring the levels of remaining, living B-cells by flow cytometry (T-cells are used as an internal standard that is not depleted by the anti-CD20 antibodies). Assay details are as described in .

Clonal Analysis of the Glycosylation of Immunoglobulin G Secreted by Murine Hybridomas†

Ronald J. Rothman,‡,§ Leonard Warren,*,‡ Johannes F. G. Vliegenthart,∥ and Karl J. Härd⊥

The Wistar Institute of Anatomy and Biology, Philadelphia, Pennsylvania 19104, and Department of Bio-Organic Chemistry, University of Utrecht, Transitorium III, P.O. Box 80.075, NL-3508 TB Utrecht, The Netherlands

Received June 7, 1988; Revised Manuscript Received September 21, 1988

ABSTRACT: A panel of 10 hybridomas was assembled to assess the influence of various genetic and biological factors upon glycosylation of secreted monoclonal IgG. After exhaustive Pronase digestion of IgG, glycopeptides were characterized chromatographically by apparent size, charge, and concanavalin A (Con A)–Sepharose and *Lens culinaris* (LcH)–agarose affinity. Six glycosylation phenotypes were found to be common among all clones studied. Despite this phenotypic heterogeneity in glycosylation of IgG, considerable similarity exists between different clones. In particular, virtually all IgG glycopeptides bear a core fucose residue. Second, the majority of the glycosylation repertoire is comprised of two phenotypes, characterized by glycopeptides which differ in affinity for Con A–Sepharose. Of these, the predominantly expressed phenotype is the same for all clones. The carbohydrate structure derived from this phenotype, elucidated by 500-MHz ^{1}H NMR spectroscopy, is

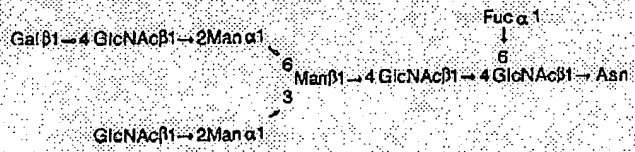

Significant variability between different hybridomas exists in the relative expression of the two major phenotypes. Other differences between clones may reflect the expression of an additional site which is glycosylated differently. However, there is no apparent correlation of phenotype with either the hybridoma's parentage or the serologically defined polypeptide structure of the IgG which it secretes. In addition to clonal variability, other sources of variability in phenotypic expression were identified. A generational variability is apparent upon continuous culturing of the same hybridoma. Also, differences in culture medium pH or proliferative state of the cells may have a modest influence upon the glycosylation phenotype.

IgG is a glycoprotein secreted by immune splenocytes and malignant myelomas. Although IgG is otherwise well characterized, few detailed, comparative studies exist of the species-specific differences in IgG carbohydrate or the clonal variability in its expression. Similarly, systematic studies are lacking as to whether glycosylation varies with polymorphism in IgG polypeptide structure, which can be defined serologically as isotype, allotype, and idiotype. Structural elucidation of the oligosaccharides expressed has been performed extensively only with human (Parekh et al., 1985; Takahashi et al., 1987; Harada et al., 1987) and rabbit (Taniguchi et al., 1985; Rademacher et al., 1983) IgG, whereas clonal variability in glycosylation has been studied solely with human myeloma IgG (Takahashi et al., 1987; Mizuochi et al., 1982; Savvidou et al., 1984; Grey et al., 1982; Kornfeld et al., 1971).

The carbohydrate structure of human (Kornfeld et al., 1971), rabbit (Taniguchi et al., 1985), murine (Mizuochi et al., 1987), bovine (Tai et al., 1975), and porcine (Rao & Mendicino, 1978) IgG is an Asn-linked oligosaccharide of the biantennary, complex type. However, instead of a single oligosaccharide, an array of structurally related yet distinct oligosaccharides is expressed, a phenomenon referred to as carbohydrate microheterogeneity. Differences exist in the frequency of expression of these various oligosaccharides on human (Parekh et al., 1985; Harada et al., 1987), rabbit (Taniguchi et al., 1985; Rademacher et al., 1983), and murine (Mizuochi et al., 1987) serum IgG. Additionally, clonal differences exist in the carbohydrate microheterogeneity of human myeloma IgG (Takahashi et al., 1987; Mizuochi et al., 1982; Savvidou et al., 1984; Grey et al., 1982; Kornfeld et al., 1971).

The phenomenon of carbohydrate microheterogeneity is a characteristic feature of protein glycosylation. Unlike proteins and nucleic acids, oligosaccharide synthesis is not guided by a template. Rather, it is the structure of the polypeptide undergoing glycosylation, as well as the proteins (enzymes and transporters) comprising the glycosylation apparatus, which is under genetic control (Hubbard & Ivatt, 1981; Kornfeld & Kornfeld, 1985; Stanley, 1984; Deutscher & Hirschberg, 1986). The phenotypic expression of the oligosaccharide, however, may be influenced by biological modulation of the cell's environment (pH and substrate availability), proliferative state, or substratum (Warren et al., 1983, 1982; Megaw & Johnson, 1979). Presumably, it is the dynamic interplay of these various genetic and biological influences which accounts

† This work was supported by USPHS (Grant CA 19130 to L.W.; Training Grant CA 01971 to R.J.R.), the Netherlands Foundation for Chemical Research (SON/ZWO), and the Netherlands Foundation for Cancer Research (KWF, Grant UUKC 88-14). This paper constitutes a portion of a thesis submitted by R.J.R. in partial fulfillment of the requirements for the degree of Doctor of Philosophy from the University of Pennsylvania.

* Author to whom correspondence should be addressed.
‡ The Wistar Institute of Anatomy and Biology.
§ Present address: Department of Pathology and Cell Biology, Jefferson Medical College, Philadelphia, PA 19107.
∥ University of Utrecht.

0006-2960/89/0428-1377$01.50/0

Table I: Panel of Hybridomas[a]

hybridoma	parental cells: splenocyte	parental cells: myeloma	IgG: isotype	IgG: antigenic specificity	references
CSAT	BALB/c	SP2/0	2b	anti-integrin	Neff et al., 1982
34-5-8S	C3H	SP2/0	2a	anti-H-2D^d	Ozato et al., 1982
H36.15.3	BALB/c	SP2/0	2a	anti-hemagglutinin	Staudt et al., 1983
H36.4.5	BALB/c	SP2/0	2a	anti-hemagglutinin	Staudt et al., 1983
H36.2.6	BALB/c	SP2/0	2a	anti-hemogglutinin	Staudt et al., 1983
H36.15.6	BALB/c	SP2/0	2a	anti-hemagglutinin	Staudt et al., 1983
S-S.1	BALB/c	SP2/0	2a	anti-sheep red blood cell	
B137.17.1	BALC/c	.653	2a	?	Perussia et al., 1987
L5.1	BALB/c	.653	2a	anti-transferrin receptor	Lebman et al., 1982
D4IE4	BALC/c	.653	1	anti-P_0	Miller et al., 1984

[a] The parentage and serologically defined polypeptide structure of the IgG secreted are indicated for each member of the panel of hybridomas employed in the clonal analysis.

for the host-dependent and tissue-dependent variability in glycosylation (Hsieh et al., 1983; Sheares & Robbins, 1986; Parekh et al., 1987).

In the present study, we describe the clonal repertoire for the glycosylation of IgG secreted by a panel of murine hybridomas, formed by the fusion of immune splenocytes with myelomas. The effect upon glycosylation of the hybridoma's parentage and the serologically defined polypeptide structure of the monoclonal IgG which it secretes are assessed. The contribution of generational differences, resulting from continuous culturing, and differences in culturing conditions are evaluated as further sources of variability in glycosylation.

Materials and Methods

Materials. D-[U-^{14}C]Glucosamine hydrochloride (284 Ci/mol), D-[6(N)-^{3}H]glucosamine hydrochloride (23.4 Ci/mmol), and En^{3}Hance were purchased from New England Nuclear (Boston, MA). Sephadex G-50 (Superfine), Sephadex G-10, Con A–Sepharose,[1] DEAE-Sephadex A-25, and protein A–Sepharose were obtained from Pharmacia (Piscataway, NJ). LcH (E-Y Laboratories, San Mateo, CA) was conjugated to Affi-Gel 10 (Bio-Rad, Richmond, CA) (7 mg/mL of resin) according to an established procedure (Knudsen et al., 1981). Bio-Gel P-2 (200–400 mesh) was also from Bio-Rad. Pronase (grade B) was purchased from Calbiochem (San Diego, CA).

Culturing and Metabolic Labeling of Hybridomas. Hybridomas (Table I) were obtained either from American Type Culture Center (Rockville, MD) or from various laboratories at the Wistar Institute (Philadelphia, PA). The fusion partners were BALB/c-derived, nonsecreting myelomas. For contrast, one hybridoma (34-5-8S) was chosen for its allogeneic C3H background, and the allotypically different IgG which it secretes. The H36 clones were a cluster of related hybridomas derived from a single fusion of one myeloma variant with immune splenocytes from one animal. All H36 clones secreted an IgG2a directed against the same antigen.

Cells were seeded at 5×10^5/mL and cultured in Dulbecco's modified Eagle's medium with low glucose (Gibco, Grand Island, NY), supplemented with 10% heat-inactivated fetal bovine serum, 10 mM sodium bicarbonate, and 25 mM Hepes (pH 7.2). After a 20-h preincubation, cultures were metabolically labeled with [^{3}H]glucosamine (2 μCi/mL) for an additional 48 h. Parallel cultures of CSAT hybridomas were labeled alternatively with [^{14}C]glucosamine (0.5 μCi/mL).

Isolation of IgG and Preparation of Glycopeptides. IgG in the spent culture medium was affinity purified chromatographically on protein A–Sepharose essentially by the procedure of Ey et al. (1978). The purified IgG was incubated with predigested Pronase for 3 days, according to an established procedure (Blithe et al., 1980). For ^{1}H NMR analysis, IgG also was obtained from the ascites fluid of CSAT hybridomas passaged in pristane-primed BALB/c mice. The IgG was affinity purified and digested with Pronase similar to IgG obtained from tissue culture.

Structural Characterization Studies. To ensure consistency of elution profiles, a common ^{14}C-labeled CSAT IgG Pronase digest was added as an internal standard to all ^{3}H-labeled samples. The resulting doubly labeled Pronase digests were analyzed chromatographically by various techiques. The radioactive distribution in each fraction, determined by liquid scintillation counting, was plotted by computer-aided graphics, which also provided peak area summations.

(1) Gel Filtration Chromatography. Blue dextran and phenol red, added to the sample, served as exclusion and inclusion volume markers, respectively. Samples were analyzed on columns (1 cm × 135 cm) of Sephadex G-50 developed with an alkaline borate buffer composed of 45.5 mM boric acid/4.5 mM sodium tetraborate/2 mM Na_2EDTA/0.02% sodium azide (pH 8.2) (Rothman & Warren, 1988).

For preparative purposes, selected fractions of the ^{3}H-labeled Pronase digests were pooled. Borate was removed by evaporation under a stream of nitrogen after repeated treatment with 1% acetic acid in methanol. The residue in a minimal volume of water was desalted further on a Bio-Gel P-2 column (1 cm × 15 cm) with a 5-cm overlayer of Sephadex G-10 that was developed with water (Blithe et al., 1980).

(2) Anion-Exchange Chromatography. The ^{3}H-labeled IgG Pronase digest was fractionated batchwise on a column of DEAE-Sephadex (0.7 cm × 4 cm). After the column was washed with 10 mM pyridine/17 mM acetic acid (pH 4.5) to remove the neutral glycopeptides, the acidic glycopeptides were eluted with 2 M ammonium acetate/3.5 M acetic acid (pH 4.5). Volatile buffers were removed by lyophilization.

(3) Lectin Affinity Chromatography. After being boiled for 5 min, IgG glycopeptides were analyzed on columns of Con A–Sepharose or LcH–agarose (0.7 cm × 4 cm) according to the procedure of Cummings and Kornfeld (1982). After the glycopeptides lacking lectin affinity were removed by washing with TBS buffer, the column was eluted stepwise. First, glycopeptides with low lectin affinity were eluted with 10 mM methyl α-glucoside in TBS; then, those with high affinity were eluted with 100 mM methyl α-mannoside in TBS, prewarmed to 60 °C.

[1] Abbreviations: Con A, concanavalin A; LcH, *Lens culinaris* agglutinin; GFC, gel filtration chromatography; DEAE, diethylaminoethyl; mAb, monoclonal antibody; Hepes, 4-(2-hydroxyethyl)-1-piperazineethanesulfonic acid; Pipes, 1,4-piperazinediethanesulfonic acid; Tes, 2-[[2-hydroxy-1,1-bis(hydroxymethyl)ethyl]amino]ethanesulfonic acid; Hepps, 4-(2-hydroxyethyl)-1-piperazinepropanesulfonic acid; Tris, 2-amino-2-(hydroxymethyl)propane-1,3-diol; TBS, 150 mM NaCl/10 mM Tris/1 mM $CaCl_2$/1 mM $MgCl_2$/0.02% NaN_3 (pH 8).

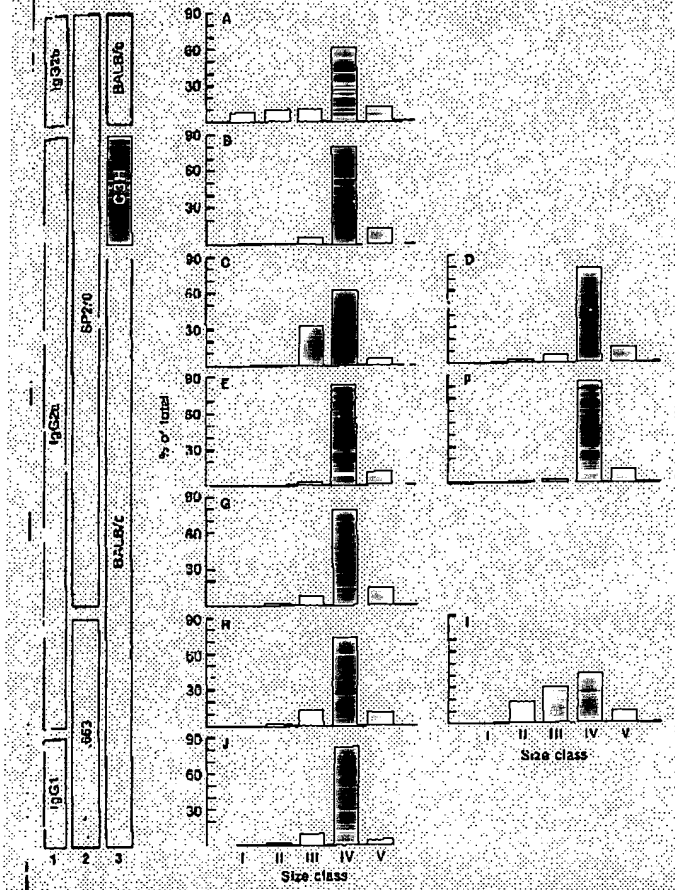

FIGURE 1: Clonal comparison of IgG glycopeptides by alkaline borate GFC. The ^{3}H-labeled IgG Pronase digests were analyzed by alkaline borate GFC. The size class distributions are shown for the IgG glycopeptides of CSAT (A), 34-5-8S (B), H36.15.3 (C), H36.4.5 (D), H36.2.6 (E), H36.15.6 (F), S-S.1 (G), B137.17.1 (H), L5.1 (I), and D4E4 (J). The panel to the left schematically represents how the hybridomas are related to each other by the isotype (1) of IgG secreted, as well as by their parentage of myeloma (2) variant and splenocyte (3) strain.

For ^{1}H NMR analysis, glycopeptides of IgG isolated from ascites fluid were resolved as described above on a column (1 cm × 8 cm) of Con A–Sepharose.

(4) 500-MHz ^{1}H NMR Spectroscopy. Glycopeptides were repeatedly exchanged in ^2H_2O with intermediate lyophilization and finally dissolved in ^2H_2O which was 99.96 atom % ^{2}H (Aldrich). ^{1}H NMR spectra were recorded on a Bruker WM-500 spectrometer (SON hf facility, Department of Biophysical Chemistry, University of Nijmegen, The Netherlands) operating at 500 MHz and a probe temperature of 27 °C. Resolution enhancement of the spectra was achieved by Lorentzian-to-Gaussian transformation. Chemical shifts are given relative to sodium 4,4-dimethyl-4-silapentane-1-sulfonate but were actually measured indirectly to acetone in ^2H_2O (δ = 2.225) (Vliegenthart et al., 1983).

Results

Characterization of IgG Glycopeptides by Apparent Size. In an attempt to observe what influence differences in polypeptide structure and parental background might have upon glycosylation, the Pronase digests of IgG secreted by the panel of hybridomas were fractionated according to apparent size by alkaline borate GFC. Clonal analysis revealed that as few as three and as many as five size classes of glycopeptides could be distinguished (Figure 1). Although there is some apparent variability between clones in the relative distribution of these various classes, the predominant size present was always class IV. The molecular weight of this glycopeptide size class is approximately 2000 (Rothman & Warren, 1988).

A second feature common among all the clones was the presence of class III, IV, and V glycopeptides. Of the 10 monoclonal IgGs surveyed, 2 (CSAT and L5.1) were found to have a pattern different by the presence of additional glycopeptides of size classes I and/or II. Although CSAT mAb differs, isotypically, L5.1 mAb is the same as the majority of the panel. Thus, a priori, the absolute number of size classes does not appear to correlate with the isotype.

The clonal differences in the elution profile of CSAT IgG glycopeptides characterized by class I and II glycopeptides have been studied more fully (Rothman & Warren, 1988). Glycopeptide classes I and II were found to differ from the other classes chiefly by sialylation. Their presence reflects the expression of an additional glycosylation site, presumably located within the Fab region, whereas, typically, IgG is glycosylated solely at a single conserved site, located within the Fc portion (Beale & Feinstein, 1976). Furthermore, extensive sialylation appears to be a feature more characteristic of the Fab (and the related Bence Jones proteins) than of the Fc (Taniguchi et al., 1985; Abel et al., 1968; Burton, 1985; Chandrasekaran et al., 1981). Typically, the site of all additional carbohydrate is located within the idiotypically defined variable region of IgG (Spiegelberg et al., 1970; Sox et al., 1970). However, this additional carbohydrate probably does not correlate with the idiotype or the related antigenic specificity. MAbs with either identical specificities (characterized by the H36 series of anti-hemagglutinin mAbs) or different specificities (characterized by the remainder of the panel) generally have similar GFC elution profiles of their glycopeptides, although they differ from that of CSAT mAb (Figure 1). Rather, the expression of an additional site of glycosylation would appear to have been acquired adventitiously in the process of generating antibody diversity.

Characterization of IgG Glycopeptides by Charge. Despite differences in structure and parental background, all hybridomas of the panel yielded IgG glycopeptides which were found to be predominantly neutral by chromatography upon DEAE-Sephadex (Figure 2). Subsequent analysis of the glycopeptides by alkaline borate GFC indicated that the neutral glycopeptides were predominantly of size classes IV and V, whereas classes I and II were composed entirely of acidic glycopeptides. A variable but significant fraction of class III glycopeptides also was acidic. This distribution of acidic glycopeptides by size is an agreement with the sensitivity of CSAT IgG glycopeptides to neuraminidase (Rothman & Warren, 1988).

Characterization of IgG Glycopeptides by Affinity for Con A. Among the clonally common glycopeptide size classes III, IV, and V, the predominant IgG glycosylation phenotype was characterized by glycopeptides of low affinity for Con A–Sepharose (Figure 3A–F). Class IV glycopeptides of low affinity for Con A–Sepharose accounted for 42–62% of the total radioactivity incorporated into IgG. One of the most prominent differences between clones occurred in the relative distribution of class IV glycopeptides of high affinity and those of low affinity for Con A–Sepharose. The ratio between these two phenotypes varied between 1:10 and 2:3. Together, these two phenotypes comprised 50–90% of the total radioactivity incorporated into IgG.

Characterization of IgG Glycopeptides by Affinity for LcH. When analyzed by LcH–agarose, glycopeptides of high affinity for the lectin were characteristic of the predominant phenotype

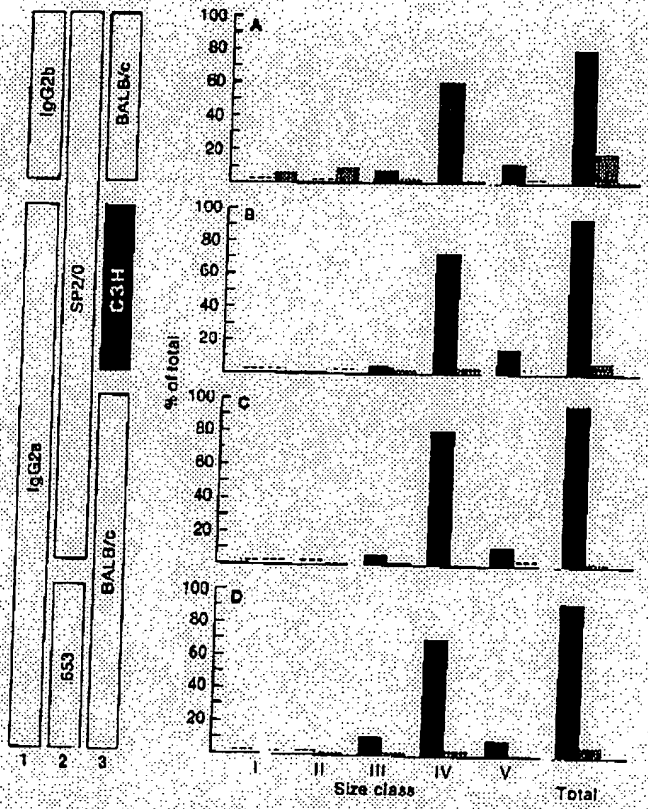

FIGURE 2: Clonal comparison of IgG glycopeptides by DEAE-Sephadex chromatography. The ^{3}H-labeled IgG Pronase digests of CSAT (A), 34-5-8S (B), S-S.1 (C), and B137.17.1 (D) were fractionated batchwise on a column of DEAE-Sephadex into neutral (black bars) and acidic (stiple) glycopeptides. An aliquot of each charge-resolved glycopeptide pool was counted to determine the distribution of acidic and neutral glycopeptides within the total Pronase digest. The balance of each pool was analyzed by alkaline borate GFC to determine the size class distribution. This was weighted for the relative distribution of acidic and neutral glycopeptides within the total digest. The panel to the left is described in Figure 1.

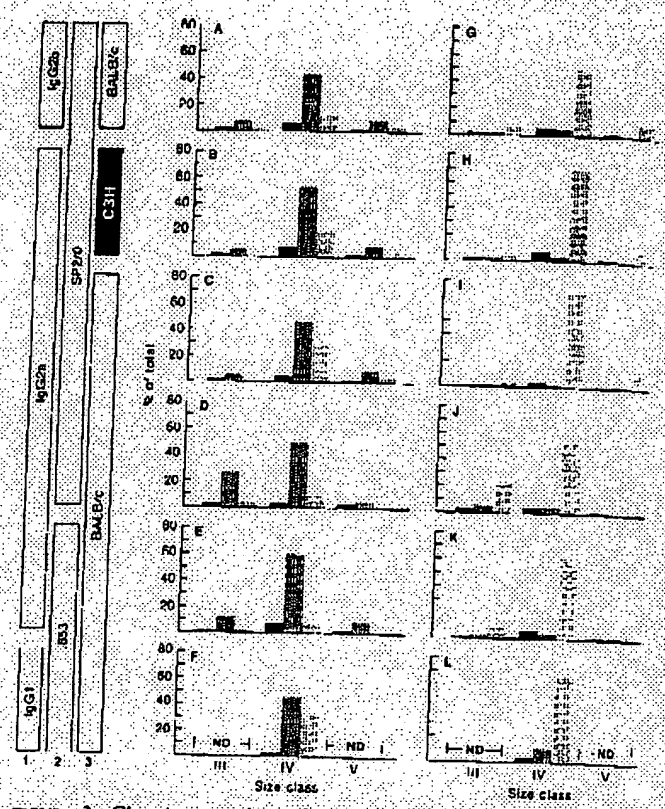

FIGURE 3: Clonal comparison of IgG glycopeptides by lectin affinity chromatography. The ^{3}H-labeled IgG Pronase digests were fractionated by alkaline borate GFC. Next, each of the isolated and desalted glycopeptides was resolved either by Con A (A–F) or LcH (G–L) affinity chromatography into glycopeptides with either no (black bars), low (dark stiple), or high (light stiple) affinity for the particular lectin. The distributions by lectin affinity were then weighted for the relative distribution of the alkaline borate GFC size classes within the total digest (as determined from Figure 2). The lectin affinity distributions are shown for the IgG glycopeptides of CSAT (A and G), 34-5-8S (B and H), S-S.1 (C and I), H36.15.3 (D and J), B137.17.1 (E and K), and D4IE4 (F and L). ND, distribution by lectin affinity not determined. The panel to the left is described in Figure 2.

(Figure 3G–L). By themselves, class IV glycopeptides of high affinity for LcH–agarose accounted for 50–75% of the total radioactivity incorporated into IgG.

Compared with classes IV and V, however, glycopeptides of size class III were found to be relatively enriched in glycopeptides of either low or no affinity for LcH–agarose. Furthermore, qualitative differences were apparent in the LcH elution profiles of glycopeptides of high affinity. Those derived from glycopeptides of size class III were eluted somewhat more quickly than the analogous ones derived from classes IV and V (data not shown). Similar subtle alterations in the Con A–Sepharose elution profiles of IgG glycopeptides have been reported to result from small differences in oligosaccharide structure (Narasimhan et al., 1979).

Another interesting common feature was that greater than 90% of the IgG glycopeptides of classes III, IV, and V, which are assumed to be derived from the Fc portion, had affinity for both LcH and Con A. Although both lectins share many carbohydrate specificities, core fucosylation is required for binding to LcH, but not to Con A (Kornfeld et al., 1981). Thus, the lectin binding data in the present study would suggest that virtually all murine monoclonal IgG expresses core fucosylation of the Fc with very little, if any, variability in its expression.

Characterization by ^{1}H NMR Spectroscopy of the Carbohydrate Structure Derived from the Predominant Phenotype. To elucidate the carbohydrate structure expressed in the predominant phenotype, the CSAT IgG glycopeptide of size class IV and low affintiy for Con A–Sepharose was analyzed by 500-MHz ^{1}H NMR spectroscopy. Its deduced structure is depicted in Figure 4. Summarized in Table II are the relevant ^{1}H NMR parameters, which are compared with those

Table II: ^{1}H Chemical Shifts of Structural Reporter Groups of the Monosaccharides Present in the Predominant Glycopeptide of CSAT IgG, Together with Those of a Reference Compound

		chemical shift (ppm)	
reporter group	residue[a]	CSAT	GP-II-3 (G Gn)
H-1	1	5.069	5.071
	2	4.681	4.682
	3	n.d.	4.766
	4	5.117	5.115
	4′	4.922	4.926
	5	4.554	4.553
	5′	4.580	4.578
	6′	4.472	4.471
H-2	3	4.250	4.253
	4	4.186	4.188
	4′	4.108	4.114
NAc	1	2.012	2.010
	2	2.093	2.091
	5	2.053	2.051
	5′	2.046	2.045
H-1	Fuc	4.872	4.873
CH_3	Fuc	1.201	1.210

[a] Residue positions refer to Figure 4.

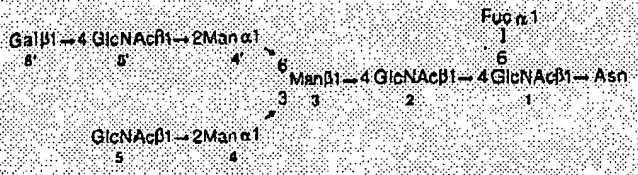

FIGURE 4: Structure of the predominant glycopeptide derived from CSAT IgG. IgG, secreted by CSAT hybridomas grown in vivo, was affinity purified, digested with Pronase, and then fractionated chromatographically. The carbohydrate structure of the size class IV glycopeptide of low affinity for Con A–Sepharose was elucidated by 500-MHz ^{1}H-NMR spectroscopy.

of a reference compound (G Gn) derived from human myeloma IgG (Grey et al., 1982).

The asparagine-bound GlcNAc-1 was characterized by the chemical shift values of its H-1 (δ = 5.069) and *N*-acetyl (δ = 2.012) signals. All GlcNAc-1 residues are α1→6 fucosylated, as revealed by the structural reporter groups for this type of Fuc, namely, H-1 (δ = 4.872) and CH_3 (δ = 1.201). The signals for GlcNAc-2 (H-1, δ = 4.681; NAc, δ = 2.093) also show the presence of the core fucose. No signals for the afuco analogue were detectable.

The biantennary type of branching was seen from the H-2 signals of Man-3, Man-4, and Man-4′, occurring at δ = 4.250, δ = 4.186, and δ = 4.108, respectively. This was consistent with the corresponding H-1 signals for Man-4 and Man-4′ at δ = 5.117 and δ = 4.922. The doublet at δ = 4.580 is assigned to GlcNAc-5′, and the doublet at δ = 4.554 to GlcNAc-5. Therefore, the *N*-acetyl signal at δ = 2.046 is assigned to GlcNAc-5′, and the signal at δ = 2.053 to GlcNAc-5.

Only one Gal seemed to be present and was localized in the Man α1→6 arm by comparison with compounds G Gn and Gn G described by Grey et al. (1982). G Gn was a biantennary glycopeptide terminating with Gal in the Man α1→6 arm and GlcNAc in the Man α1→3 arm. In glycopeptide Gn G, the terminal Gal was located in the Man α1→3 arm instead. The chemical shift of H-1 of Gal in the CSAT IgG glycopeptide was assigned at δ = 4.472. The placement of the Gal in the Man α1→6 arm is based on the chemical shift values of the NAc resonances of GlcNAc-5 and GlcNAc-5′ as well as the value of Man-4′ H-1 (see above). These values are in closer agreement with the structure of G Gn than of Gn G.

Evaluation of Variability in Expression of Glycosylation Phenotypes. Typically, parallel cultures of the same clone, grown under identical conditions, yielded very similar IgG glycopeptide elution profiles (Figure 5). However, comparison of the glycopeptide profiles of IgG secreted by different generations of the same clone revealed an interexperimental (generational) variability (Figure 5). Although the number of size classes remained constant, the relative distribution of all classes varied in a random fashion. One of the most dramatic changes was in the distribution of class III glycopeptides. The percentage of the total radioactivity incorporated into this size class varied nearly 3-fold between the different generations. This generational variability characterized by class III glycopeptides might account for the apparent clonal difference observed in the glycopeptide elution profile of H36.15.3 IgG (Figure 1C).

As culturing conditions are known to influence phenotypic heterogeneity in glycosylation (Buck et al., 1971; van Beek et al., 1975; Megaw & Johnson, 1979), several typical cultural differences were evaluated as a possible source of the interexperimental variability observed in this study. One such difference might be the pH of the culturing medium. Culturing hybridomas at either a lower or higher pH than normal

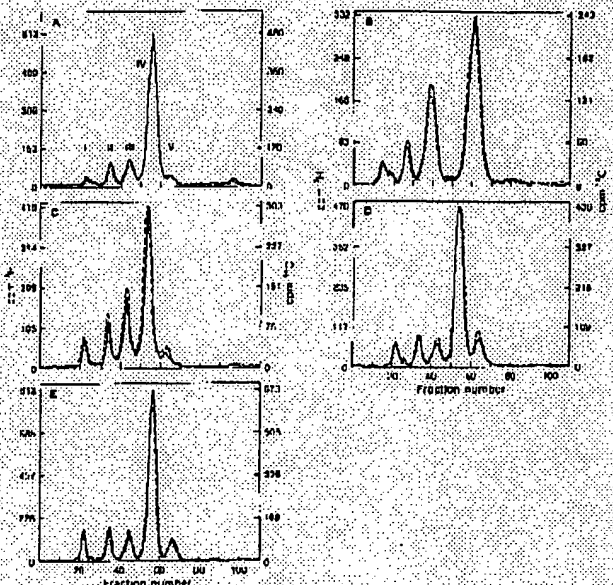

FIGURE 5: Generational variability in the glycosylation of IgG. CSAT hybridomas were cultured continuously in vitro for 16.5 months. At various times, parallel cultures were metabolically labeled with either [^{3}H]- or [^{14}C]glucosamine. The secreted IgG was affinity purified and digested with Pronase. The ^{14}C-labeled (—) and ^{3}H-labeled (---) Pronase digests obtained from parallel cultures of the same generation of CSAT were cochromatographed by alkaline borate GFC. The initial profile (A) and the profiles after culturing for an additional 2 (B), 10 (C), 13.5 (D), and 16.5 (E) months are presented.

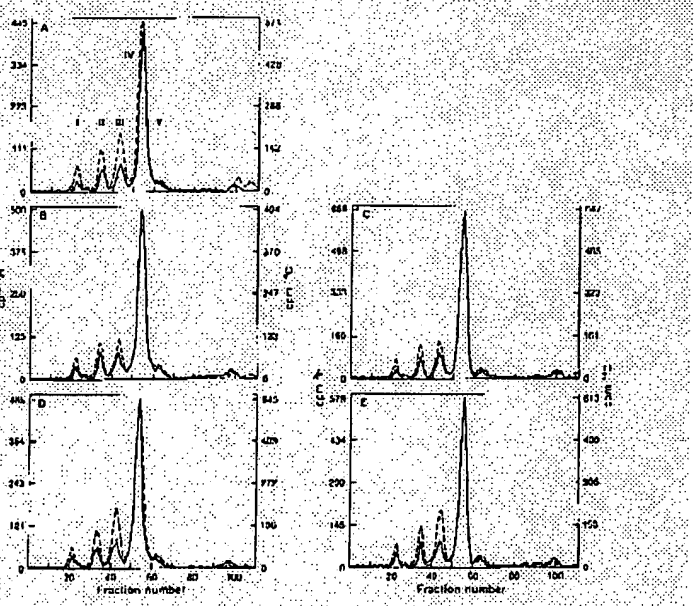

FIGURE 6: Effect of culture medium pH upon IgG glycosylation. Parallel cultures of CSAT, buffered with 10 mM $NaHCO_3$ and either 25 mM Pipes, pH 6.7 (A), 25 mM Hepes, pH 7.2 (B), 25 mM Tes, pH 7.2 (C), 25 mM Hepes, pH 8.0 (D), or 25 mM Hepps, pH 8.0 (E), were metabolically labeled with [^{3}H]glucosamine. The ^{3}H-labeled IgG Pronase digests (– –) were analyzed by alkaline borate GFC. A ^{14}C-labeled IgG Pronase digest (—) derived from an earlier generation of CSAT served as a common internal standard.

did enhance the distribution of glycopeptides of size classes I, II, and III (Figure 6). However, the variability in the relative distribution of class III glycopeptides was not as extensive as the observed generational variability depicted in Figure 5.

A second possible cultural difference could be the proliferative state of the hybridomas. To assess its effect upon the IgG glycopeptide elution profile, different inhibitors were

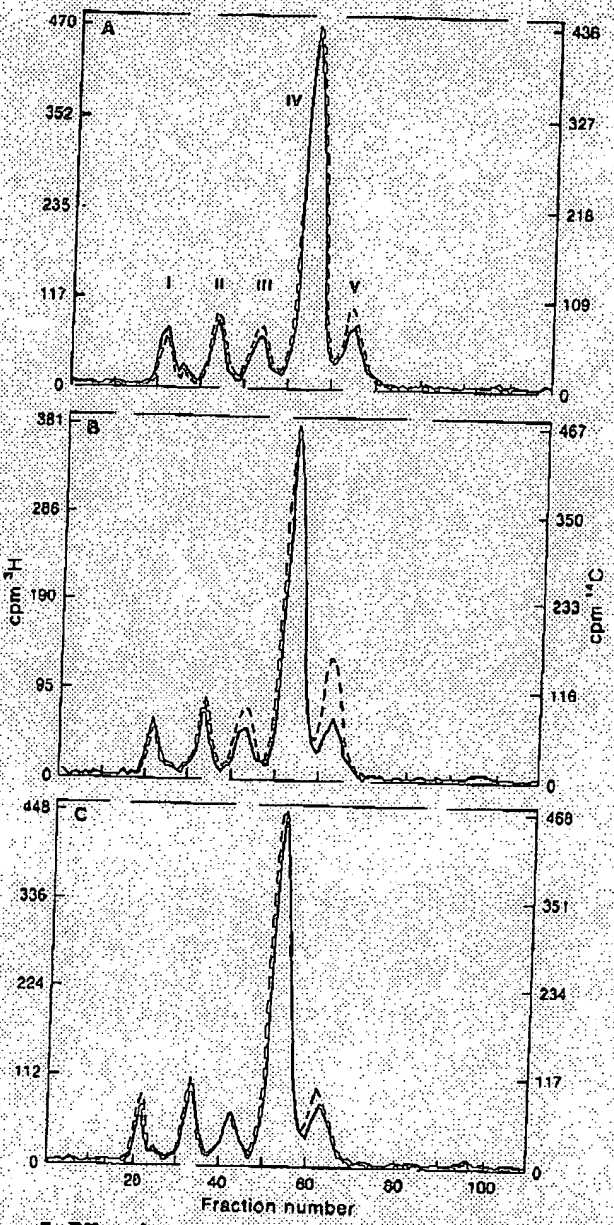

FIGURE 7: Effect of growth inhibitors upon IgG glycosylation. Parallel cultures of CSAT were metabolically labeled with [^{3}H]glucosamine in the absence (A) or presence of either 0.1 μg/mL vinblastine sulfate (B) or 10 mM thymidine (C) by the protocol described in under Materials and Methods. An additional culture of CSAT was metabolically labeled with [^{14}C]glucosamine in the absence of inhibitors. The secreted IgG was affinity purified and digested with Pronase. Aliquots of the ^{14}C-labeled digest (—), added as an internal standard, were cochromatographed by alkaline borate GFC with the ^{3}H-labeled digest (– –). Treatment with either inhibitor resulted in a 60% reduction in cell number.

chosen to synchronize the growth of the hybridomas at various stages of the cell cycle. Whereas thymidine (inhibition at G_1/S interphases) had no apparent influence upon glycosylation, vinblastine (inhibition in M phase) had a modest effect. This effect was particularly noticeable in the enhanced percentage of class V glycopeptides (Figure 7).

Discussion

Previously, we have shown that the CSAT hybridoma repertoire for glycosylation of IgG comprises a minimum of eight distinct phenotypes (Rothman & Warren, 1988). In the present study, six of these eight phenotypes were found to be commonly expressed by all ten clones analyzed and presumably reflect glycosylation of the same site located within the Fc portion of IgG. These clonally common phenotypes were characterized by glycopeptides of either low affinity, high affinity, or no affinity for Con A–Sepharose and were distributed differently by size between classes III and IV (plus V). Class IV and V glycopeptides differ from each other only by the size of the peptide remaining after exhaustive Pronase digestion (Rothman & Warren, 1988). The inability of Pronase to completely remove all amino acid residues surrounding the glycosylation site is characteristic of most glycoproteins and appears to be dependent upon the nature of the oligosaccharide (Kobata, 1984).

Despite the phenotypic heterogeneity in glycosylation of IgG, there is considerable similarity between different clones. In particular, virtually all Fc-derived oligosaccharides are believed to express a core fucose residue, as, typically, greater than 90% of IgG glycopeptides have affinity for LcH–agarose. Moreover, the majority of the IgG glycosylation by all hybridomas is of only two phenotypes. Of these, the predominantly expressed phenotype is the same for all clones. Upon digestion of IgG by Pronase, this phenotype is characterized chromatographically by neutral glycopeptides of size class IV (M_r ~2000) which are of high affinity for LCH–agarose but of low affinity for Con A–Sepharose. The second most prevalent phenotype is characterized by neutral glycopeptides also of size class IV, but which are of high affinity for Con A–Sepharose.

For CSAT IgG, the carbohydrate structure derived from the predominant phenotype has been identified by ^{1}H NMR. Similar structures are also the predominant ones expressed on rabbit (Taniguchi et al., 1985) and bovine (Tai et al., 1975) serum IgG, as well as on human myeloma IgG (Kornfeld & Kornfeld, 1980; Kornfeld et al., 1971). Chromatographic similarity of glycopeptides by four criteria (apparent size, charge, and affinity for two lectins) suggests that a similar oligosaccharide also is the predominant one expressed on all IgG secreted by our panel of murine hybridomas. Due to its high affinity for Con A–Sepharose, the second most prevalent phenotype is consistent with the expression of an oligosaccharide similar to the predominant one, but lacking the single galactosyl residue, such that both branches terminate with *N*-acetylglucosamine (Narasimhan et al., 1979).

Very recently, Mizuochi et al. (1987) have elucidated the structure of the oligosaccharides expressed on IgG from pooled murine serum. The major structure is identical with the predominant one identified for CSAT IgG in the present study. Furthermore, they have reported that 94% of the oligosaccharides are core fucosylated and that 80% bear either a single galactose residue or none, which is consistent with our analysis by lectin affinity.

Interestingly, though, we find that a lesser percentage of sialylated structures are expressed on IgG secreted by murine hybridomas than Mizuochi et al. (1987) reported for murine serum IgG. Whereas a comparable percentage of murine, rabbit, and human serum IgG is sialylated, there is considerable variability in the (Fc) sialylation of human myeloma IgG (Mizuochi et al., 1987, 1982; Taniguchi et al., 1985). Thus, the reduction in sialylation we observe may be a feature of murine hybridomas, perhaps as a consequence of the somatic hybridization of two cell types.

Variability in Expression of Glycosylation Phenotypes. As anticipated, there is some variability in the relative expression of the various phenotypes. In part, some of this variability is clonal in origin. For example, significant variability between different hybridomas exists in the relative expression of the two major phenotypes characterized by glycopeptides which

bind to Con A–Sepharose but which differ in their affinity. In some instances, other differences between clones may reflect the expression of an additional site which is glycosylated differently. This is exemplified by class I and II IgG glycopeptides derived from CSAT, which are sialylated and lack affinity for Con A (Rothman & Warren, 1988). However, there is no phenotype which appears to be uniquely characteristic of either the hybridoma's parentage or the serologically defined polypeptide structure of the IgG which it secretes.

Instead, there appears to be a continuum of shared phenotypes. Although the predominantly expressed one is always the same, these phenotypes otherwise are variably expressed in an apparently random fashion by the different clones. To some extent, this may be a consequence of the variability in glycosylation evident between different generations of the same hybridoma upon continuous culturing. This generational variability does not influence the number of phenotypes expressed. Rather, it results in a random drift in the relative expression of these phenotypes, particularly the one characterized by class III glycopeptides.

Anderson et al. (1985) also have reported what appears to be a generational variability in glycosylation of mouse myeloma IgM. By contrast, Sweidler et al. (1985) have reported stability in glycosylation of major histocompatibility complex (MHC) antigens by lymphomas. Whether this discrepancy reflects intrinsic differences between cell surface and secreted glycoproteins is uncertain. Alternatively, generational variability may be an intrinsic feature of immunoglobulins.

Lastly, some variability in phenotypic expression of glycosylation may be a consequence of differences in culturing conditions of the hybridomas. However, typical culturing differences which would be anticipated, such as culture medium pH and proliferation status, have only a modest influence upon the IgG glycopeptide elution profile. In fact, a survey of environmental challenges, including a comparison of the effect of growth of hybridomas in vitro with that in vivo, revealed only occasional differences in the relative expression of the various phenotypes, whereas the nature of the predominant phenotype remained conserved (unpublished data).

The relative clonal similarity in IgG glycosylation poses an intriguing question. If a single, predominant phenotype is sufficiently important enough to have been conserved, why is there phenotypic heterogeneity? One possibility might be that glycosylation defines functional subsets of mAb. Thus, heterogeneity in effector function might be a consequence of structural heterogeneity in glycosylation. Studies to determine the effect of metabolically induced structural alterations in glycosylation upon IgG effector function should help to answer this question.

ACKNOWLEDGMENTS

The secretarial assistance of Marie Lennon and editing by Marina Hoffman are gratefully acknowledged.

Registry No. IgG carbohydrate, 70308-40-6.

REFERENCES

Abel, C. A., Spiegelberg, H. L., & Grey, H. M. (1968) *Biochemistry 7*, 1271–1278.

Anderson, D. R., Atkinson, P. H., & Grimes, W. J. (1985) *Arch. Biochem. Biophys. 243*, 605–618.

Beale, D., & Feinstein, A. (1976) *Q. Rev. Biophys. 9*, 135–180.

Blithe, D. L., Buck, C. A., & Warren, L. (1980) *Biochemistry 19*, 3386–3395.

Buck, C. A., Glick, M. C., & Warren, L. (1971) *Biochemistry 10*, 2176–2180.

Burton, D. R. (1985) *Mol. Immunol. 22*, 161–206.

Chandrasekaran, E. V., Mendicino, A., Garver, F. A., & Mendicino, J. (1981) *J. Biol. Chem. 256*, 1549–1555.

Cummings, R. D., & Kornfeld, S. (1982) *J. Biol. Chem. 257*, 11235–11240.

Deutscher, S. L., & Hirschberg, C. B. (1986) *J. Biol. Chem. 261*, 96–100.

Ey, P. L., Prowse, S. J., & Jenkin, C. R. (1978) *Immunochemistry 15*, 429–436.

Grey, A. A., Narasimhan, S., Brisson, J.-R., Schachter, H., & Carver, J. P. (1982) *Can. J. Biochem. 60*, 1123–1131.

Haruda, H., Kamei, M., Tokumoto, Y., Yui, S., Koyama, F., Kochibe, N., Endo, T., & Kobata, A. (1987) *Anal. Biochem. 164*, 374–381.

Hsieh, P., Rosner, M. R., & Robbins, P. W. (1983) *J. Biol. Chem. 258*, 2548–2554.

Hubbard, S. C., & Ivatt, R. J. (1981) *Annu. Rev. Biochem. 50*, 555–583.

Knudsen, K. A., Rao, P. E., Damsky, C. H., & Buck, C. A. (1981) *Proc. Natl. Acad. Sci. U.S.A. 78*, 6071–6075.

Kobata, A. (1984) in *Biology of Carbohydrates* (Ginsburg, V., & Robbins, P. W., Eds.) Vol. 2, pp 87–161, Wiley, New York.

Kornfeld, K., Reitman, M. L., & Kornfeld, R. (1981) *J. Biol. Chem. 256*, 6633–6640.

Kornfeld, R., & Kornfeld, S. (1980) in *Biochemistry of Glycoproteins and Proteoglycans* (Lennarz, W. J., Ed.) Chapter 1, Plenum Press, New York.

Kornfeld, R., & Kornfeld, S. (1985) *Annu. Rev. Biochem. 54*, 631–664.

Kornfeld, R., Keller, J., Baenziger, J., & Kornfeld, S. (1971) *J. Biol. Chem. 246*, 3259–3268.

Lebman, D., Trucco, M., Bottero, L., Lange, B., Pessano, S., & Rovera, G. (1982) *Blood 59*, 671–678.

Mcgaw, J. M., & Johnson, L. D. (1979) *Proc. Soc. Exp. Biol. Med. 161*, 60–65.

Miller, S. L., Pleasure, D., Herlyn, M., Atkinson, B., Ernst, C., Tachovsky, T. G., & Baird, L. (1984) *J. Neurochem. 43*, 394–400.

Mizuochi, T., Taniguchi, T., Shimizu, A., & Kobata, A. (1982) *J. Immunol. 129*, 2016–2020.

Mizuochi, T., Hamako, J., & Titani, K. (1987) *Arch. Biochem. Biophys. 257*, 387–394.

Narasimhan, S., Wilson, J. R., Martin, E., & Schachter, H. (1979) *Can. J. Biochem. 57*, 83–96.

Neff, N. T., Lowrey, C., Decker, C., Tovar, A., Damsky, C., Buck, C., & Horwitz, A. F. (1982) *J. Cell Biol. 95*, 654–666.

Ozato, K., Mayer, N. M., & Sachs, D. H. (1982) *Transplantation 34*, 113–120.

Parekh, R. B., Dwek, R. A., Sutton, B. J., Fernandes, D. L., Leung, A., Stanworth, A. L., Rademacher, T. W., Mizuochi, T., Taniguchi, T., Matsuta, K., Takeuchi, T., Nagano, Y., Miyamoto, T., & Kobata, A. (1985) *Nature 316*, 452–457.

Parekh, R. B., Tse, A. G. D., Dwek, R. A., Williams, A. F., & Rademacher, T. W. (1987) *EMBO J. 6*, 1233–1244.

Perussia, B., Kobayashi, M., Rossi, M. E., Anegon, I., & Trinchieri, G. (1987) *J. Immunol. 138*, 765–774.

Rademacher, T. W., Homans, S. W., Fernandes, D. L., Dwek, R. A., Mizuochi, T., Taniguchi, T., & Kobata, A. (1983) *Biochem. Soc. Trans. 11*, 132–134.

Rao, A. K., & Mendicino, J. (1978) *Biochemistry 17*, 5632–5638.

Rothman, R., & Warren, L. (1988) *Biochim. Biophys. Acta 955*, 143–153.

Savvidou, G., Klein, M., Grey, A. A., Dorrington, K. J., & Carver, J. P. (1984) *Biochemistry 23*, 3736–3740.
Sheares, B. T., & Robbins, P. W. (1986) *Proc. Natl. Acad. Sci. U.S.A. 83*, 1993–1997.
Sox, H. C., Jr., & Hood, L. (1970) *Proc. Natl. Acad. Sci. U.S.A. 66*, 975–982.
Spiegelberg, H. L., Abel, C. A., Fishkin, B. G., & Grey, H. M. (1970) *Biochemistry 9*, 4217–4223.
Stanley, P. (1984) *Annu. Rev. Genet. 18*, 525–552.
Staudt, L. M., & Gerhard, W. (1983) *J. Exp. Med. 157*, 687–704.
Swiedler, S. J., Freed, J. H., Tarentino, A. L., Plummer, T. H., Jr., & Hart, G. (1985) *J. Biol. Chem. 260*, 4046–4054.
Tai, T., Setsuko, I., Yamashita, K., Muramatsu, T., & Kobata, A. (1975) *Biochem. Biophys. Res. Commun. 65*, 968–974.
Takahashi, N., Ishii, I., Ishihara, H., Mori, M., Tejima, S., Jefferis, R., Endo, S., & Arata, Y. (1987) *Biochemistry 26*, 1137–1144.
Taniguchi, T., Mizuochi, T., Beale, M., Dwek, R. A., Radcmacher, T. W., & Kobata, A. (1985) *Biochemistry 24*, 5551–5557.
van Beek, W. P., Smets, L. A., & Emmelot, P. (1975) *Nature (London) 253*, 457–460.
Vliegenthart, J. F. G., Dorland, L., & van Halbeek, H. (1983) *Adv. Carbohydr. Chem. Biochem. 41*, 209–374.
Warren, L., Blithe, D. L., & Cossu, G. (1982) *J. Cell. Physiol. 113*, 17–22.
Warren, L., Baker, S. R., Blithe, D. L., & Buck, C. A. (1983) in *Biomembranes* (Nowotny, A., Ed.) Vol. 11, pp 53–77, Plenum Press, New York.

Effect of Homo Poly(L-amino acids) on Fibrin Assembly: Role of Charge and Molecular Weight

Marcus E. Carr, Jr.,[‡] Roy Cromartie,[§] and Don A. Gabriel*[,§]

Division of Hematology/Oncology, Department of Medicine, Medical College of Virginia, Richmond, Virginia 23249, and Center for Thrombosis and Hemostasis, Department of Medicine, University of North Carolina School of Medicine, Chapel Hill, North Carolina 27599-7035

Received June 27, 1988; Revised Manuscript Received August 23, 1988

ABSTRACT: Positively charged molecules such as protamine, leukocyte cationic protein, and the carboxyl terminus of platelet factor 4 have been shown to increase fibrin fiber thickness. Synthetic homo poly(L-amino acids) were used to explore the role of charge and molecular weight of cationic molecules on fibrin assembly. The effects of poly(L-lysine) (PLL), poly(L-glutamic acid) (PLG), poly(L-aspartic acid) (PLA), poly(L-histidine) (PLH), and poly(L-arginine) (PLArg) on the assembly and structure of fibrin gels were studied by using light-scattering techniques. At a PLG (M_r 60 000) concentration of 80 μg/mL and a PLA (M_r 20 000) concentration of 64 μg/mL, neither of these negatively charged polymers produced a detectable change in either fibrin assembly kinetics or final structure. Positively charged PLArg (16 μg/mL) caused a 30% increase in fibrin fiber mass/length ratio without calcium. In contrast, PLH (16 μg/mL), also positively charged, had no effect in the absence of $CaCl_2$ but produced a 40% increase in fiber mass/length ratio with 5 mM $CaCl_2$. At concentrations as low as 1 μg/mL, positively charged PLL increased the initial fibrin assembly kinetics and led to larger fiber mass/length ratio. The impact on fibrin mass/length ratio was equivalent for three different molecular weight preparations of PLL (M_r 25 000, 90 000, and 240 000). The lack of a molecular weight effect on fiber thickness and the low polymer concentrations required to produce the perturbation argue against an excluded volume effect as the mechanism by which lateral fiber growth is augmented. Mechanisms by which poly(L-amino acids) may perturb fibrin assembly are discussed.

Fibrinogen normally circulates as a soluble asymmetric protein, M_r 340 000, until the amino-terminal peptide, fibrinopeptide A, is enzymatically removed by thrombin. The subsequent fibrin polymerization kinetics and resulting fibrin structure are exquisitely sensitive to and modified by the microenvironment in which fibrin assembly occurs (Jones & Gabriel, 1988). Small shifts in pH, ionic strength, or calcium concentration during the assembly process result in dramatic changes in the material properties of fibrin (Ferry, 1947; Shulman et al., 1953a,b; Shen et al., 1975; Latallo et al., 1962; Carr et al., 1986a,b). Agents with known positive charge, including protamine (Stewart et al., 1969), dextran (Carr & Gabriel, 1980), and hydroxyethyl starch (Carr, 1986), have been shown to modify the final clot structure. Recently, native plasma proteins such as immunoglobulins (Gabriel et al., 1983), histidine-rich protein (Leung, 1986), leukocyte cationic protein (Carr et al., 1986a,b), thrombospondin (Bale et al., 1986), platelet factor 4 (Carr et al., 1987), and actin (Janmey et al., 1985) have been reported to alter fibrin assembly kinetics and fibrin material properties. The roles of molecular charge and size of nonpolymerizing perturbing molecules in determining fibrin assembly kinetics and structure remain incompletely examined. This study reports the effects of charged synthetic homo poly(L-amino acids) of varying size and charge

* Address correspondence to this author at the Division of Hematology, Department of Medicine, CB 7035, University of North Carolina School of Medicine, Chapel Hill, NC 27599-7035.
‡ Medical College of Virginia.
§ University of North Carolina School of Medicine.

0006-2960/89/0428-1384$01.50/0

Biochemistry

Volume 28
Number 3
February 7, 1989

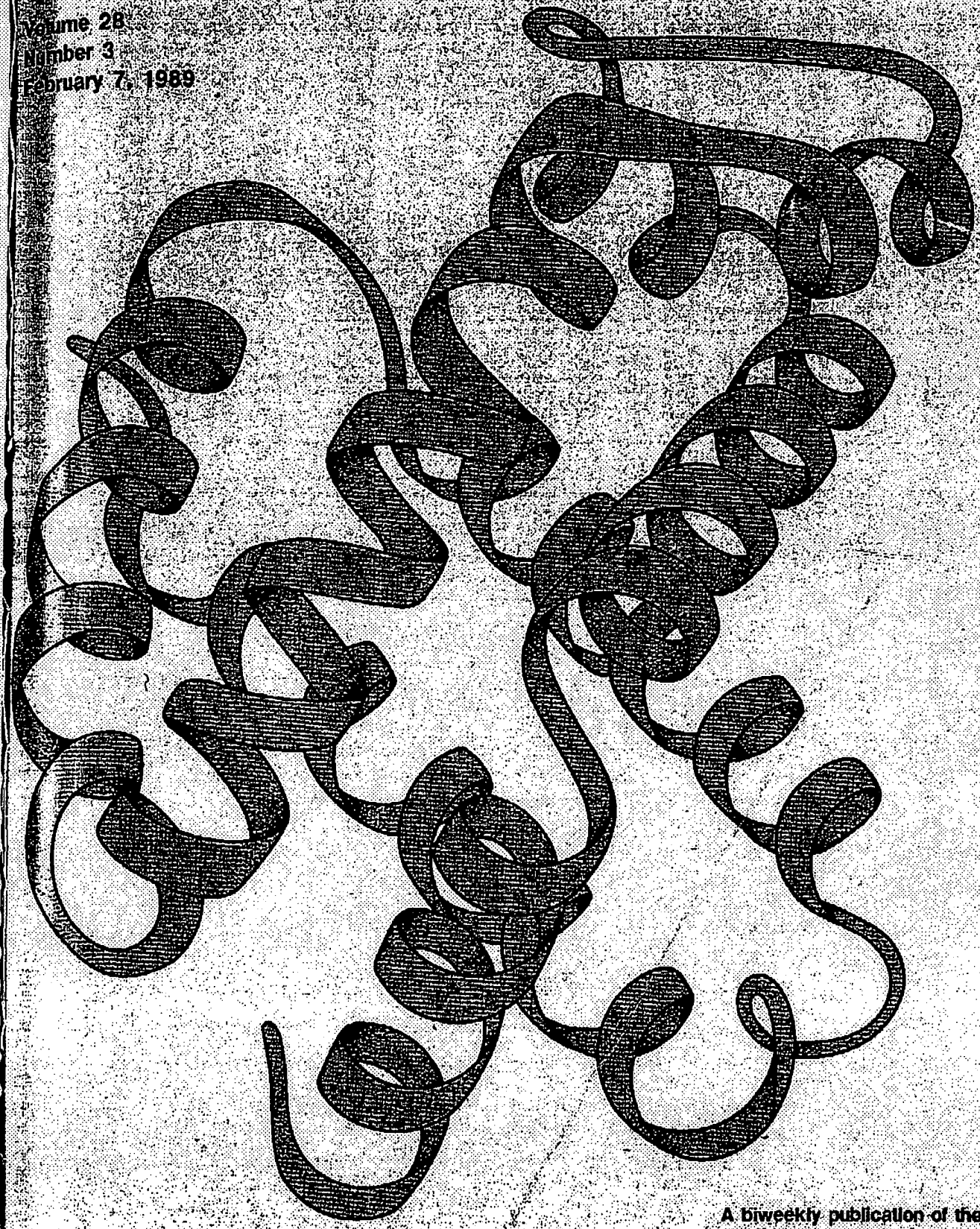

A biweekly publication of the
American Chemical Society

Biochemistry

Biochemistry (ISSN 0006-2960) is published biweekly by the American Chemical Society at 1155 16th Street, N.W., Washington, D.C. 20036. Second-class postage paid at Washington, D.C., and additional mailing offices. POSTMASTER: Send address changes to *Biochemistry*, Member & Subscriber Services, P.O. Box 3337, Columbus, Ohio 43210.

American Chemical Society
1155 16th Street, N.W.
Washington, D.C. 20036
(202) 872-4600
TDD (202) 872-8733

Member & Subscriber Services
American Chemical Society
P.O. Box 3337, Columbus, Ohio 43210
(614) 447-3776
(800) 333-9511

Journals Department
American Chemical Society
2540 Olentangy River Road
P.O. Box 3330, Columbus, Ohio 43210
(614) 447-3600, ext 3171
TELEX 6842086; FAX (614) 447-3745

Publications Division
Robert H. Marks, Director

JOURNALS DEPARTMENT
Charles R. Bertsch, Head; Marianne C. Brogan, Associate Head; Mary E. Scanlan and Joseph E. Yurvati, Journals Editing Managers; Deborah K. Miller, Senior Associate Editor; Darrell McGeorge, Eileen M. Richardson, Beth A. Rogers, and Barbara I. Taylor, Assistant Editors; Brenda S. Wooten, Staff Editor

Advertising Office: Centcom, Ltd., 500 Post Road East, Westport, Connecticut 06880

The paper used in this publication meets the minimum requirements of American National Standard for Information Sciences—Permanence of Paper for Printed Library Materials, ANSI Z39.48-1984. ♾

Editorial Information

Instructions to authors and copyright status form are printed in the first issue of each volume. Please conform to these instructions when submitting manuscripts.

Manuscripts for publication should be submitted to the Editor, Hans Neurath, Department of Biochemistry, University of Washington, Seattle, Washington 98195. Correspondence regarding accepted papers and proofs should be directed to the Journals Department at the address above. Page charges of $30.00 per page may be paid for papers published in this journal. Payment does not affect acceptance or scheduling of papers. Bulk reprints of individual articles are available. For information write to Distribution Office at the ACS Washington address.

The American Chemical Society and its Editors assume no responsibility for the statements and opinions advanced by contributors.

Registered names and trademarks, etc., used in this publication, even without specific indication thereof, are not to be considered unprotected by law.

Subscription and Business Information

Subscriptions are available only on a calendar year basis. (For membership information, contact Office of Membership Development at the ACS Washington address.)

New and renewal subscriptions should be sent with payment to Financial Operations & Controller, ACS, P.O. Box 57136, West End Station, Washington, D.C. 20037. Rates do not apply to nonmember subscribers in Japan, who must enter subscription orders with Maruzen Company Ltd., 3-10 Nihonbashi 2-chome, Chuo-ku, Tokyo 103, Japan. Tel: (03) 272-7211.

1989 subscription prices including postage.

	U.S.	Canada and Mexico	Europe*	All Other Countries*
Printed				
Members—1 yr	$ 80	$140	$237	$342
2 yr	$144	$264	$458	$668
Nonmembers	$549	$609	$706	$811
Microfiche				
Members—1 yr	$ 80	$ 80	$105	$105
2 yr	$144	$144	$194	$194
Nonmembers	$549	$549	$574	$574
Supplementary material on microfiche	$ 30	$ 44	$ 44	$ 44

* Air service included.

Printed edition single issue prices: current year $21.50; prior year $23.00. Back volume price: $584.00. Foreign postage additional. Mail orders should be sent to Microforms & Back Issues Office at the ACS Washington address.

Phone orders can be placed for printed, microfiche, and microfilm editions by calling the ACS TOLL FREE at (800) 333-9511 from anywhere in the continental United States. Phone orders can be charged to Visa, MasterCard, or American Express accounts.

Changes of address must include both old and new addresses with ZIP code and a recent mailing label. Send all address changes to Member & Subscriber Services. Please allow 6 weeks for change to become effective. Claims for missing numbers will not be allowed if loss was due to failure of notice of change of address to be received in the time specified; if claim is dated (a) North America, more than 90 days beyond issue date; (b) all other foreign, more than 180 days beyond issue date. Hard copy claims are handled by Member & Subscriber Services.

Supplementary material is noted in the table of contents with a ■. It is available as photocopy ($10.00 for up to 3 pages and $1.50 per page for additional pages, plus $2.00 for foreign postage) or as 24× microfiche ($10.00, plus $1.00 for foreign postage). See supplementary material notice at end of journal article for number of pages. Orders *must* state whether for photocopy or microfiche and give complete title of article, names of authors, journal, issue date, and page numbers. Prepayment is required and prices are subject to change. Order from Microforms & Back Issues Office at the ACS Washington address. Supplementary material except structure factors also appears in the microfilm edition and may be ordered by subscription (in microfiche only).

Cover: Based on apohemoglobin β subunit—courtesy of Jane S. Richardson.

Volume 26, Number 12, December 1989 ISSN 0161-5890

Molecular Immunology

The List of Contents and Author Index for Volume 26, 1989, are bound in at the back of this issue

Pergamon Press

Oxford · New York · Beijing · Frankfurt · São Paulo · Sydney
Tokyo · Toronto

Molecular Immunology

Publishing and Advertising Offices: Pergamon Press plc, Headington Hill Hall, Oxford OX3 0BW, U.K., and Pergamon Press Inc., Maxwell House, Fairview Park, Elmsford, NY 10523, U.S.A. Published monthly. Annual institutional subscription rate (1990) DM 1160.00. Two year institutional rate (1990/91) DM 2204.00. Personal subscription rate for those whose library subscribes at the regular rate (1990) DM 167.00. Subscription enquiries from customers in North America should be sent to: Pergamon Press Inc., Maxwell House, Fairview Park, Elmsford, NY 10523, U.S.A., and for the remainder of the world to: Pergamon Press plc, Headington Hill Hall, Oxford OX3 0BW, U.K. Prices are subject to change without notice.

Microform Subscriptions and Back Issues

Back issues of all previously published volumes are available direct from Pergamon Press offices.

™ The paper used in this publication meets the minimum requirements of American National Standard for Information Sciences—Permanence of Paper for Printed Library Materials, ANSI Z39.48-1984.

Molecular Immunology, Vol. 26, No. 12, pp. 1113–1123, 1989
Printed in Great Britain.

0161-5890/89 $3.00 + 0.00
Pergamon Press plc

ANTIBODY-DEPENDENT CYTOTOXICITY MEDIATED BY NATURAL KILLER CELLS IS ENHANCED BY CASTANOSPERMINE-INDUCED ALTERATIONS OF IgG GLYCOSYLATION*

RONALD JAY ROTHMAN,† BICE PERUSSIA, DOROTHEE HERLYN and LEONARD WARREN‡
The Wistar Institute of Anatomy and Biology, Philadelphia, PA 19104, U.S.A.

(*First received 22 February 1989; accepted in revised form 18 May 1989*)

Abstract—Inhibitors of glycosylation and carbohydrate processing were used to probe the functional consequences of specific, differential alterations in glycosylation of monoclonal IgG secreted by hybridoma clones. Neither the absence of glycosylation nor the presence of atypical oligosaccharides significantly influenced binding of the monoclonal antibody to the cell surface antigen recognized. However, lymphocyte-mediated antibody-dependent cytotoxicity was enhanced significantly, as compared to native (unmodified) IgG-sensitized target cells, when target cells were sensitized with IgG bearing the atypical oligosaccharides induced metabolically by castanospermine, *N*-methyldeoxynojirimycin, deoxymannojirimycin or monesin, but not by swainsonine. The enhanced cytotoxicity was mediated by natural killer cells but not by monocytes or interferon-activated polymorphonuclear leukocytes. By contrast, antibody-dependent cytotoxicity mediated by activated polymorphonuclear leukocytes against target cells sensitized with the IgG glycosylation phenotypes induced by swainsonine and tunicamycin, but not by castanospermine, was decreased in comparison to cytotoxicity against target cells sensitized with native IgG.

The enhanced lymphocyte-mediated cytotoxicity was Fc receptor-dependent.

A panel of monoclonal antibodies directed against different human tumor target cells was used to demonstrate that the castanospermine-induced IgG phenotype generally enhanced antibody-dependent tumoricidal activity mediated by natural killer cells. However, differences in lymphocyte response to an alteration in IgG glycosylation were observed.

INTRODUCTION

A similar site of glycosylation is located within the Fc portion of IgG from different species (Howell *et al.*, 1967). Conservation of Fc glycosylation would suggest a functional importance for this moiety. The role of glycosylation has been studied by depleting IgG of its carbohydrates either enzymatically, by treatment of hyperimmune rabbit IgG with glycosidases (Winkelhake *et al.*, 1980, Koide *et al.*, 1977), or metabolically by treatment of IgG-secreting murine hybridomas and myelomas with tunicamycin (Leatherbarrow *et al.*, 1985; Nose and Wigzell, 1983).

Carbohydrates covalently bound to the IgG protein backbone are not necessary for either proper assemblage or secretion of IgG, as shown in studies using IgG from murine myeloma or hybridoma cells cultured in the presence of tunicamycin (Leatherbarrow *et al.*, 1985; Leatherbarrow and Dwek, 1983; Nose and Wigzell, 1983; Hickman and Kornfeld, 1978). Similar results have been obtained by Weitzman and Scharff (1976), using a mutant mouse myeloma that synthesized a polypeptide-deleted IgG heavy chain with a partial block in glycosylation.

Deglycosylation does not seem to alter significantly the antigen-binding properties of IgG antibodies, as aglycosylated IgG secreted by tunicamycin-treated hybridomas have been shown to maintain the same antigen-binding affinity as their glycosylated forms (Nose and Wigzell, 1983; Leatherbarrow and Dwek, 1983). Similarly, enzymatic deglycosylation of hyperimmune rabbit IgG with β-aspartyl-*N*-acetylglucosamidohydrolase has no effect upon antigen-binding (Winkelhake *et al.*, 1980).

However, depletion of carbohydrates, either from rabbit IgG or from murine IgG secreted by hybri-

*This work was supported by grants CA 19130, CA 37155, and CA 45284 from USPHS. R. J. Rothman was supported by training grant CA 09171 from USPHS. B. Perussia is a Scholar of The Leukemia Society of America.

†Present address: Jefferson Medical College, Department of Pathology and Cell Biology, Philadelphia, PA 19107, U.S.A.

‡Author to whom correspondence should be addressed.

Abbreviations: FcR, receptor for the Fc fragment of IgG; ADCC, antibody-dependent cell-mediated cytotoxicity; Cs, castanospermine; DMM, deoxymannojirimycin; MdNM, *N*-methyldeoxynojirimycin; Mon, monensin; Sw, swainsonine; Tm, tunicamycin; NK, natural killer; PBL, peripheral blood lymphocyte; PMN, polymorphonuclear leukocyte; GFC, gel filtration chromatography; Endo H, endo-β-*N*-acetylglucosaminidase H; Con A, concanavalin A; LcH, *Lens culinaris* agglutinin; RIA, radioimmunoassay; mAb, monoclonal antibody; r-IFNγ, recombinant immune interferon; HI-FBS, heat-inactivated fetal bovine serum; PBS, 137 m*M* NaCl/3 m*M* KCl/8 m*M* Na_2HPO_4/1.5 m*M* KH_2PO_4 (pH 7.4); TBS, 150 m*M* NaCl/10 m*M* Tris/1 m*M* $CaCl_2$/1 m*M* $MgCl_2$/0.02% NaN_3 (pH 8).

domas, results in significantly lower binding to Fc receptors (FcR) expressed on human monocytes and murine macrophages (Leatherbarrow *et al.*, 1985; Nose and Wigzell, 1983; Koide *et al.*, 1977). Presumably, the decreased binding of carbohydrate-deficient IgG antibodies to FcR I accounts for the decreased antibody-dependent cytotoxicity (ADCC) mediated by murine macrophages and splenocytes against target cells sensitized with carbohydrate-deficient IgG (Nose and Wigzell, 1983; Koide *et al.*, 1977).

Although these studies suggest that glycosylation of the IgG antibodies used to sensitize the target cell plays a role in ADCC, these studies do not address the question of the functional significance of individual types of IgG oligosaccharides. In fact, an array of 31 structurally distinct, yet related, oligosaccharides are expressed on human IgG (Parekh *et al.*, 1985) and approximately half of these oligosaccharides are found on mouse IgG as well (Mizuochi *et al.*, 1987).

Recently, a series of carbohydrate processing inhibitors have become available. These inhibitors interfere with discrete steps involved in the maturation of protein-bound oligosaccharides (Elbein, 1987). Castanospermine (Cs) and *N*-methyldeoxynojirimycin (MdNM) are chemically dissimilar glucosidase inhibitors that interfere with an early step of carbohydrate processing. The next steps involve removal of different mannosyl residues by two distinct mannosidases. The first of these mannosidases is inhibited by deoxymannojirimycin (DMM), whereas the later-acting mannosidase is inhibited by swainsonine (Sw). These trimming reactions are necessary for the oligosaccharides to acquire structures able to interact subsequently with glycosyltransferases. These transferases catalyze the terminal elongations characteristic of the mature oligosaccharides found on secreted glycoproteins. Although the effect of monensin (Mon) is less certain, it appears to uncouple the trimming reactions from the terminal elongations of the oligosaccharides. Several of these inhibitors, tested on rat hybridomas, have no effect upon IgG secretion (Hashim and Cushley, 1987, 1988).

In this report, we describe the functional effects of alterations in IgG glycosylation induced by inhibitors of glycosylation and carbohydrate processing. The structural alterations have been characterized and correlated with their effect upon ADCC mediated by various populations of human peripheral blood leukocytes. Our data suggests a possible involvement of core fucosylation of IgG in NK cell-mediated ADCC.

MATERIALS AND METHODS

Materials

D-[1-^{14}C]-Glucosamine hydrochloride (284 Ci/mol), D-[6(*N*)-^{3}H]-glucosamine hydrochloride (23.4 Ci/mmol), $Na_2{}^{51}CrO_4$ and En^{3}Hance were purchased from New England Nuclear (Boston, MA). Sephadex G-50 (Superfine), Con A–Sepharose and Protein A–Sepharose were obtained from Pharmacia Fine Chemicals (Piscataway, NJ). LcH (E-Y Laboratories, San Mateo, CA) was conjugated to Affigel 10 (Bio-Rad, Richmond, CA) (7 mg/ml resin) according to an established procedure (Knudsen *et al.*, 1981). Endoglycosidase H (endo-β-*N*-acetylglucosaminidase H) was purchased from Genzyme (Boston, MA), and Pronase (grade B) was from CalBiochem (San Diego, CA). r-IFNγ was purchased from Genentech, Inc. (San Francisco, CA).

Castanospermine was supplied initially by Dr R. J. Molyneux (Agricultural Research Service, USDA, Albany, CA), and later was purchased from Genzyme. Deoxymannojirimycin similarly was purchased from Genzyme; tunicamycin and monensin were from Sigma (St Louis, MO). *N*-Methyldeoxynojirimycin was a gift from Dr R. J. Schwarz (Institut für Virologie der Justus-Liebig, Giessen, F.R.G.). Swainsonine was obtained from Drs D. R. P. Tulsiani (Vanderbilt University, Nashville, TN) and P. R. Dorling (Murdoch University, Murdoch, Western Australia).

Murine hybridoma clones and monoclonal IgG

Description of hybridomas. 34-5-8S hybridomas were obtained from the American Type Culture Collection (Rockville, MD). These cells secrete an IgG2a mAb with specificity for the H-2D^{d} alloantigen (Ozato *et al.*, 1982).

A panel of hybridomas that secrete mAbs to human tumor antigens was previously described (Herlyn *et al.*, 1979, 1983, 1985; Mazauric *et al.*, 1982; Mitchell *et al.*, 1982). All mAbs were of IgG2a isotype. The mAbs ME-288, ME-5073 and ME-37-7 are directed against antigens expressed on WM-9, a human melanoma cell line. CO-17-1A is directed against an antigen expressed on SW-1116, a human colorectal carcinoma cell line, and LU-16B13 recognizes an antigen present on both tumor cell lines.

Culturing conditions. Hybridomas, seeded at 5×10^5/ml, were cultured in Dulbecco's Modified Eagle Medium with low glucose (Gibco, Grand Island, NY), supplemented with 10% HI-FBS, 10 m*M* sodium bicarbonate and 25 m*M* Hepes (pH 7.2). Parallel cultures were grown in the presence or absence of either Tm (0.25 μg/ml), Cs (10 μg/ml), MdNM (1 m*M*), DMM (1 m*M*), Sw (2 μg/ml), or Mon (0.25 μ*M*). For structural characterization studies, cultures were pre-incubated for 20 hr, and then metabolically labelled with either [^{3}H]-glucosamine (2 μCi/ml) or [^{14}C]-glucosamine (0.5 μCi/ml) for an additional 48 hr. Replicate cultures for each condition remained unlabelled for functional studies. In some instances, the cells were cultured in RPMI 1640 medium supplemented with 10% HI-FBS and 2 m*M* glutamine (complete RPMI).

Isolation of IgG. IgG in the spent culture medium were affinity-purified chromatographically on Protein

A-Sepharose by a modification of the procedure of Ey *et al.* (1978). Unlabelled, affinity-purified IgG used for functional studies were dialyzed against PBS. All manipulations were performed at 4°C. Protein concn in each IgG preparation was determined fluorimetrically by conjugation with fluorescamine (Bohlen *et al.*, 1973).

Pronase and Endo H digestions. For structural characterization studies, metabolically labelled, affinity-purified IgG were incubated with pre-digested pronase for 3 days according to an established procedure (Blithe *et al.*, 1980). The pronase digests were heat-inactivated by boiling for 5 min, and then lyophilized. In some instances, the residue was suspended in 200 m*M* sodium citrate/citric acid (pH 5.5), and incubated at 37°C for 21 hr with 10 mU of Endo H (50 mU/ml, final concn).

Structural characterization studies of IgG glycosylation

To insure consistency of elution profiles, a ^{14}C-labelled IgG pronase digest was added as an internal standard to all ^{3}H-labelled samples. The resulting doubly-labelled mixture of pronase digests was analyzed chromatographically using various techniques. The radioactive distribution in each chromatographic fraction, determined by liquid scintillation counting, was plotted by computer-aided graphics, which also provided peak area summations.

Alkaline borate gel filtration chromatography. Blue dextran and phenol red, added to the sample, served as exclusion and inclusion volume markers, respectively. Samples were analyzed on Sephadex G-50 columns (1 × 135 cm), equilibrated and developed with an alkaline borate buffer composed of 45.5 m*M* boric acid/4.5 m*M* sodium tetraborate/2 m*M* Na_2-EDTA/0.02% sodium azide (pH 8.2) (Rothman and Warren, 1988). The nominal flow rate was 3 ml/hr, and fractions of 0.7 ml were collected.

Lectin affinity chromatography. After boiling for 5 min, the pronase digests were analyzed on Con A Sepharose or LcH–agarose columns (0.7 × 4 cm) according to the procedure of Cummings and Kornfeld (1982). Glycopeptides lacking lectin affinity were removed by washing the column with TBS buffer. Lectin-bound glycopeptides were eluted stepwise: first, glycopeptides with low lectin affinity were eluted with 10 m*M* α-methylglucoside in TBS. Afterwards, glycopeptides with high affinity were eluted with 100 m*M* α-methylmannoside in TBS, pre-warmed to 60°C.

Functional studies of the influence of IgG glycosylation

Target cell lines. The murine mastocytoma P815y of DBA/2 origin (H-2^d) was maintained in culture in complete RPMI medium.

The human tumor cell lines WM-9 (melanoma) and SW-1116 (colorectal carcinoma) were cultured in Leibovitz's L-15 medium supplemented with 10% HI-FBS. Single-cell suspensions of these adherent cell lines were obtained after brief incubation at room temp with trypsin (1.25 mg/ml in 0.1% versene).

Peripheral blood leukocyte preparations. Peripheral blood, obtained from healthy donors by venipuncture and anticoagulated with heparin, was processed using an established protocol (Perussia *et al.*, 1987*a*). Blood was centrifuged on a Ficoll/Hypaque gradient (F/H, density = 1.077 g/ml). Mononuclear cells at the upper F/H interface were fractionated into PBL and monocytes by adherence to plastic surfaces after a 1-hr incubation at 37°C in complete RPMI. Adherent monocytes were recovered by scraping. Cells from the lower F/H interface were mixed with plasma, and diluted with 3% Dextran T500 in 0.15 *M* NaCl. After incubation at 37°C, the leukocyte-rich plasma was separated from agglutinated erythrocytes; PMN were isolated from this fraction after hypotonic lysis and a second centrifugation on F/H. All leukocytes were maintained in complete RPMI. In some cases, PMN (4×10^6/ml) were incubated overnight at 37°C with r-IFNγ (200 U/ml).

NK cells were purified from short-term bulk cultures of peripheral blood mononuclear cells co-cultured for 10 days with an irradiated B lymphoblastoid cell line (Daudi or RPMI-8866) (Perussia *et al.*, 1987*b*). NK cells were negatively selected from these lymphocyte cultures using a mixture of T cell- and monocyte-specific monoclonal antibody- and anti-globulin-rosetting as previously described in detail (Perussia *et al.*, 1983).

Binding studies. Triplicate samples of P815y cells (10^5 cells/50 μl/well) were incubated at room temp for 30 min in the presence or absence of serial log dilutions (initially, 10 μg/ml) of the various glycosylation phenotypes of 34-5-8S mAb, produced in the presence or absence of inhibitors of glycosylation and carbohydrate processing. After extensive washing, the cells were incubated for an additional hr at 4°C with ^{125}I-labelled goat Ig anti-mouse IgG. Cell-bound radioactivity was determined, after extensive washing, in a γ-counter. All incubations and washes were performed at 4°C with PBS/0.1% gelatin/0.1% sodium azide (pH 7.2).

The titer of anti-human tumor mAbs in the spent hybridoma culture fluid was determined similarly by indirect RIA binding studies using 1:3 dilutions of the culture fluid.

Antibody-dependent cell-mediated cytotoxicity. Cytotoxicity mediated by peripheral blood leukocytes was determined in a 3-hr ^{51}Cr release assay (Trinchieri *et al.*, 1984). After labelling overnight with ^{51}Cr (100 μCi/10^6 cells), P815y target cells (5×10^5/ml) were sensitized with 34-5-8S mAb (1 μg/ml) for 20 min at room temp, and then washed free of excess, unbound mAb. A constant number of these target cells (10^4/well) was added to serial dilutions of effector cells in a 96-well microtiter plate in complete RPMI. The plates were spun for 1 min at 800 rpm, and after a 3-hr incubation at 37°C, the ^{51}Cr released into the supernatant was measured in a

γ-counter. The percentage specific cytotoxicity was calculated as

$$\frac{\text{OBS} - \text{S.R.}}{\text{MAX} - \text{S.R.}} \times 100\%,$$

where OBS is the release observed in the presence of effectors; S.R. is the spontaneous release in the absence of effectors; and MAX, the maximal release in the presence of 1% Triton X-100. Typically, maximal release from target cells corresponded to 90% of the cell-incorporated isotope; and spontaneous release was less than 10% of maximal release. Values represent the mean of triplicate determinations.

ADCC of human tumor target cells was performed similarly, but with slight modifications. WM-9 and SW-1116 target cells were labelled overnight with ^{51}Cr (50 μCi/10^6 cells and 100 μCi/10^6 cells, respectively). The trypsinized suspensions of labelled target cells were sensitized with a 1:2 dilution of the spent hybridoma culture fluid. By indirect RIA binding studies, this concn had been determined previously to be saturating. Effector cells were NK cells that had been trypsin-treated in order to abrogate their ability to mediate spontaneous cytotoxicity (Perussia *et al.*, 1979). For this, NK cells (10^7/ml) in serum-free RPMI medium were incubated with trypsin (1 mg/ml) at 37°C for 20 min, and then washed with complete (serum-supplemented) medium. Release of ^{51}Cr from target cells was determined after a 6 hr incubation at 37°C.

RESULTS

Characterization of IgG glycopeptide alterations induced by inhibitors of carbohydrate processing

The effect of Cs, Mon or Sw upon glycosylation was determined by analyzing the glycopeptides derived from IgG secreted by 34-5-8S hybridomas cultured in the presence of these inhibitors. Although some similarities existed between glycopeptides derived from the different pharmacologically-induced glycosylation phenotypes, each altered phenotype was characterized by a unique set of IgG glycopeptides. For instance, when analyzed according to apparent size by alkaline borate GFC, only the glycopeptides derived from the Sw-induced phenotype were characterized by a relatively increased amount of class III glycopeptides (Fig. 1B). By contrast, culturing hybridomas in the presence of Cs or Mon induced small, but notably opposite, effects upon the apparent size of class IV glycopeptides (Fig. 1C and D). Relative to glycopeptides from the natively expressed phenotype (produced in the absence of inhibitors), Cs slightly increased (Fig. 1C), whereas Mon slightly decreased (Fig. 1D), the apparent size of class IV glycopeptides. Although small, these differences in apparent size induced by Mon and Cs probably are not artefactual, since in the absence of these inhibitors no differences in the elution profiles are apparent between class IV glycopeptides derived from IgG secreted by two parallel cultures differently labelled with ^{14}C and ^{3}H (Fig. 1A).

Unlike the IgG glycopeptides from the natively expressed phenotype, glycopeptides from each of the altered phenotypes were sensitive to Endo H digestion (Fig. 1E–H). However, comparison of the glycopeptide elution profiles after Endo H digestion would suggest that the Sw- and Mon-induced phenotypes are structurally related and distinct from the phenotype induced by Cs. Particularly apparent are differences in the late-eluting oligosaccharide fragment which is released from the glycopeptides upon Endo H digestion. When derived from glycopeptides of the Cs-induced phenotype, a lesser amount of the total radioactivity is released, and this fragment is eluted later than the analogous fragments released from glycopeptides of the other altered phenotypes.

Previously, we had shown that pronase-digested IgG from murine hybridomas can be resolved by apparent size into as many as five *size* classes of glycopeptides by GFC in the presence of an alkaline borate buffer (Rothman *et al.*, 1989; Rothman and Warren, 1988). Unlike class IV and V glycopeptides, a significant fraction of class III glycopeptides was sialylated. Moreover, class III glycopeptides were found to be relatively enriched in glycopeptides of low or no affinity for LcH agarose. Additionally, class III glycopeptides of high affinity had qualitatively different LcH elution profiles than the analogous class IV glycopeptides.

Thus, structural alterations in glycosylation induced by Cs, Mon and Sw, as suggested by differences in GFC elution profiles, are apparent especially from the quantitative and qualitative differences in the lectin affinity chromatographic elution profiles of the IgG glycopeptides. In particular, the glycopeptides of low affinity for Con A derived from the altered phenotypes had a more retarded elution pattern than those of low affinity derived from the native phenotype (Fig. 2A–D). However, of all of the altered phenotypes, only the phenotype induced by Mon is characterized by an increase in the distribution of glycopeptides of high affinity for Con A (Fig. 2D).

Unlike the phenotype induced by Sw, both the Cs- and Mon-induced phenotypes are characterized by a five-fold increase in the distribution of glycopeptides which lack affinity for LcH (Fig. 2G and H). Of more importance, there is no comparable increase in the distribution of glycopeptides which lack affinity for Con A. Presumably, the majority of the glycopeptides derived from the Cs- and Mon-induced phenotypes which do not bind to LcH will bind to Con A.

Effect of alterations in glycosylation upon antigen-binding

The influence of the 34-5-8S IgG glycosylation phenotype upon binding to the target cell P815y was determined by indirect RIA (Fig. 3). Similar amounts

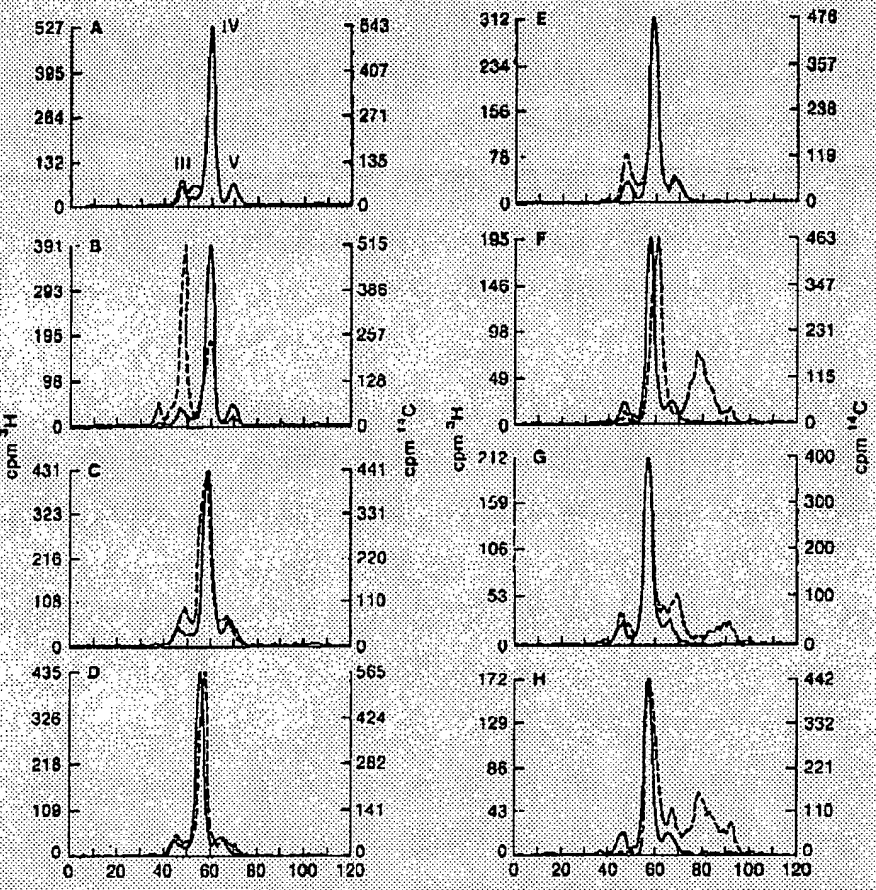

Fig. 1. Effect of carbohydrate processing inhibition upon alkaline borate GFC elution profiles of IgG glycopeptides. Parallel cultures of 34-5-8S hybridoma were metabolically labelled with [^{3}H]-glucosamine in the absence or presence of either Sw, Cs or Mon. An additional culture was labelled with [^{14}C] glucosamine in the absence of inhibitors. The secreted IgG was affinity-purified and digested with pronase. The alterations in glycosylation were characterized on a column of Sephadex G-50 by alkaline borate GFC before (A–D) and after (E–H) Endo H digestion of the ^{3}H-labelled (---) pronase digest. The ^{14}C-labelled (——) digest, added before chromatography, served as a common internal standard. The elution profiles are shown for the glycopeptides derived from the native phenotype (A and E) as well as the Sw-induced (B and F), Cs-induced (C and G) and Mon-induced (D and H) phenotypes.

of mAb bound to P815y targets regardless of the nature, or even the absence, of the IgG oligosaccharide. Saturation of target cells occurred at a mAb concn of 1 μg/ml for all glycosylation phenotypes.

Effect of alterations in glycosylation upon antibody-dependent cell-mediated cytotoxicity

All effector cell populations tested mediated significant levels of ADCC against P815y target cells sensitized with a control polyclonal rabbit antiserum (data not shown). ADCC mediated by PBL and monocytes against 34-5-8S mouse monoclonal antibody-sensitized targets was lower than that mediated against polyclonal antibody-sensitized targets, whereas PMN mediated similar levels of ADCC against monoclonal or polyclonal antibody-sensitized target cells.

When their ability to promote ADCC were compared, the various altered phenotypes of 34-5-8S mAb were found to differ. Sensitizing P815y target cells with IgG produced in the presence of Mon, or of the chemically dissimilar glucosidase inhibitors Cs and MdNM, enhanced ADCC mediated by PBL (Fig. 4A). This enhancement in cytotoxicity was observed consistently with PBL obtained from various donors (lymphocytes from 24 donors assayed with the Cs-induced, and five donors with the Mon-induced phenotypes of 34-5-8S mAb) (data not shown).

In addition to being specific for certain altered phenotypes, the enhanced cytotoxicity was specific for the effector cell population. The Cs- and Mon-induced phenotypes did not enhance cytotoxicity mediated by monocytes or r-IFNγ-treated PMN obtained from the same donor of the PBL (Fig. 4B and C).

Instead, the Cs-induced phenotype was as active as the native phenotype at promoting ADCC mediated by activated PMN. Additionally, PMN-mediated ADCC against target cells sensitized with the Tm- or Sw-induced phenotypes was significantly lower than that against native IgG-sensitized cells. However, unlike what is observed with PBL, all IgG phenotypes were effective in promoting ADCC by PMN.

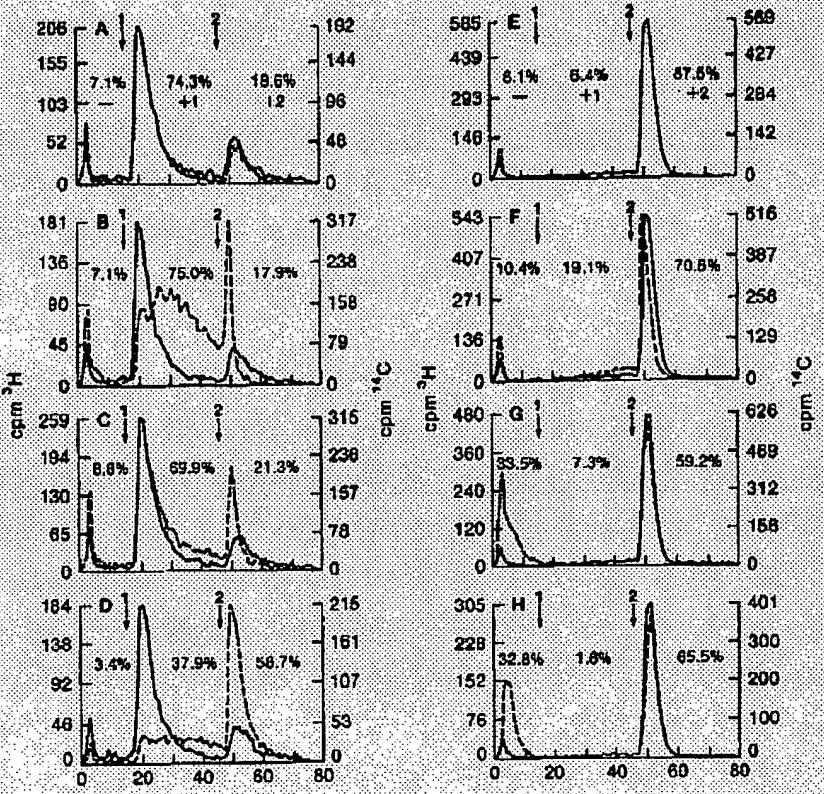

Fig. 2. Effect of carbohydrate processing inhibition upon lectin affinity elution profiles of IgG glycopeptides. The pronase digests of the various phenotypes of 34-5-8S IgG (described in Fig. 1) were analyzed by either Con A (A–D) or LcH (E–H) affinity chromatography. Arrows indicate the start of the stepwise application of 10 m*M* α-methylglucoside (1) and 100 m*M* α-methylmannoside (2). The percentage of ^3H recovered in each of the three lectin affinity fractions is also shown. The elution profiles are shown for the glycopeptides derived from the native phenotype (A and E), as well as the Sw-induced (B and F), Cs-induced (C and G) and Mon-induced (D and H) phenotypes.

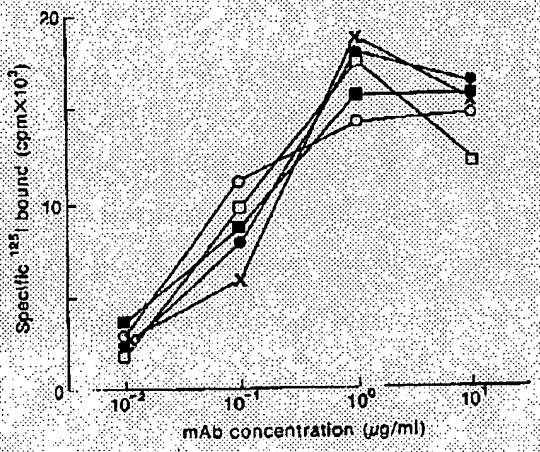

Fig. 3. Effect of IgG glycosylation phenotype upon antigen-binding. Serial log dilutions of equal amounts of 34-5-8S mAb of the various glycosylation phenotypes were incubated with a constant number of P815y cells. The amount of mAb bound at each dilution was determined by indirect RIA with ^{125}I-labelled goat Ig anti-mouse IgG. This was corrected for the amount of label bound non-specifically in the absence of 34-5-8S mAb, approximately 5–7% of maximal bound. The IgG glycosylation phenotypes assayed were the natively expressed (□), and the altered phenotypes induced by Sw (○), Tm (×), Cs (■) or Mon (●).

Virtually all ADCC observed with PBL is mediated by FcR-bearing NK cells (Perussia *et al.*, 1983). For further studies, NK cells were purified to homogeneity from bulk cultures of peripheral blood mononuclear cells. As previously described (Perussia *et al.*, 1987*b*), these purified NK cells had the phenotype and functions of freshly obtained NK cells, and mediated high levels of ADCC against polyclonal antibody-sensitized P815y target cells (data not shown). As observed with fresh PBL, these NK cell preparations mediated minimal levels of ADCC against P815y targets sensitized with native 34-5-8S murine IgG2a monoclonal antibodies, but were able to mediate high levels of ADCC against P815y target cells which had been sensitized with either the Cs- or Mon-induced phenotype of 34-5-8S mAb (Fig. 5A). A similar enhancement in NK-mediated ADCC also was observed using target cells sensitized with the DMM-induced phenotype of 34-5-8S mAb (Fig. 5B), and was observed consistently with NK cells from a total of five donors (data not shown). As described for the other phenotypes, indirect RIA binding studies revealed that the enhanced cytotoxicity promoted by the DMM-induced phenotype could not be ascribed to a significantly greater binding of this IgG phenotype to the target cell (data not shown).

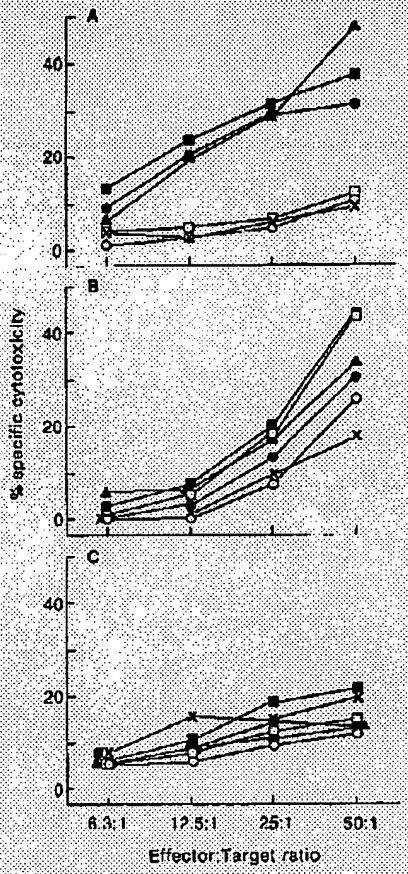

Fig. 4. Effect of IgG glycosylation phenotype upon ADCC mediated by different leukocyte populations. A constant number of ^{51}Cr-labelled P815y cells, sensitized with saturating amounts of 34-5-8S mAb of the various glycosylation phenotypes, was added to serial dilutions of various populations of human peripheral blood leukocytes. Specific ADCC mediated by either PBL (A), PMN (activated with r-IFNγ) (B) or monocytes (C) was then determined in a 3-hr ^{51}Cr release assay. The IgG glycosylation phenotypes assayed were the natively expressed (□), and the altered phenotypes induced by Sw (○), Tm (×), Cs (■), MdNM (▲) or Mon (●).

The enhanced lymphocyte-mediated cytotoxicity was found to be FcR-dependent (Fig. 6). ADCC was specifically abrogated by pre-incubation of PBL with 3G8, an anti-FcR mAb (Perussia and Trinchieri, 1984; Fleit *et al.*, 1982), but not by other irrelevant monoclonal antibodies (data not shown). Pre-treatment of NK cells with trypsin did not abrogate ADCC (Fig. 7), although FcR-independent spontaneous cytotoxicity of K562 or human tumor target cells was abrogated (data not shown). Trypsin resistance is a characteristic feature of the FcR expressed on NK cells (Perussia *et al.*, 1979).

Generality of the influence of the Cs-induced phenotype upon ADCC mediated against tumor target cells sensitized with a panel of mAbs

The generality of the phenomenon of enhanced NK cell-mediated ADCC was explored using various human tumor target cell lines sensitized with a panel

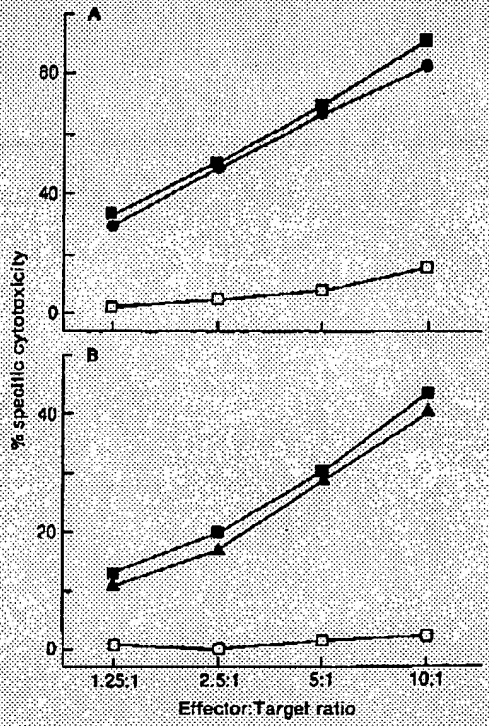

Fig. 5. Effect of IgG glycosylation phenotype upon NK-mediated ADCC. P815y target cells labelled with ^{51}Cr were sensitized with saturating amounts of 34-5-8S mAb of either native (□) or the Cs- (■), Mon- (●) or DMM-induced (▲) phenotype. The effect upon ADCC was determined in a 3-hr ^{51}Cr release assay using serial dilutions of NK effector cells purified from two donors, (A) and (B).

of murine mAbs. As observed with P815y target cells, the native IgG phenotype of relevant antigenic specificity induced only minimal ADCC by NK cells. ADCC activity generally was enhanced when WM-9 melanoma cells were sensitized with the

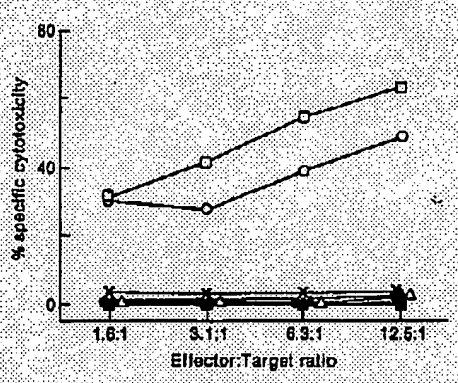

Fig. 6. Fc receptor-dependence of enhanced PBL-mediated ADCC. Serial dilutions of PBL (initially, 1.25×10^5/well) were pre-incubated at room temp for 1 hr in the presence (closed symbols) or absence (open symbols) of 3G8 ascites fluid (1:100 dilution). The effect upon ADCC was determined after the addition of ^{51}Cr-labelled P815y target cells (10^4/well) which had been sensitized with saturating amounts of 34-5-8S mAb of either native (△, ▲), Cs- (□, ■) or Mon-induced (○, ●) phenotype. Spontaneous cytotoxicity against labelled P815y targets which had not been sensitized with 34-5-8S mAb was determined in the absence of 3G8 ascites fluid (×).

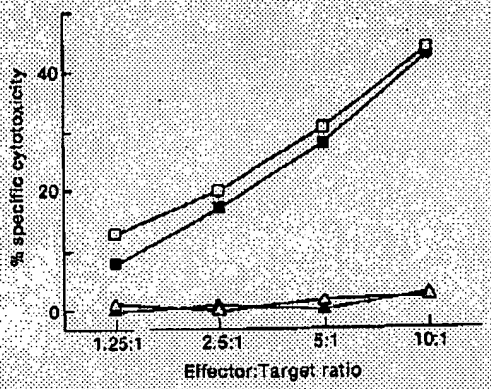

Fig. 7. Effect of trypsin treatment of NK cells upon enhanced NK-mediated ADCC. Purified NK cells were incubated at 37°C for 30 min with trypsin (1 mg/ml/10⁷ cells). The effect of the treatment upon ADCC was determined in a 3-hr ^{51}Cr release assay using P815y target cells that had been sensitized with saturating amounts of either the native (△, ▲) or Cs-induced (□, ■) phenotype of 34-5-8S mAb. Trypsin-treated NK cells are indicated by closed symbols, untreated NK cells by open symbols.

Cs-induced phenotype of mAbs of relevant antigenic specificity (Fig. 8). From a total of five donors assayed, NK cells from four donors mediated significantly greater ADCC when WM-9 cells were sensitized with the Cs-induced phenotype of either LU-16B13 or ME-288 mAb (data not shown). Although the level of ADCC was too low to be conclusive, ADCC of WM-9 cells also appeared to be enhanced by sensitizing target cells with the Cs-induced phenotype of either ME-5073 or ME-37-7 mAb (enhancement observed with NK cells from three donors; total of four donors assayed; data not shown).

A second tumor cell line SW-1116 also was used as a target (Fig. 9). The Cs-induced phenotype of LU-16B13 was found to augment cytotoxicity against both tumor lines by NK cells derived from the same donor. Cytotoxicity by the same NK cells, however, was enhanced, though only modestly, when SW-1116 target cells were sensitized with the Cs-induced

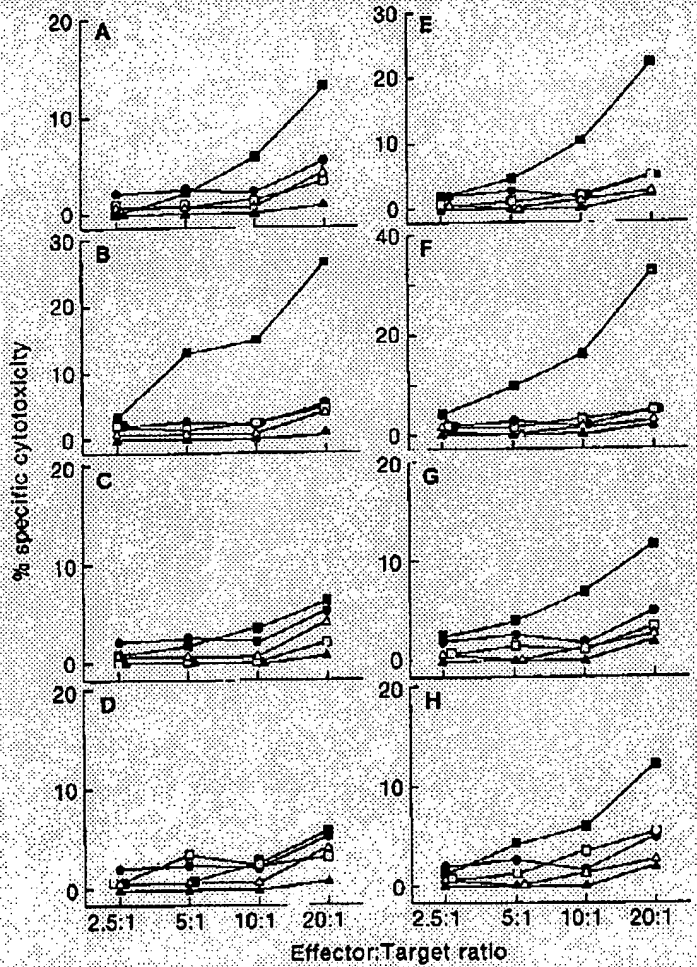

Fig. 8. Effect of the Cs-induced phenotype of a panel of anti-WM-9 mAbs upon NK-mediated ADCC. WM-9 target cells were sensitized with saturating amounts of either the native (□) or Cs-induced (■) phenotype of LU-16B13 (A and E), ME-288 (B and F), ME-5073 (C and G), or ME-37-7 (D and H) mAbs (1:2 dilution of spent hybridoma culture fluid). The effect of the altered IgG phenotype upon ADCC activity was measured in a 6-hr ^{51}Cr release assay using serial dilutions of purified NK effector cells from either donor A (A–D) or donor B (E–H). To assess spontaneous cytotoxicity, WM-9 cells either were not sensitized with mAb (●), or were sensitized with CO-17-1A, an isotype-matched mAb of irrelevant antigenic specificity, of either the native (△) or Cs-induced (▲) phenotype.

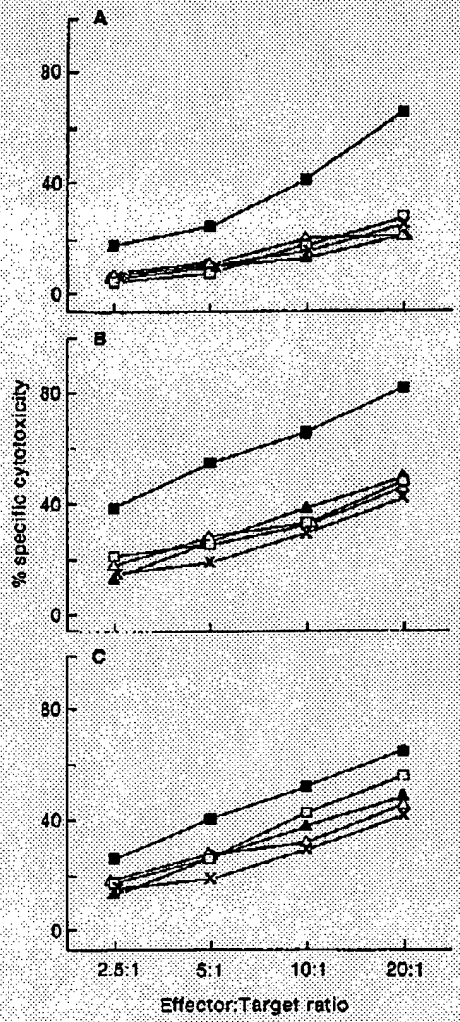

Fig. 9. Effect of the Cs-induced IgG phenotype upon NK-mediated ADCC of several human tumors. SW-1116 target cells were sensitized with saturating amounts of either the native (□) or Cs-induced (■) phenotype of LU-16B13 (B) or CO-17-1A (C) mAb (1:2 dilution of spent hybridoma culture fluid). WM-9 target cells were sensitized similarly with LU-16B13 mAb (A). The effect of the altered IgG phenotype upon ADCC activity was measured in a 6-hr ^{51}Cr release assay with serial dilutions of purified NK cells from the same donor. To assess spontaneous cytotoxicity, target cells either were not sensitized with mAb (×); or were sensitized with an isotype-matched mAb of irrelevant antigenic specificity, of either the native (△) or Cs-induced (▲) phenotype. MF-288 and CO-17-1A mAbs were used as irrelevant mAbs for SW-1116 and WM-9 target cells, respectively.

phenotype of CO-17-1A mAb instead. Sensitizing SW-1116 cells with the Cs-induced phenotype of either LU-16B13 or CO-17-1A mAb enhanced ADCC mediated by NK cells from three donors (total of five donors assayed; data not shown).

In these latter ADCC studies, human tumor cells were sensitized with saturating amounts of the spent culture medium of the hybridoma, rather than with purified mAb. However, the use of the unpurified mAb preparations did not seem to interfere with the cytotoxicity assays. Dialysis of the spent culture medium to deplete it of the carbohydrate processing inhibitors did not influence ADCC (data not shown). Also, it should be noted that the cytotoxicity assays were done in the absence of the inhibitors, as target cells, after brief sensitization with mAb, routinely were washed free of the sensitizing hybridoma culture medium prior to incubation with NK cells. Furthermore, sensitization of tumor target cells with the spent culture medium from Cs-treated hybridomas that secrete an isotype-matched mAb of irrelevant antigenic specificity did not enhance spontaneous cytotoxicity (Figs 8 and 9). Rather, it is specifically the relevant mAbs of the Cs-induced phenotype which account for the enhanced ADCC activity mediated by NK cells.

DISCUSSION

IgG secreted by the same hybridoma clone, but cultured in the presence of various inhibitors of glycosylation or carbohydrate processing, were used to probe the functional consequences of alterations in glycosylation. Neither the absence of glycosylation (resulting from inhibition by Tm) nor the presence of atypical oligosaccharides (as a consequence of inhibition by Cs, MdNM, Mon or Sw) significantly influenced antigen-binding of mAb to their target cells. Despite this similarity in the degree of sensitization of target cells with mAb, a correlation was observed between the efficiency of promoting ADCC and the glycosylation phenotype of the mAb.

The effect of the phenotype upon ADCC varied with the type of cytotoxic effector cell. Sensitization of target cells with mAb of either the Cs-, MdNM-, DMM- or Mon-induced phenotypes significantly enhanced ADCC mediated by PBL (and NK cells purified from this fraction), but not by fresh monocytes or r-IFNγ-treated PMN. However, sensitization of target cells with the native phenotype was as efficient as the Cs-induced phenotype at promoting ADCC mediated by PMN which had been activated by r-IFNγ. Regardless of the glycosylation phenotype, the various mAbs all promoted ADCC with activated PMN. Because NK cells bear only one FcR type (CD16), it is likely that alterations of glycosylation play a major role in binding of IgG Fc to this receptor. PMN share with NK cells FcR (CD16); however, like monocytes but unlike NK cells, they also constitutively express a distinct FcR (gp40) (Shen *et al.*, 1987) which has been shown to mediate ADCC. An enhancing effect of the altered IgG phenotypes on CD16-mediated ADCC could be masked on PMN if efficacy of this second FcR type in mediating ADCC is not altered by these IgG glycosylation phenotypes.

The enhanced lymphocyte-mediated ADCC observed with the Cs- and Mon-induced phenotypes cannot be attributed simply to a functional inactivity of the other altered phenotypes because all

phenotypes bound equally well to their target cells when assayed by RIA, and all phenotypes promoted PMN-mediated ADCC. Furthermore, the enhanced cytotoxicity depends on specific alterations of IgG glycosylation, as the Sw-induced phenotype, although also characterized by a radical alteration in glycosylation, was ineffective at enhancing lymphocyte-mediated ADCC.

Enhancement of NK cell-mediated ADCC correlates with the expression of phenotypes characterized by IgG glycopeptides which bind to Con A but not to LcH. Glycopeptides from human myeloma IgG with similar lectin-binding properties have been identified as complex-type oligosuccharides in which core fucosylation is absent (Kornfeld *et al.*, 1981). In addition to these complex-type structures, high mannose-type structures also would be expected to lack fucosylation, as these oligosaccharides are not substrates for the core fucosyl transferase (Hubbard and Ivatt, 1981).

The mere exposure of peripheral mannosyl residues, however, seems to be insufficient to enhance ADCC, as the Sw-induced phenotype did not alter lymphocyte-mediated ADCC even though peripheral mannosyl residues are expressed in this phenotype. Although functionally distinct, both the Sw- and Mon-induced phenotypes appear related structurally, as evidenced by their similar susceptibility to Endo H digestion as a probe for exposure of mannosyl residues. However, of more importance is the fact that they also differ structurally, as the hybrid structures induced by Sw are core fucosylated, unlike a subset of those oligosaccharides expressed in the Mon-induced phenotype.

Glucosylation, characteristic of the phenotypes induced by the chemically dissimilar glucosidase inhibitors Cs and MdNM, likewise would appear to be unrelated to ADCC activity. Despite the putative absence of glucosylation, the DMM-induced phenotype was as effective as the glucosylated Cs-induced phenotype at enhancing NK cell-mediated ADCC. Moreover, incubation of the Cs-induced IgG phenotype with α-glucosidase did not affect ADCC of targets sensitized with the glucosidase-modified mAb (data not shown). Thus, absence of core fucosylation itself would appear to be a likely candidate as a structural feature necessary for enhancement of NK cell-mediated ADCC.

Because NK cells, unlike monocytes and PMN, bear only one FcR type (CD16), our data suggest that such alterations of glycosylation mainly affect the functional consequences of IgG binding to FcR (CD16) and not to other FcR types. Also in support of this hypothesis is the observation that murine monoclonal antibodies are as efficient as rabbit polyclonal antisera in inducing ADCC by PMN, whereas rabbit polyclonal antisera are more efficient than murine mAbs in promoting antibody-dependent cytotoxicity mediated by human NK cells that express only CD16 (Ortaldo *et al.*, 1987; Christiaansen and Scars, 1984). Several obvious reasons may account for this observation, such as recognition by polyclonal IgG of numerous antigens and epitopes, each with a different orientation, organization and binding affinity (Christiaansen *et al.*, 1987; Christiaansen and Scars, 1984), but perhaps glycosylation also may be involved.

Although the absence of core fucosylation may not be expressed natively in the murine hybridoma repertoire for glycosylation of IgG (Rothman *et al.*, 1989), species-specific differences exist in its expression. Approximately 15% of human IgG, and 68% of rabbit IgG, lack core fucosylation (Mizuochi *et al.*, 1987). Thus, it is tempting to speculate that polyclonal variability in the expression of core fucosylation may confer a functional advantage to host defense by diversifying the effector activity of IgG.

The influence of the glycosylation phenotype may have implications for immunotherapy of neoplasias with murine mAbs. Its possible general applicability is demonstrated by our findings with a panel of anti-tumor mAbs. Typically, expression of the Cs-induced phenotype enhanced the ADCC activity of human NK cells against two human tumor cell lines.

Differences in reactivity are apparent between the Cs-induced phenotypes of the various anti-tumor mAbs of the panel. Glycosylation of the mAb might have to act in concert with other features, such as the orientation and organization of the immune complex on the tumor cell, for the efficient presentation of a determinant that will elicit an immune response. Thus, it may be either the recognition of this determinant or else its presentation which is perceived differently by NK cells.

Perhaps other glycosylation phenotypes will be detected which may result in their preferential interaction with different populations of cytotoxic leukocytes and this may provide a means by which the immune response can be fine-tuned.

Acknowledgements—The secretarial assistance of Marie Lennon is gratefully acknowledged. This study constitutes a portion of a thesis submitted by R. J. Rothman in partial fulfilment of the requirements for the degree of Doctor of Philosophy from the University of Pennsylvania.

REFERENCES

Blithe D. L., Buck C. A. and Warren L. (1980) Comparison of glycopeptides from control and virus-transformed baby hamster kidney fibroblasts. *Biochemistry* **19**, 3386–3395.

Bohlen P., Stein S., Dairman W. and Udenfriend S. (1973) Fluorometric assay of proteins in the nanogram range. *Archs Biochem. Biophys.* **155**, 213–220.

Christiaansen J. E., Burnside S. S. and Scars D. W. (1987) Apparent sensitivity of human K lymphocytes to the spatial orientation and organization of target cell-bound antibodies as measured by the efficiency of antibody-dependent cellular cytotoxicity (ADCC). *J. Immun.* **138**, 2236–2243.

Christiansen J. E. and Scars D. W. (1984) Unusually efficient tumor cell lysis by human effectors of antibody-dependent cellular cytotoxicity mediated by monoclonal antibodies. *Cancer Res.* 44, 3712–3718.

Cummings R. D. and Kornfeld S. (1982) Fractionation of asparagine-linked oligosaccharides by serial lectin agarose affinity chromatography. A rapid, sensitive and specific technique. *J. biol. Chem.* 257, 11,235–11,240.

Elbein A. D. (1987) Inhibitors of the biosynthesis and processing of N-linked oligosaccharide chains. *A. Rev. Biochem.* 56, 497–534.

Ey P. Y., Prowse S. J. and Jenkin C. R. (1978) Isolation of pure IgG1, IgG2a, and IgG2b immunoglobulins from mouse serum using Protein A Sepharose. *Immunochemistry* 15, 429–436.

Fleit H. R., Wright S. D. and Unkeless J. C. (1982) Human neutrophil Fcγ receptor distribution and structure. *Proc. natn. Acad. Sci. U.S.A.* 79, 3275–3279.

Hashim O. H. and Cushley W. (1987) Role of processing of N-linked oligosaccharides in control of immunoglobulin secretion from rat hybridomas. *Molec. Immun.* 24, 1087–1096.

Hashim O. H. and Cushley W. (1988) Simultaneous inhibition of multiple steps in the processing of N-linked oligosaccharides does not impair immunoglobulin secretion from rat hybridoma cells. *Immunology* 63, 383–388.

Herlyn D., Powe J., Ross A. II., Herlyn M. and Koprowski H. (1985) Inhibition of human tumor growth by IgG2a monoclonal antibodies correlates with antibody density on tumor cells. *J. Immun.* 134, 1300–1304.

Herlyn M., Steplewski Z., Herlyn D., Clark W. II., Ross A. H., Blaszczyk M., Pak K. Y. and Koprowski H. (1983) Production and characterization of monoclonal antibodies against human malignant melanoma. *Cancer Invest.* 1, 215–224.

Herlyn M., Steplewski Z., Herlyn D. and Koprowski H. (1979) Colorectal carcinoma-specific antigen: detection by means of monoclonal antibodies. *Proc. natn. Acad. Sci. U.S.A.* 76, 1438–1482.

Hickman S. and Kornfeld S. (1978) Effect of tunicamycin on IgM, IgA, and IgG secretion by mouse plasmacytoma cells. *J. Immun.* 121, 990–996.

Howell J. W., Hood L. and Sanders B. G. (1967) Comparative analysis of the IgG heavy chain carbohydrate peptide. *J. molec. Biol.* 30, 555–558.

Hubbard S. D. and Ivatt R. J. (1981) Synthesis and processing of asparagine-linked oligosaccharides. *A. Rev. Biochem.* 50, 555–583.

Knudsen K. A., Rao P. E., Damsky C. H. and Buck C. A. (1981) Membrane glycoproteins involved in cell-substratum adhesion. *Proc. natn. Acad. Sci. U.S.A.* 78, 6071–6075.

Koide N., Nose M. and Muramatsu T. (1977) Recognition of IgG by Fc receptor and complement: effects of glycosidase digestion. *Biochem. biophys. Res. Commun.* 75, 838–844.

Kornfeld K., Reitman M. L. and Kornfeld R. (1981) The carbohydrate-binding specificity of pea and lentil lectins. Fucose is an important determinant. *J. biol. Chem.* 256, 6633–6640.

Leatherbarrow R. J. and Dwek R. (1983) The effect of aglycosylation on the binding of mouse IgG to staphylococcal protein A. *FEBS Lett.* 164, 227–230.

Leatherbarrow R. J., Rademacher T. W., Dwek R. A., Woof J. M., Clark A. and Burton D. R. (1985) Effector functions of a monoclonal aglycosylated mouse IgG2a: binding and activation of complement component C1 and interaction with human monocyte Fc receptor. *Molec. Immun.* 22, 407–415.

Mazauric T., Mitchell K. F., Lotchworth III, G. J., Koprowski H. and Steplewski Z. (1982) Monoclonal antibody-defined lung cell surface protein antigens. *Cancer Res.* 42, 150–154.

Mitchell K. F., Ward P. E. and Koprowski H. (1982) DR antigens on melanoma cells: analysis with monoclonal antibodies. *Human Immun.* 4, 15–26.

Mizuochi T., Hamako J. and Titani K. (1987) Structures of the sugar chains of mouse immunoglobulin G. *Archs Biochem. Biophys.* 257, 387–394.

Nose M. and Wigzell H. (1983) Biological significance of carbohydrate chains on monoclonal antibodies. *Proc. natn. Acad. Sci. U.S.A.* 80, 6623–6636.

Ortaldo J. R., Woodhouse C., Morgan A. C., Herberman R. B., Cheresh D. A. and Reisfeld R. (1987) Analysis of effector cells in human antibody-dependent cellular cytotoxicity with murine monoclonal antibodies. *J. Immun.* 138, 3566–3572.

Ozato K., Mayer N. M. and Sachs D. H. (1982) Monoclonal antibodies to mouse major histocompatibility complex antigens. IV. A series of hybridoma clones producing anti-H-2 antibodies and an examination of expression of H-2 antigens on the surface of these cells. *Transplantation* 34, 113–120.

Parekh R. B., Dwek R. A., Sutton B. J., Fernandes D. L., Leung A., Stanworth A. L., Rademacher T. W., Mizuochi T., Taniguchi T., Matsuta K., Takeuchi F., Nagano Y., Miyamoto T. and Kobata A. (1985) Association of rheumatoid arthritis and primary osteoarthritis with changes in the glycosylation pattern of total serum IgG. *Nature* 316, 452–457.

Perussia B., Kobayashi M., Rossi M. E., Anegon I. and Trinchieri G. (1987*a*) Immune interferon enhances functional properties of human granulocytes: role of Fc receptors and effect of lymphotoxin, tumor necrosis factor and granulocyte–macrophage colony-stimulating factor. *J. Immun.* 138, 765–774.

Perussia B., Ramoni C., Anegon I., Curturi M. C., Faust J. and Trinchieri G. (1987*b*) Preferential proliferation of natural killer cells among peripheral blood mononuclear cells cocultured with B lymphoblastoid cell lines. *Nat. Immun. Cell. Growth Regul.* 6, 171–188.

Perussia B., Starr S., Abraham S., Fanning V. and Trinchieri G. (1983) Human natural killer cells analyzed by B73.1, a monoclonal antibody blocking Fc receptor functions. I. Characterization of the lymphocyte subset reactive with B73.1. *J. Immun.* 130, 2133–2141.

Perussia B., and Trinchieri G. (1984) Antibody 3G8, specific for the human neutrophil Fc receptor, reacts with natural killer cells. *J. Immun.* 132, 1410–1415.

Perussia B., Trinchieri G. and Cerottini J. C. (1979) Functional studies of Fc receptor-bearing human lymphocytes: effect of treatment with proteolytic enzymes. *J. Immun.* 123, 681–687.

Rothman R. J. and Warren L. (1988) Analysis of IgG glycopeptides by alkaline borate gel filtration chromatography. *Biochim. biophys. Acta* 955, 143–153.

Rothman R. J., Warren J., Vliegenthart J. F. G. and Hard K. J. (1989) Clonal analysis of the glycosylation of IgG secreted by murine hybridomas. *Biochemistry* 28, 1377–1384.

Shen L., Guyre P. M. and Fanger M. W. (1987) Polymorphonuclear leukocyte function triggered through the high affinity Fc receptor for monomeric IgG. *J. Immun.* 139, 534–538.

Trinchieri G., O'Brien T., Shade M. and Perussia B. (1984) Phorbol esters enhance spontaneous cytotoxicity of human lymphocytes, abrogate Fc receptor expression, and inhibit antibody-dependent lymphocyte-mediated cytotoxicity. *J. Immun.* 133, 1869–1877.

Weitzman S. and Scharff M. D. (1976) Mouse myeloma mutants blocked in the assembly, glycosylation and secretion of immunoglobulin. *J. molec. Biol.* 102, 237–252.

Winkelhake J. L., Kunicki T. J., Elcombe B. M. and Aster R. H. (1980) Effects of pH treatments and deglycosylation of rabbit immunoglobulin G on the binding of C1q. *J. biol. Chem.* 255, 2822–2828.

Effect of Altered C_H2-associated Carbohydrate Structure on the Functional Properties and In Vivo Fate of Chimeric Mouse-Human Immunoglobulin G1

By Ann Wright and Sherie L. Morrison

From the Department of Microbiology and Molecular Genetics and the Molecular Biology Institute, University of California, Los Angeles, Los Angeles, California 90024

Summary

Immunoglobulin G (IgG) molecules are glycosylated in C_H2 at Asn297; the N-linked carbohydrates attached there have been shown to contribute to antibody (Ab) stability and various effector functions. The carbohydrate attached to the IgG constant region is a complex biantennary structure. Alterations in the structure of oligosaccharide have been associated with human diseases such as rheumatoid arthritis and osteoarthritis. To study the effects of altered carbohydrate structure on Ab effector function, we have used gene transfection techniques to produce mouse-human chimeric IgG1 Abs in the Chinese hamster ovary (CHO) cell line Lec 1, which is incapable of processing the high-mannose intermediate through the terminal glycosylation steps. We also produced IgG1 Abs in Pro-5, the wild-type CHO cell line that is the parent of Lec 1. The Pro-5–produced Ab (IgG1-Pro-5) was similar to IgG1-My 1, a myeloma-produced IgG1 Ab of the same specificity, in its biologic properties such as serum half-life, ability to effect complement-mediated cytolysis, and affinity for FcγRI. Although the Lec 1–produced Ab, IgG1-Lec 1, was properly assembled and retained antigen specificity, it was incapable of complement-mediated hemolysis and was substantially deficient in complement consumption, C1q binding, and C1 activation. IgG1-Lec 1 also showed reduced but significant affinity for FcγR1 receptors. The in vivo half-life of IgG1-Lec 1 was shorter than that of either the myeloma- or Pro-5–produced counterpart, with more being cleared during the α-phase and with more rapid clearance during the β-phase. Clearance of IgG1-Lec 1 could be inhibited by the administration of yeast-derived mannan. Thus the uptake of IgG1-Lec 1 appears to be accelerated by the presence of terminally mannosylated oligosaccharide. Therefore, certain Ab functions as well as the in vivo fate of the protein are dramatically affected by altered carbohydrate structure. Expression of Igs in cell lines with defined glycosylation mutations is shown to be a useful technique for investigating the contribution of carbohydrate structure to Ab function.

All Abs are glycoproteins and are glycosylated at characteristic positions according to their isotype. The IgG molecule has one conserved glycosylation site, at Asn297, within the C_H2 domain of each of its two heavy chains. The oligosaccharides attached there are accommodated within the internal space between the two C_H2 domains (1) and are thought to stabilize the molecule and to contribute to the tertiary structure of the Fc (2). Aglycosylated IgGs have been shown to be deficient in such effector functions as complement activation, Fc receptor recognition, and Ab-dependent cell-mediated cytotoxicity (ADCC)[1] (3–5).

The oligosaccharides associated with the C_H2 of IgG are complex biantennary structures whose core structure consists of two α-mannosyl structures attached to a β-mannosyl-di-*N*-acetylchitobiose unit (see Fig. 1 *A*). The composition of the outer arms varies with the degree of terminal processing and considerable heterogeneity of carbohydrate structures is observed. This heterogeneity has been observed both in the IgG component of normal human serum (6, 7) as well as in IgG paraproteins (8). Whereas heterogeneity is always seen, the relative concentration of different carbohydrate structures is altered in some diseases. Among individuals with rheumatoid arthritis, the proportion of agalactosylated IgG sugars is increased, both in serum and synovial fluid (9, 10). Fc agalactosylation has also been observed in patients with chronic juvenile arthritis, Crohn's disease, and tuberculosis (11, 12). In some clinical studies, the degree of agalactosylation correlated with disease activity in rheumatoid arthritis patients (13). It has been proposed that the presence of agalactosylated

[1] *Abbreviations used in this paper:* ADCC, Ab-dependent cell-mediated cytotoxicity; CHO, Chinese hamster ovary; DNS, dansyl; Endo H, Endoglycosidase H; Gel-HBS, Hepes-buffered saline.

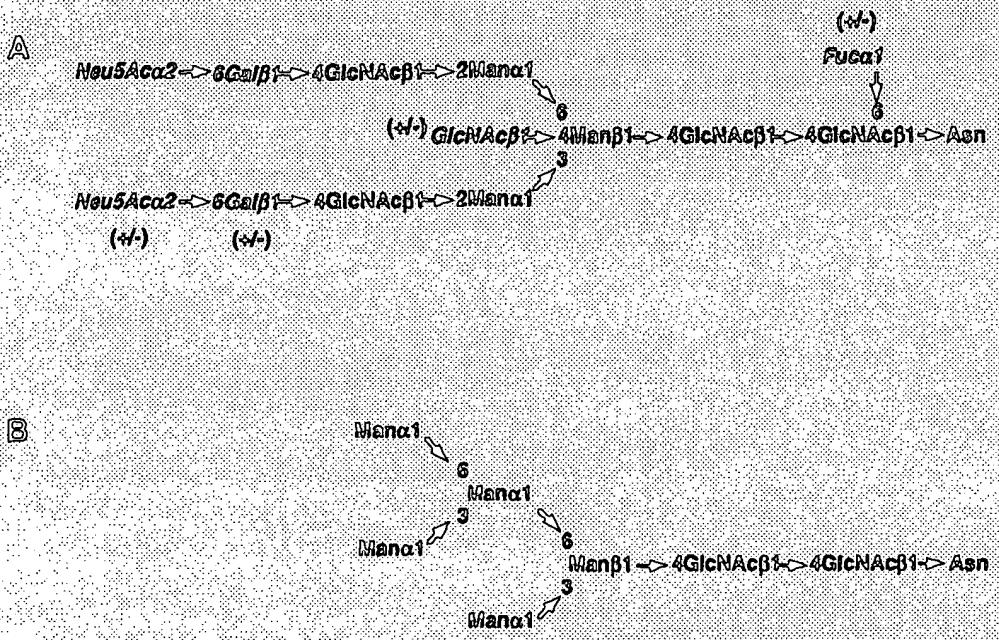

Figure 1. (*A*) Schematic representation of the complex biantennary structure characteristic of C_H2-associated oligosaccharide (7). The core residues are shown in plain type, and the terminal residues, whose variable addition confers heterogeneity upon the structure, are italicized and highlighted with (+/−) symbols. (*B*) The truncated oligosaccharide produced by the CHO glycosylation mutant Lec 1 is shown (16).

carbohydrate causes conformational changes that result in aberrant activity in the Ig, such as increased tendency for self-aggregation.

It is therefore of interest to obtain populations of Abs with defined alterations in carbohydrate structure so that the contributions of specific oligosaccharide residues to glycoprotein function can be assessed. Sequential exoglycosidase digestion of glycoprotein hormones such as choriogonadotropin has shown that successive removal of the outer sugars results in decreased biologic activity (14). Agalactosylated IgG prepared by glycosidase digestion showed decreased complement activation and Fc receptor binding activity (15). However, enzymatic or chemical treatment may damage the protein backbone. Therefore, in this study Igs were produced in Chinese hamster ovary (CHO) cells that have defined defects in oligosaccharide processing. Numerous mutants have been derived by selection for lectin resistance and mostly possess single glycosylation defects (16). These mutations occur at distinct steps in the oligosaccharide biosynthesis pathway, resulting in the accumulation of intermediate structures with reduced overall carbohydrate heterogeneity. In previous studies (17) glycosylation mutants transfected with choriogonadotropin genes produced proteins that were deficient in signal transduction.

CHO cells are widely used as recipient cells for the production of recombinant proteins. In particular, several studies have documented the production and characterization of Igs produced in CHO cells. When compared to their lymphoid cell–produced counterparts, these Abs were found to retain Ag specificity and affinity (18–20), as well as effector functions such as complement- and cell-mediated cytotoxicity (21) and Fc receptor recognition (22). Thus it was reasonable to assume that Igs produced in wild-type CHO cells are functionally equivalent to those in myeloma cells and that Ig production in the CHO glycosylation mutants would permit the study of the specific effects of altered glycosylation on otherwise normal proteins.

In the present studies chimeric mouse-human IgG1 Abs were produced in Lec 1, a CHO cell line deficient in *N*-acetylglucosaminyltransferase I activity (23). Lec 1 synthesizes oligomannosyl structures which are truncated sugars not normally found on IgG (see Fig. 1 *B*). The resulting Abs were assembled and secreted correctly, but were shown to be altered in their biologic properties and significantly deficient in numerous effector functions. Chimeric IgG1 Abs were also produced in Pro-5, the wild-type CHO parent of Lec 1. As expected, the biologic properties of these Abs were similar to their myeloma-produced counterparts.

Materials and Methods

Cell Lines. The CHO cell lines cell lines Lec 1 and Pro-5 were obtained from the American Type Culture Collection (Rockville, MD), having been deposited by Dr. Pamela Stanley (Albert Einstein College of Medicine, New York, NY) (23). The original cell lines and transfectants were maintained at 37°C under 5% CO_2 in IMDM (Irvine Scientific, Santa Ana, CA) supplemented with 5% FCS (Hyclone Laboratories, Logan, UT). The cells were maintained as monolayers on tissue culture–treated petri dishes (Falcon Labware, Lincoln Park, NJ).

The transfectoma cell line TPR1.3 (3; for clarity, referred to in this paper as IgG1-My 1, the myeloma-produced chimeric IgG1) was produced by transfecting the Ig nonproducing mouse myeloma cell line P3X63Ag8.653 with chimeric heavy and light chain genes with murine variable regions from the anti-dansyl (DNS) hybridoma 27-44 and human γ1 and κ constant regions. Cells were maintained in IMDM supplemented with 5% iron-supplemented calf serum (Hyclone).

The human monocyte-like cell line U937, which expresses FcγRI and FcγRII receptors, was maintained in RPMI 1640 medium (GIBCO BRL, Gaithersburg, MD) supplemented with 10% FCS.

Vector Design for Transfection of CHO Cells. The heavy and light chain constructs used to produce DNS-specific IgG1 chimeric Abs

in lymphoid cells were modified to allow the expression of Ig genes in nonlymphoid cells by replacing the Ig-specific promoter and enhancer with the SV40 promoter and enhancer. To construct the heavy chain vector, the 2.1-kb-BamHI fragment containing the leader and Ig promoter was subcloned into the BamHI site of pBR322. Complete digestion with EcoRI and partial digestion with HindIII removed the Ig promoter but retained the leader sequence. The SV40 promoter/enhancer was obtained from the pSV2*gpt* expression vector, where it is flanked by PvuII and HindIII restriction sites. The PvuII site at the 5′ end of the SV40 promoter was converted to an EcoRI restriction site by linker tailing. The EcoRI-HindIII fragment containing the SV40 promoter/enhancer was then cloned into the homologous restriction sites 5′ of the anti-DNS leader sequence. The BamHI-SalI fragment, which contains the V_H gene and the J-C intron, was then cloned into the BamHI and SalI sites of this pBR322 derivative, so that it adjoined the promoter/leader sequence. The heavy chain enhancer, which is flanked by two XbaI restriction sites in the J-C intron, was deleted by XbaI digestion and religation. The EcoRI-SalI fragment was then joined to human IgG1 in the expression vector pSV2ΔH*gpt* (see Fig. 2 *A*). Nucleotide sequencing of the vector showed that no mutations had been introduced in the heavy chain coding region during vector construction.

To construct the light chain vector, a PvuII site 5′ of the leader sequence but 3′ of the light chain promoter was converted to a HindIII site by linker tailing. The EcoRI-HindIII fragment encoding the SV40 promoter/enhancer was joined to the V_κ at that site. The intronic κ enhancer was deleted by EcoRI digestion and religation. The resulting light chain expression vector lacks Ig-specific controlling elements but instead contains the SV40 promoter and enhancer (see Fig. 2 *B*). Large scale plasmid purification was performed for both the expression vectors with a plasmid purification kit (Qiagen, Chatsworth, CA).

Transfection of CHO Cells by Lipofection. The Lec 1 and Pro-5 cells were each grown to 50–75% confluence on three tissue culture–treated 60 × 15-mm petri dishes. For either recipient cell line, the dishes were rinsed three times with serum-free IMDM before transfection. 30 μg each of the heavy and light chain expression vectors were combined and diluted in sterile water to a final volume of 200 μl in a polystyrene tube. 90 μl of Lipofectin (Bethesda Research Laboratories, Bethesda, MD) was then added, the contents mixed, and the tube allowed to stand at room temperature for 15 min. The mixture was then diluted to a final volume of 9 ml with serum-free IMDM. To each dish of Lec 1 or Pro-5 cells three ml of the Lipofectin mixture was added dropwise, with the drops distributed over the surface of the plate. The plates were incubated overnight at 37°C in a humidified 5% CO_2 incubator. The next day, an equal volume of IMDM with 10% FCS was added to each dish. On the following day, each plate was trypsinized and the cells diluted in 24 ml selection medium (IMDM supplemented with 10% FCS, 1% Nystatin [GIBCO BRL], 1% gentamicin and 1 mM histidinol [Sigma Chemical Co., St. Louis, MO]) and distributed 100 μl/well into 96-well flat-bottomed microtiter plates (Corning, Inc., Corning, NY). Fresh selection medium was added 3 d later. Colonies were generally seen within 10 d.

Transfectants were screened for Ab production by an ELISA using microtiter plates (Immulon 2; Dynatech Laboratories, Inc., Chantilly, VA) coated with DNS-BSA or goat anti–human IgG. The detecting Ab was alkaline phosphatase–conjugated goat anti–human κ light chain (Sigma Chemical Co.). Positive clones were expanded and subcloned.

Biosynthetic Labeling and Endoglycosidase H Hydrolysis. Secreted Abs were obtained from [^{35}S]methionine-labeled transfectants. Approximately 3 × 10^6 cells were trypsinized, washed in methionine-free DME (Irvine Scientific), and resuspended in the same medium supplemented with 15 μCi [^{35}S]methionine (Amersham, Arlington Heights, IL) and 400 μg/ml proline, and incubated at 37°C for 3 h. The supernatants were harvested and the Ab immunoprecipitated with a mixture of rabbit anti–human Fc and rabbit anti–human Fab antisera (both prepared by Letitia A. Wims in this laboratory) followed by precipitation with *Staphylococcus aureus* protein A (IgG Sorb; The Enzyme Center, Boston, MA) and washing. The Abs were resuspended in sample buffer (25 mM Tris, pH 6.7, 2% SDS, 10% glycerol, and 0.008% bromophenol blue) and eluted from protein A by boiling. The samples were analyzed by SDS-PAGE and autoradiography.

For Endoglycosidase H (Endo H) hydrolysis, ^{35}S-labeled supernatants were treated with 50 mM sodium citrate (pH 5.5), 100 mM 2-ME (Eastman Kodak Co., Rochester, NY), 2 mM PMSF (Sigma Chemical Co.), and 0.005 U Endo H (Boehringer Mannheim, Indianapolis, IN) in a final vol of 1 ml. After incubation for 24 h at 37°C, the reactions were terminated by the addition of 5

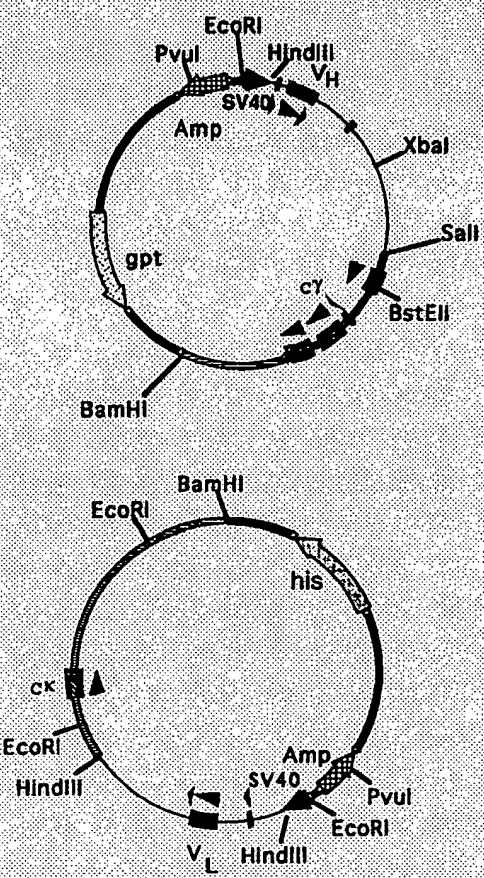

Figure 2. Vectors for the expression of Ig genes using SV40 controlling elements. The SV40 early promoter and enhancer are shown on the heavy chain (*A*) and light chain (*B*) vectors by a darkly cross-hatched arrowhead, and the murine leader and variable region genes by dark boxes. Murine intronic sequences are indicated by a thin black line. Human constant region exons are shown by diagonally striped boxes and the intervening sequences by striped black lines. The pSV2-derived sequences are represented by filled lines, with the prokaryotic selectable marker (*Amp*) and the eukaryotic selectable markers (*gpt* and *his*) shown by stippled and lightly shaded arrows, respectively. Arrows indicate the direction of transcription. Restriction sites discussed in the text are shown.

μl/sample 2 M Tris, pH 8.0. The samples were then spun briefly in a microcentrifuge to pellet debris and Ab was immunoprecipitated as described. The samples were analysed by SDS-PAGE using Tris-glycine gels.

Protein Purification. Purified Ab for biological characterization was obtained by affinity chromatography as previously described (24). Transfectoma cells were grown in roller bottle cultures in IMDM plus 2% α-calf serum (Hyclone). Supernatants from saturated cultures were buffered with 10 mM phosphate buffer (0.43 M Na_2PO_4, 0.57 M Na_2HPO_4) and supplemented with 0.45 M NaCl, 0.02 M EDTA, and 0.02% NaN_3. Supernatants were sterile filtered, degassed, and passed through AH-Sepharose columns to which the DNS isomer 2-dimethyl-aminonaphthalene-5 sulfonyl chloride had been coupled (Molecular Probes, Inc., Eugene, OR). Ab was eluted with a second DNS isomer, *N*-(5-carboxy-pentyl)-2-dimethyl-aminonaphthyl-5-sulfonamide. The bound hapten was removed by extensive dialysis against Tris-buffered saline (TBS). The concentration of purified protein was determined with the bicinchoninic acid (BCA) protein assay (Pierce, Rockford, IL).

Measurement of Ag Affinity. A competitive binding assay was used to compare the affinity for DNS of the chimeric Abs. Immulon 2 microtiter plates were coated overnight at 4°C with DNS-BSA (5 μg/ml diluted in PBS, 50 μl/well) and blocked with 3% BSA. The murine DNS-specific Ab 27-44 was diluted to 200 ng/ml in BBS/1% BSA and mixed in equal vol with serial dilutions of IgG1-My 1, IgG1-Pro-5, or IgG1-Lec 1. The dilutions ranged from 0 to 24 μg/ml. The mixtures of murine and chimeric anti-DNSs were added in duplicate (50 μl/well) to the DNS-coated plate and incubated overnight at 4°C. Bound 27-44 Ab was detected by incubation with an alkaline phosphatase–conjugated goat anti–mouse κ Ab (Zymed Laboratories, Inc., S. San Francisco, CA), followed by the addition of substrate (*p*-nitrophenyl phosphate disodium, obtained from Sigma Chemical Co.). The data were plotted to compare the percentage of maximal binding (in the absence of competitor) to the amount of competitor present, and the point at which 50% inhibition of Ag binding by 27-44 occurred was determined. As a negative control, a chimeric dextran–specific IgG1 Ab was diluted and incubated in similar fashion with 27-44.

Measurement of Complement Fixation. The capacity of Abs for complement fixation was measured by several methods. In the direct assay, SRBC (Pocono Rabbit Farm, Canadensis, PA) were coated with DNS-BSA by the chromic chloride coupling procedure (25). The Ag-coated SRBC were loaded with ^{51}Cr, washed, and brought to a 2% suspension in Hepes-buffered saline with 0.1% gelatin (Gel-HBS). Ab at various concentrations, 0–20 μg/ml and diluted in the same buffer, was added in duplicate 50-μl aliquots to round-bottomed microtiter plates that were kept on ice throughout preparation. Chromium-loaded SRBC were added (50 μl), followed by 25 μl guinea pig complement (C'; Colorado Serum Co., Denver, CO) that had been preabsorbed with DNS-coated SRBC and adjusted to 10 LU/25 μl. Controls included spontaneous lysis (SRBC in Gel-HBS alone), total lysis (SRBC in water), SRBC incubated with Ab but without complement, and SRBC with complement and buffer alone. Experimental samples were plated in duplicate, and controls in quadruplicate. The plates were then covered and incubated in a 37°C water bath for 45 min. The plates were spun at 800 rpm in a countertop centrifuge (Beckman Instruments Inc., Fullerton, CA) to pellet red cells and debris and 50 μl from each well was withdrawn and counted in a gamma counter (model Gamma 5500; Beckman Instruments Inc.). Percent lysis was calculated as: 100 × [(mean experimental cpm − mean cpm SRBC lysis in the presence of complement alone)/(total lysis − spontaneous lysis)].

For the complement consumption assay (25) Ab (8 μg/25 μl) was incubated in duplicate with increasing amounts of DNS-BSA (0–5 μg/well) and 2 CH_{50} U of guinea pig complement in round-bottomed microtiter plates for 45 min at 37°C. [^{51}Cr]-loaded hemolysin-sensitized SRBC were then added and incubation was continued for another 45 min. The plates were centrifuged as before and the amount of ^{51}Cr release measured with a gamma counter. The percentage of complement consumption was calculated as 100 × [1−(cpm of Ab + Ag + C'/cpm Ab + C')].

C1q Binding Assay. A solid phase assay was used to measure the capacity of Abs to bind C1q, the first step in the complement cascade (26). Immulon 2 microtiter plates were coated with 100 μl/well of DNS-BSA diluted to 10 μg/ml in PBS. The plates were then blocked with PBS plus 3% BSA overnight at 4°C and washed. The DNS-specific Abs were diluted serially from a stock concentration of 10 μg/ml in PBS plus 1% BSA, were added in duplicate 100 μl/well, and incubated overnight at 4°C. After washing with HBS, 100 μl 0.125% normal human serum diluted in HBS was added to each well and the plates were incubated at 37°C for 2 h. HBS was used for washing and as the diluent at this point because phosphate inactivates complement. Goat anti–human C1q was then diluted 1:10,000 in PBS plus 1% BSA and incubated at room temperature for 2 h, after which the plates were washed and incubated at room temperature for 2 h more with alkaline phosphatase–conjugated swine and anti–goat IgG (Boehringer Mannheim). After a final washing with PBS, substrate was added and the plates were read at 410 nm on a plate reader (model MR 700; Dynatech). IgG4, which does not bind C1q, was included on each plate as a negative control.

Fc Receptor Binding. Purified Abs (10–20 μg) were iodinated using Iodobeads (Pierce). ^{125}I was obtained from ICN (Irvine, CA). Before the assay, U937 cells were harvested, washed with PBS, and resuspended in fresh RPMI supplemented with 10% FCS and 100 U/ml recombinant human IFN-γ (the gift of Dr. Jorge Gavilondo-Cowley, Centro de Ingenieria Genetica y Biotecnologica, La Habana, Cuba). After a 48-h incubation, the cells were washed and incubated in serum-free DMEM at 37°C for 2 h to dissociate any serum Ig that might be bound to the Fc receptors. The cells were then washed again and resuspended to 5 × 10^6 cells/ml in assay buffer (Hepes buffer; 0.1 M Hepes, pH 7.4, 0.12 M NaCl, 0.005 M KCl, 0.0012 M $MgSO_4$, 0.015 M HAc, 0.01 M glucose, and 1% BSA).

The radiolabeled Ab diluted in assay buffer to ~ 10 ng/50 μl was mixed in 0.6 ml Eppendorf tubes with increasing amounts of the homologous unlabeled Ab in the same volume. Threefold dilutions from a 100-fold excess of unlabeled Ab were tested in duplicate. To measure nonspecific binding, a 1,000-fold excess of commercial human IgG (Miles Inc., Kankakee, IL) was used as inhibitor. 400 μl of stimulated U937 cells were added to each tube, and the tubes were rotated on a Labquake rotator (Labindustries, Inc., Berkeley, CA) at 18°C for 2.5 h. The tubes were then spun briefly in a microfuge, the supernatants were withdrawn, and 100 μl was measured in a gamma counter. The pellets were washed three times with PBS and the supernatant carefully removed by aspiration. Each tube was then placed in the gamma counter to measure the radioactivity retained by the pellets. Scatchard analysis was applied to determine the binding constants and number of receptors per cell (27).

In Vivo Half-Life. Female BALB/c mice were fed for at least 1 wk with water treated with potassium iodide (3 drops of 10 mg/ml per 100 ml water). For each ^{125}I-labeled protein, three mice were injected intraperitoneally with 10^6 cpm labeled Ab (28). Whole-body radioactivity was measured with a scaler/ratemeter (model

JS-5A; Wm. B. Johnson & Assoc., Ronceverte, WV) using a NaI crystal large enough to accommodate a mouse. Measurements commenced at 3 min after injection and continued at regular intervals for 300 h. The percentage of radioactive counts remaining in each sample (background subtracted) was: 100 × [(cpm from each sample)/(cpm observed immediately after injection)]. To calculate the half-life of each protein, the percentage of radioactivity remaining was plotted against the intervals at which cpm were measured.

In further experiments, mice were injected intravenously with the IgG1-Lec 1 prepared as described previously, but were coinjected with either 10 mg mannan (purified yeast polysaccharide from *Saccharomyces cerevisiae*, purchased from Sigma, and dissolved to 10 mg/100 μl PBS) or the equivalent vol of PBS (29). After 1 h, the mannan-injected mice were given a second intravenous injection of 10 mg mannan. The mice were monitored for whole-body radioactivity as before, and clearance of radioactivity over time was plotted as described.

Results

Chimeric mouse-human mAbs provide useful tools for the study of Ig function. In previous studies, the human IgG1 constant region joined to the murine DNS-specific variable region expressed in murine myeloma cells was used to investigate the functional properties of the resulting protein (30, 31). In the current study, by substituting the Ig-specific promoters and enhancers with those of SV40, the same Ab has been produced in Pro-5, a wild-type CHO cell line, and Lec 1, a variant of Pro-5 deficient in *N*-acetylglucosaminyltransferase I activity. The Ab expressed in Lec 1 will have a high-mannose carbohydrate of a type that is not normally seen on IgG attached to C_H2 in place of the normal complex carbohydrate. Thus it is possible without clinical or enzymatic modification to obtain large quantities of purified Ab with a defined, altered carbohydrate structure.

The CHO cells were refractory to electroporation, but efficient transfection was attained by lipofection. Transfectants selected for resistance to 1 mM histidinol were obtained from both Pro-5 and Lec 1. The transfectants fully assembled H_2L_2 molecules at a level ~5 μg/ml of Ab/10^6 cells/24 h, sufficient to produce adequate amounts of purified Ab from roller bottle culture. One clone of each, IgG1-Pro-5 and IgG1-Lec 1, was chosen for further study.

To confirm that carbohydrate with altered structure was present on the Lec 1–produced Ab, the Lec 1 transfectant and myeloma cells producing a chimeric Ab of the same isotype were biosynthetically labeled and the supernatants from each were treated with Endo H, which hydrolyzes high-mannose and hybrid but not complex oligosaccharides. Hydrolysis was conducted under reducing conditions to expose the sugar to the enzyme and the proteins were immunoprecipitated and analyzed by SDS-PAGE. The myeloma-produced IgG, IgG1-My 1, is mostly unaffected by treatment with Endo H although a small amount of enzyme hydrolysis is observed (Fig. 3). In contrast, the Lec 1–produced IgG, IgG1-Lec 1, is sensitive to Endo H and the heavy chain of the treated protein shows a faster mobility than the untreated one. Furthermore, the heavy chain of untreated IgG1-Lec 1 shows faster migration than does that of untreated IgG1-My 1, consistent with

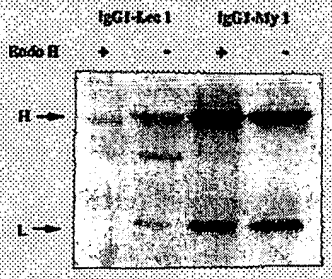

Figure 3. Endo H hydrolysis of transfectoma proteins. Transfectoma proteins were subjected to hydrolysis with Endo H under reducing conditions and were analyzed by SDS-PAGE. Heavy and light chains are indicated.

the presence of a truncated carbohydrate on IgG1-Lec 1. The identity of the band migrating between the heavy and light chains is not clear, but it appears to be a CHO cell–specific product that is not glycosylated.

To evaluate the biologic activity of these Abs in Ag-dependent assays it was necessary to confirm that the Abs' affinity for Ag is equivalent. The IgG1-Lec 1, IgG1-Pro-5, and IgG1-My 1 Abs were tested in competition experiments for their ability to inhibit Ag binding by the murine anti-DNS 27-44 with identical variable regions (Fig. 4). With all the chimeric Abs, 50% inhibition of binding by 27-44 was attained at a concentration of ~3 μg/ml. The inhibition curves of these Abs are very similar overall, thus their Ag binding capacity should be equivalent at the Ab concentrations employed in the various functional assays.

Previous work from this laboratory and others (3–5) had shown that the presence of carbohydrate in the C_H2 region of IgG1 is essential for Fc-associated functions such as complement activation and Fc receptor binding. The IgG1-Lec 1 protein containing a carbohydrate with altered structure, as well as the Pro-5–produced Ab, were now compared to the biologically active IgG1-My 1 Ab produced in murine myeloma cells.

The ability of the IgG1 Abs to activate complement was determined using several assays designed to investigate different aspects of the complement cascade. In the direct assay, which determines the ability of the Ab to complete the complement cascade and effect hemolysis, increasing amounts of Ab

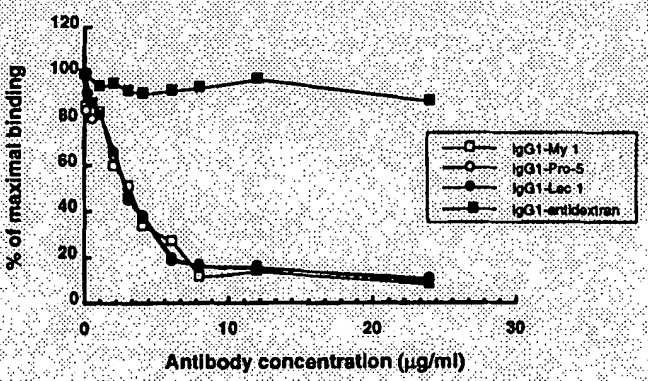

Figure 4. Competition of IgG1-My 1, IgG1-Pro-5, and IgG1-Lec 1 with the binding of murine anti-DNS 27-44 to Ag, as determined by ELISA. The data are plotted as percentage of maximum binding in the absence of competing Ab, against the increasing amount of competitor. The negative control is a chimeric IgG1 Ab specific for dextran.

were incubated with constant amounts of complement and Ag-coated SRBC. As shown in Fig. 5 *A*, red cell lysis increased as the amount of IgG1-My 1 or IgG1-Pro-5 was increased to a maximal lysis of ~35%. In contrast, IgG1-Lec 1 failed to mediate lysis at any of the concentrations tested.

In the complement comsumption assay, the capacity of Ab to deplete the complement components is measured. A constant amount of Ab is first incubated with complement in the presence of increasing amounts of Ag; if the Ag–Ab complexes consume any of the complement components, they will not be available to lyse the hemolysin-coated indicator cells. Decreased lysis therefore indicates an increase in complement activation. The ability of the IgG1-My 1, as well as IgG1–Pro-5 Ab, to consume complement is Ag dependent with total consumption ranging from of 0.5 to 50 μg Ag/well (Fig. 5 *B*). In contrast, IgG1-Lec 1 consumes only a low level of complement (<15%) in an Ag-independent manner.

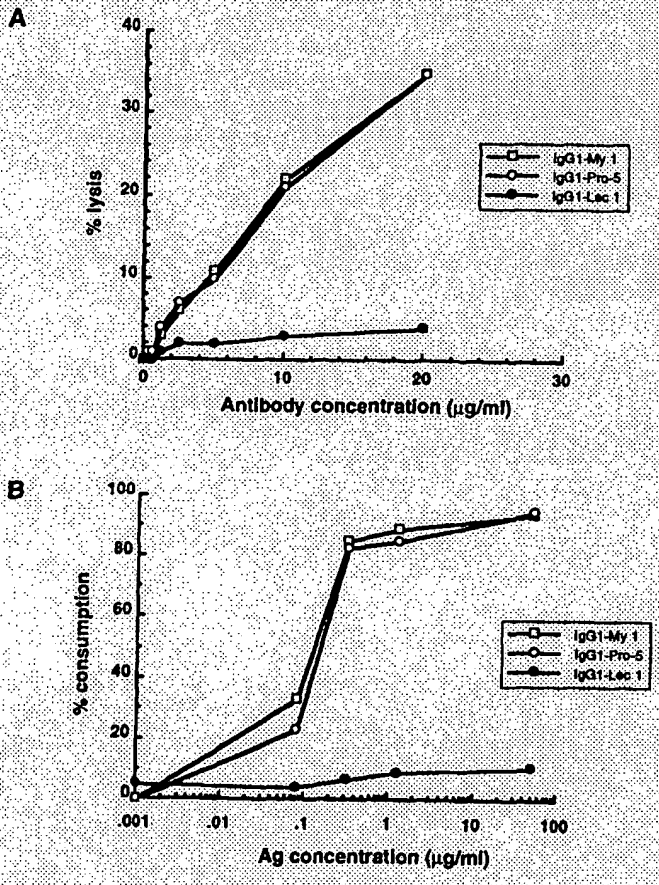

Figure 5. Complement activation by IgG1 chimeric Abs. (*A*) Direct lysis of ^{51}Cr-loaded, DNS/BSA-coated SRBC. Cells were incubated with complement and increasing amounts of Ab (in duplicate) for 45 min at 37°C. Supernatants were then harvested and the amount of lysis was quantitated with a gamma counter as described. The percent lysis is plotted against the Ab concentration. (*B*) Complement consumption. Ab (8 μg/25 μl) was incubated with complement and with increasing amounts of Ag at 37°C for 45 min. SRBC were sensitized with hemolysin, loaded with ^{51}Cr, and added to the reaction for a further incubation of 45 min. Complement consumption was calculated from chromium release as described.

To determine whether the defect in complement activation by IgG1-Lec 1 lies in the initial steps of the complement cascade, we compared the ability of these Abs to bind C1q, the first step in the activation of the classical complement pathway. Because C1q binds poorly to monomeric IgG, a solid-phase assay was used in which Ag–Ab complexes are formed on a plastic surface at sufficient density to allow C1q binding, which is then quantitated by C1q specific antiserum. An IgG4 Ab, which does not bind C1q, was included as a negative control. Both IgG1-My 1 and IgG1–Pro-5 bound C1q well, the IgG4 Ab, as expected, did not bind, and IgG1-Lec 1 showed significant but reduced C1q binding capacity (Fig. 6).

Fc Receptor Binding. To determine the affinity of binding of the IgG to the FcγRI present on IFN-γ–stimulated U937 cells, a constant amount of radiolabeled Ab was incubated with increasing amounts of unlabeled homologous ligand and the amount of radioactivity bound determined. Values for the dissociation constant and numbers of receptors per cell were obtained through Scatchard analysis; a representative experiment is shown in Fig. 7. U937 cells stimulated with IFN-γ displayed ~4.2×10^4 receptors per cell. The mean K_d of IgG1-My 1 was 1.79×10^{-9} M^{-1}, in agreement with previously published values (31). The K_d of IgG1–Pro-5 was very similar, at 1.55×10^{-9} M^{-2}. The K_d of IgG1-Lec 1 was reduced approximately four- to sixfold, with a mean value of 8.2×10^{-9} M^{-1}. Thus, the ability of the mannosylated IgG1-Lec 1 to bind FcγRI is slightly reduced but still substantial.

In Vivo Half-life. To determine the in vivo half-life of the molecules, ^{125}I-labeled Abs were introduced into BALB/c mice by intraperitoneal injection, and the amount of radioactivity present in each mouse determined by whole-body counting. The half-life values obtained by this method have been found to correlate well with those obtained by intravenous injection of labeled Abs and counting of blood samples (28). IgG1-My 1 was cleared in the β-phase with a half-life of 6.3 d (Fig. 8). In this experiment, virtually all of the IgG1-My 1 was cleared in the β-phase, but in other experiments,

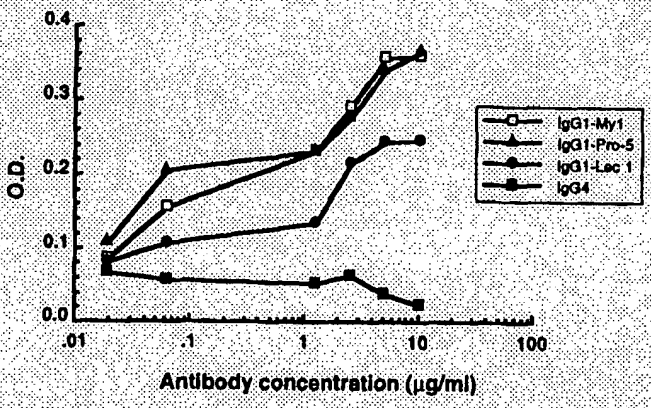

Figure 6. C1q binding by DNS-specific Abs. Binding was measured by ELISA as described using Ag-coated microtiter plates. An IgG4 Ab, which does not bind C1q, was included as a negative control.

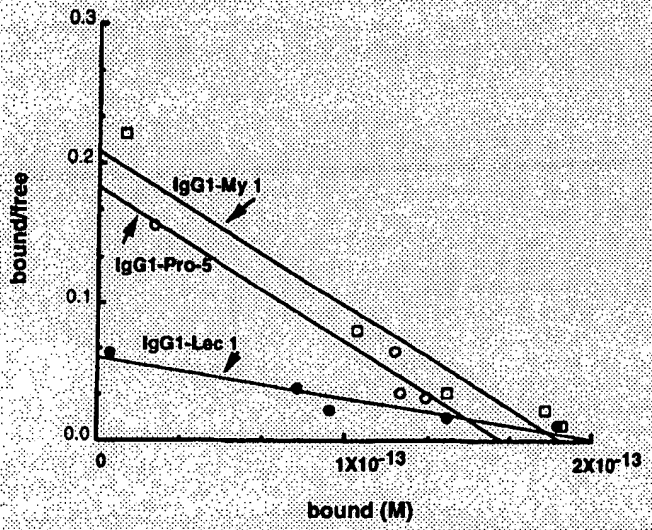

Figure 7. Scatchard analysis of the binding of IgG1-My 1 (●), IgG1-Pro-5 (○), and IgG1-Lec 1 (□) to U937 cells. The U937 cells had been stimulated for 48 h with 100 U/ml IFN-γ to increase expression of FcγR1 receptors. A constant amount of ^{125}I-labeled Ab was incubated with U937 cells with increasing amounts of unlabeled homologous competitor, and the amount of radioactivity bound to pelleted and washed cells was measured with a gamma counter. The line represents a least squares fit of the data and was calculated using Excel.

up to 40% of the protein was cleared in the α-phase. Approximately 40% of the IgG1-Pro-5 Ab was rapidly cleared in the α-phase; the remaining Ab had a β-phase half-life of 5.7 d, very similar to that of IgG1-My 1. In contrast, over 80% of IgG1-Lec 1 is consistently cleared rapidly whereas the remaining protein has a greatly reduced in vivo half-life of 4 d. Thus the IgG produced in the myeloma and Pro-5 CHO cells persists in the circulation considerably longer than does its mannosylated counterpart.

To investigate whether the rapid clearance of IgG-Lec 1

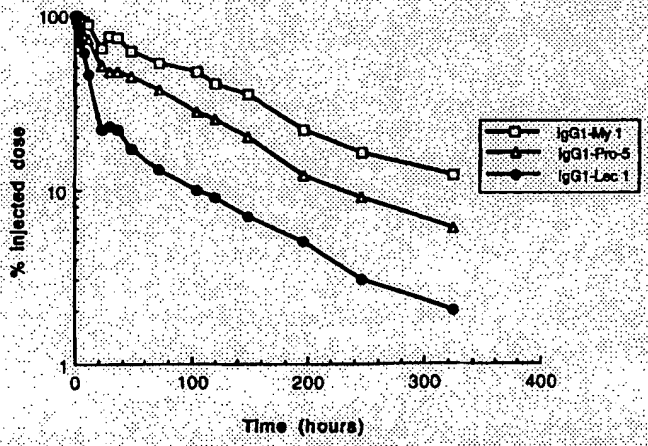

Figure 8. In vivo half-life of IgG1-My 1, IgG1-Pro-5, and IgG1-Lec 1 Abs. BALB/c mice were injected intraperitoneally with ^{125}I-labeled Ab and the persistence of radioactivity was measured by whole-body counting and is displayed as a percentage of injected dose over time. The β-phase half-life was determined from the values obtained after 48 h.

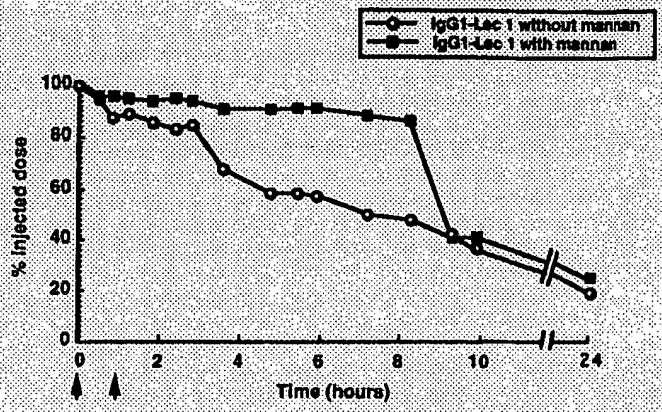

Figure 9. Effect of mannan on the in vivo clearance of IgG1-Lec 1. Mice were given intravenous injections of radiolabeled protein, either concurrently with 10 mg mannan or without. The mice receiving mannan were given a second injection 1 h later; the times of mannan injection are indicated by arrows along the *x*-axis. The percentage of radioactivity remaining was measured over time; the initial measurement was taken immediately after injection.

was mediated through mannose receptors on cells in the reticuloendothelial system, mice injected intravenously (tail vein) with ^{125}I-IgG1-Lec 1 were concurrently injected with either 10 mg of yeast mannan or with an equal volume of PBS. 1 h after injection, those mice receiving mannan were given a second injection of 10 mg mannan, and all mice were monitored by whole-body counting for 24 h. As shown in Fig. 9, the control mice injected with PBS demonstrated continuous and rapid loss of radioactivity. In contrast, the mannan-injected mice retained virtually all radioactivity for over 8 h, after which rapid clearing abruptly ensued. This result suggests that clearance takes place using the mannose receptors and these were blockaded temporarily by the yeast polysaccharide. By 24 h, the level of remaining radioactivity was the same in all the mice.

Discussion

The presence of carbohydrate in C_H2 is essential for biological activity of IgG. Although the carbohydrate attached there is heterogeneous, a considerable body of evidence shows that certain glycosylation patterns can contribute to aberrant Ig activity. Previous studies (15) had indicated that IgG rendered deficient in galactose by glycosidase treatment is deficient in C1q and Fc receptor binding. However, to rule out any diminution of Ab function that might be a consequence of the conditions of enzyme treatment, it would be desirable to produce biosynthetically Abs with defined alterations in carbohydrate structure and to determine their functional properties.

Proteins with altered carbohydrate structures can be produced in well-characterized glycosylation mutants of CHO cells (32). Wild-type CHO cells have been widely used for Ab production (18–22), so the variety of available mutants provides an expression system appropriate for the study of specific glycosylation defects of interest. Additionally, genetic engineering techniques provide the means to produce homo-

geneous populations of isotypes of interest. Therefore, we designed expression vectors for the production of DNS-specific IgG1 Abs in CHO cells. In this initial study using this experimental approach, the Igs were produced in wild-type CHO cells as well as Lec 1, a cell line incapable of processing the high mannose intermediate through the terminal glycosylation steps (Fig. 1). The resulting Abs were properly assembled and secreted and retained Ag affinity. Using this approach, Abs with novel oligosaccharide structures were made available for study.

The classical pathway of complement activation is initiated by the binding of Ab to Ag with the subsequent binding and activation of C1. Unlike the myeloma- or CHO-produced chimeric Abs, the IgG1-Lec 1 Ab was incapable of complement-mediated lysis of hapten-coated erythrocytes, although the Lec 1–produced Ab did demonstrate a reduced but significant amount of C1q binding. The C1q binding site on IgG defined by residues Glu318, Lys320, and Lys322 lies along an exposed β-strand on C_H2 (33). Other residues within this region have been shown to contribute to isotypic differences in complement activation capability (34). It is possible, therefore, that a conformational change introduced into the C_H2 domain by the altered carbohydrate serves to decrease C1q binding.

The level of C1q binding possessed by IgG1-Lec 1 might not be sufficient to activate the subsequent steps of the complement cascade. That C1q binding does not necessarily lead to cell lysis has been documented in studies of the comparative lytic efficiencies of different Ab isotypes (26, 35, 36). Additionally the IgG1-Lec 1 Ab might be an impaired substrate for interaction with complement proteins involved in the later stages of the complement cascade. The IgG1-Lec 1 differs from aglycosylated IgG1 which appears unable to bind C1q (3).

Compared to the wild-type Ab, the K_d of IgG1-Lec 1 for FcγR1 receptors on U937 cells was reduced approximately four- to sixfold. Whereas the loss of carbohydrate abolishes Fc receptor binding, changing the oligosaccharide structure has demonstrable but less drastic effects, consistent with previous reports (15, 37). Degalactosylated IgG produced by glycosidase treatment showed reduced IgG binding to U937 cells, although a binding constant was not determined (15). Intact chimeric Abs produced in yeast were as capable of ADCC as the murine counterpart, but could not activate complement (37). The oligosaccharide produced by yeast is a bulky structure with 30–100 terminal mannose residues (38) and is quite different from the truncated structure with terminal mannose residues produced by Lec 1 cells. Residues on IgG critical for Fc receptor binding lie in the lower hinge region and in the hinge proximal region, and whereas glycosylation is required for Fc receptor binding and ADCC (39–41), our results suggest that the presence of a truncated carbohydrate is sufficient to allow at least some Fc receptor binding. Additional studies are required to define precisely the carbohydrate structure necessary for different effector functions.

The in vivo fate of the IgG1-Lec 1 in mice is drastically affected by the presence of a carbohydrate of altered structure in C_H2. Whereas in vivo persistence of aglycosylated IgG1 was equivalent to that of wild type (3, 42), that of the mannosylated Ab was reduced substantially. Moreover, 80% of IgG1-Lec 1 was rapidly cleared in the α phase. Comparative in vitro protease digestion showed that IgG1-Lec 1 was no more sensitive to protease than was the wild-type Ab (data not shown). Rather, it seemed possible that clearance of IgG1-Lec 1 might occur by a different mechanism than does the clearance of IgG1-My 1 and IgG1-Pro-5.

Numerous studies have described systems for glycoprotein clearance in the liver that are localized to different compartments and that recognize different terminal sugar residues (43, 44). Liver endothelial cells bear receptors that recognize terminal mannose residues through which rapid clearance of mannosylated proteins such as ricin, OVA, and the COOH-terminal propeptide of type I procollagen has been observed (43–47). Mannose receptor–mediated clearance of glycoproteins occurred more rapidly than did clearance via galactose receptors, which were compartmentalized to liver endothelial and parenchymal cells, respectively (46, 47). Since the administration of mannan effectively inhibited the clearance of IgG1-Lec 1, although with the injection protocol used the effect was temporary, the Ab appears susceptible to uptake by mannose receptors. This result was somewhat surprising, since the Fc-associated carbohydrate normally is "buried" between the heavy chains. Indeed, the IgG1-Lec 1 Ab failed to show binding to Sepharose–Con A (data not shown). However, a report that IgG–Ag complexes injected into rats were rapidly cleared from the circulation, suggested that Ag-induced conformational changes in IgG caused the Fc carbohydrate to be exposed and susceptible to clearance by the galactose receptors on liver parenchymal cells (48). Although DNS-specific Abs are unlikely to encounter Ag in vivo, a conformational change may have been triggered in some way, perhaps through aggregation, exposing the mannose residues.

By expressing Abs in CHO cells with defined mutations in glycosylation, we have produced Abs with novel (and reasonably homogeneous) carbohydrate structures. Changing the structure of the carbohydrate may profoundly affect the behavior of Abs. In particular, the presence of a carbohydrate-bearing terminal mannose residues in C_H2 of IgG1 abolishes complement activation, attenuates Fc receptor binding, and profoundly shortens the in vivo half-life of the protein. Whereas in the current study the carbohydrate present on the IgG differed in structure from the naturally occurring carbohydrate, in future studies it will be possible to produce Abs with carbohydrate structures similar to those found on the circulating Igs in patients with certain diseases. Thus, it will be possible to determine the biologic properties of these Abs. Such studies may yield insights into the relationship between Ab structure and pathogenesis. With this technology it is possible not only to produce and study proteins with a wide variety of glycosylation defects but also to analyze a "family" of proteins, such as IgG with different isotypes, to see if effects are universal or are seen only with a particular protein. Studies like these not only may provide information about the role of carbohydrate in protein function but may also yield insights into how changes in carbohydrate structure affect protein conformation.

We thank Dr. Jorge Galvilondo-Cowley for the gift of IFN-γ. We also thank Kham Trinh and Nguyen Dinh Thien for their excellent technical assistance.

This study was supported by grants CA-16858 and AI-29470 from the National Institutes of Health and by fellowship support from Centocor (Malvern, PA).

Address correspondence to Dr. Sherie L. Morrison, Department of Microbiology and Molecular Genetics and the Molecular Biology Institute, University of California, Los Angeles, 609 Circle Drive East, Suite 1602, Los Angeles, CA 90024.

Received for publication 8 November 1993 and in revised form 6 June 1994.

References

1. Sutton, B.J., and D.C. Phillips. 1983. The three-dimensional structure of the carbohydrate within the Fc fragment of immunoglobulin G. *Biochem. Soc. Trans.* 11:130.
2. Deisenhofer, J. 1981. Crystallographic refinement and atomic models of a human Fc fragment and its complex with fragment B of protein A from *Staphylococcus aureus* at 2.9- and 2.8. A resolution. *Biochemistry.* 20:2361.
3. Tao, M.-H., and Morrison, S.L. 1989. Studies of aglycosylated chimeric mouse-human IgG. Role of carbohydrate in the structure and effector functions mediated by the human IgG constant region. *J. Immunol.* 143:2595.
4. Nose, M., and H. Wigzell. 1983. Biological significance of carbohydrate chains on monoclonal antibodies. *Proc. Natl. Acad. Sci. USA.* 80:6632.
5. Leatherbarrow, R.J., T.W. Rademacher, R.A. Dwek, J.M. Woof, A. Clark, D.R. Burton, N. Richardon, and A. Feinstein. 1985. Effector functions of monoclonal glycosylated mouse IgG2a: binding and activation of complement component C1 and interaction with human Fc receptor. *Mol. Immunol.* 22, 407.
6. Mizuochi, T., T. Taniguchi, A. Shimizu, and A. Kobata. 1982. Structural and numerical variations of the carbohydrate moiety of immunoglobulin G. *Immunology.* 129:2016.
7. Rademacher, T.W., S.W. Homans, R.B. Parekh, and R.A. Dwek. 1985. Immunoglobulin G as a glycoprotein. *Biochem. Soc. Symp.* 51:131.
8. Jefferis, R., J. Lund, H. Mizutani, H. Nakagawa, Y. Kawazoe, Y. Arata, and N. Takahashi. 1990. A comparative study of the N-linked oligosaccharide structures of human IgG subclass proteins. *Biochem. J.* 268:529.
9. Mullinax, F., A.J. Hymes, and G.L. Mullinax. 1976. Molecular site and enzymatic origin of IgG galactose deficiency in rheumatoid arthritis and SLE. *Arthritis Rheum.* 19:813.
10. Parekh, R.B., R.A. Dwek, B.J. Sutton, D.L. Fernandes, A. Leung, D. Stanworth, and T.W. Rademacher. 1985. Association of rheumatoid arthritis and primary osteoarthritis with changes in the glycosylation pattern of total serum IgG. *Nature (Lond.).* 316:452.
11. Axford, J.S., N. Sumar, A. Alavi, D.A. Isenberg, A. Young, K.B. Bodman, and I.M. Roitt. 1992. Changes in normal glycosylation mechanisms in autoimmune rheumatic disease. *J. Clin. Invest.* 89:1021.
12. Rademacher, T.W., R.B. Parekh, R.A. Dwek, G. Rook, J.S. Axford, and I. Roitt. 1988. The role of IgG glycoforms in the pathogenesis of rheumatoid arthritis. *Springer Semin. Immunopathol.* 10:231.
13. Parekh, R.B., D.A. Isenberg, B.M. Ansell, I.M. Roitt, R.A. Dwek, and T.W. Rademacher. 1988. Galactosylation of IgG-associated oligosaccharides is reduced in patients with adult and juvenile onset rheumatoid arthritis and is related to disease activity. *Lancet.* 1:966.
14. Channing, C.P., C.N. Sakai, and O.P. Bahl. 1978. Role of the carbohydrate residues of human chorionic gonadotropin in binding and stimulation of adenosine 3',5'-monophosphate accumulation by porcine granulosa cells. *Endocrinology.* 103:341.
15. Tsuchiya, N., T. Endo, K. Matsuta, S. Yoshinoya, T. Aikawa, E. Kosuge, F. Takeuchi, T. Miyamoto, and A. Kobata. 1989. Effects of galactose depletion from oligosaccharide chains on immunological activities of human IgG. *J. Rheumatol.* 16:285.
16. Stanley, P. 1987. Glycosylation mutants and the functions of mammalian carbohydrates. *Trends Genet.* 3:77.
17. Keene, J.L., M.M. Matzuk, and I. Boime. 1989. Expression of recombinant human choriogonadotropin in Chinese hamster ovary glycosylation mutants. *Mol. Endocrinol.* 3:2011.
18. Weidle, U.H., A. Borgya, H. Lenz, and P. Buckel. 1987. Reconstitution of functionally active antibody directed against creatine kinase from separately expressed heavy and light chains in non-lymphoid cells. *Gene.* 51:21.
19. Neumaier, M., L. Shively, F.-S. Chen, F.-J. Gaida, C. Ilgen, R.J. Paxton, J.E. Shively, and A.D. Riggs. 1990. Cloning of the genes for T84.66, an antibody that has a high specificity and affinity for carcinoembryonic antigen, and expression of chimeric human/mouse T84.66 genes in myeloma and Chinese hamster ovary cells. *Cancer Res.* 50:2128.
20. F. Bulens, A.-M. Vandamme, H. Bernat, L. Nelles, R.H. Lijnen, and D. Collen. 1991. Construction and characterization of a functional chimeric murine-human antibody directed against human fibrin fragment-D dimer. *Eur. J. Biochem.* 195:235.
21. Crowe, J.S., S. Hall, M.A. Smith, H.J. Cooper, and J.P. Tite. 1992. Humanized monoclonal antibody CAMPATH-1H: myeloma cell expression of genomic constructs, nucleotide sequence of cDNA constructs and comparison of effector mechanisms of myeloma and Chinese hamster ovary cell-derived material. *Clin. Exp. Immunol.* 87:105.
22. Morton, H.C., J.D. Atkin, R.J. Owens, and J.M. Woof. 1993. Purification and characterization of chimeric human IgA1 and IgA2 expressed in COS and Chinese hamster ovary cells. *J. Immunol.* 151:4743.
23. Stanley, P., and S. Siminovitch. 1977. Complementation between mutants of CHO cells resistant to a variety of plant lectins. *Somatic Cell Genet.* 3:391.
24. Shin, S.-U., and S.L. Morrison. 1989. Production and properties of chimeric antibody molecules. *Methods Enzymol.* 178:459.

25. Hardy, R.R. 1985. Complement fixation by monoclonal antibody-antigen complexes. *In* Handbook of Experimental Immunology, Vol. 1. D.M. Weir, L.A. Herzenberg, C.A. Blackwell, and L.A. Herzenberg, editors. Blackwell Scientific, Oxford, UK. 40.1–40.12.
26. Bindon, C.I., G. Hale, M. Brüggemann, and H. Waldmann. 1988. Human monoclonal IgG isotypes differ in complement activating function at the level of C4 as well as C1q. *J. Exp. Med.* 168:127.
27. Scatchard, G. 1949. The attraction of proteins for small molecules. *Ann. N.Y. Acad. Sci.* 51:660.
28. Zuckier, L.S., L. Georgescu, C.J. Chang, M.D. Scharff, and S.L. Morrison. 1994. The use of SCID mice to study the metabolism of immunoglobulin G. *Cancer.* 73 (Suppl. 3):794.
29. Bourrie, B.J., P. Casellas, H.E. Blythman, and F.K. Jansen. 1986. Study of the plasma clearance of antibody-ricin-A-chain immunotoxins. *Eur. J. Biochem.* 155:1.
30. Morrison, S.L., M.J. Johnson, L.A. Herzenberg, and V.T. Oi. 1984. Chimeric human antibody molecules: mouse antigen-binding domains with human constant region domains. *Proc. Natl. Acad. Sci. USA.* 81:6851.
31. Canfield, S.M., and S.L. Morrison. 1991. The binding affinity of human IgG for its high affinity receptor is determined by multiple amino acids in the C_H2 domain and is modulated by the hinge region. *J. Exp. Med.* 173:1483.
32. Stanley, P. 1984. Glycosylation mutants of animal cells. *Annu. Rev. Genet.* 18:525.
33. Duncan, A.R., and G. Winter. 1988. The binding site for C1q on IgG. *Nature (Lond.).* 332:738.
34. Tao, M.-H., R.I.F. Smith, and S.L. Morrison. 1993. Structural features of human immunoglobulin G that determine isotype-specific differences in complement activation. *J. Exp. Med.* 178:661.
35. Bindon, C.I., G. Hale, and H. Waldmann. 1990. Complement activation by immunoglobulin does not depend solely on C1q binding. *Eur. J. Immunol.* 20:277.
36. Michaelsen, T.E., P. Garred, and A. Aase. 1991. Human IgG subclass pattern of inducing complement-mediated lysis depends on antigen concentration and to a lesser extent on epitope patchiness, antibody affinity and complement concentration. *Eur. J. Immunol.* 21:11.
37. Horwitz, A.H., C.P. Chang, M. Better, K.E. Hellstrom, and R.R. Robinson. 1988. Secretion of functional antibody and Fab fragment from yeast cells. *Proc. Natl. Acad. Sci. USA.* 85:8678.
38. Kukuruzinska, M.A., M.L.B. Bergh, and B.J. Jackson. 1987. Protein glycosylation in yeast. *Annu. Rev. Biochem.* 56:915.
39. Walker, M.R., J. Lund, K.M. Thompson, and R. Jefferis. 1989. Aglycosylation of human IgG1 and IgG3 monoclonal antibodies can eliminate recognition by human cells expressing FcγRI and/or FcγRII receptors. *Biochem. J.* 259:347.
40. Lund, J., T. Tanaka, K.M. Thompson, and R. Jefferis. 1990. A protein structural change in aglycosylated IgG3 correlates with loss of huFcγR1 and huFcγR111 binding and/or activation. *Mol. Immunol.* 11:1145.
41. Burton, D.R., and J.M. Woof. 1992. Human antibody effector function. *Adv. Immunol.* 51:1.
42. Dorai, H., B.M. Mueller, R.A. Reisfeld, and S.D. Gillies. 1991. Aglycosylated chimeric mouse/human IgG antibody retains some effector function. *Hybridoma.* 10:211.
43. Gross, V., P. Heinrich, D. vom Berg, K. Steube, T. Andus, T.-A. Tran-Thi, K. Decker, and W. Gerok. 1988. Involvement of various organs in the initial plasma clearance of differently glycosylated rat liver secretory proteins. *Eur. J. Biochem.* 173:653.
44. Mattes, M.J. 1987. Biodistribution of antibodies after intraperitoneal or intravenous injection and effect of carbohydrate modifications. *J. Natl. Cancer Inst.* 79:855.
45. Kuiper, J., M. Otter, D.C. Rijken, and T.J.C. van Berkel. 1988. Characterization of the interaction *in vivo* of tissue-type plasminogen activator with liver cells. *J. Biol. Chem.* 263:18220.
46. Kindberg, G.M., S. Magnusson, T. Berg, and B. Smedsrod. 1990. Receptor-mediated endocytosis of ovalbumin by two carbohydrate-specific receptors in rat liver cells. *Biochem. J.* 270:197.
47. Smedsrod, B., J. Melkko, L. Risteli, and J. Risteli. 1990. Circulating C-terminal propeptide of type I procollagen is cleared mainly via the mannose receptor in liver endothelial cells. *Biochem. J.* 271:345.
48. Thornburg, R.W., J.F. Day, J.W. Baynes, and S.R. Thorpe. 1980. Carbohydrate-mediated clearance of immune complexes from the circulation. *J. Biol. Chem.* 255:6820.